



THE UNIVERSITY *of* EDINBURGH

This thesis has been submitted in fulfilment of the requirements for a postgraduate degree (e.g. PhD, MPhil, DClinPsychol) at the University of Edinburgh. Please note the following terms and conditions of use:

This work is protected by copyright and other intellectual property rights, which are retained by the thesis author, unless otherwise stated.

A copy can be downloaded for personal non-commercial research or study, without prior permission or charge.

This thesis cannot be reproduced or quoted extensively from without first obtaining permission in writing from the author.

The content must not be changed in any way or sold commercially in any format or medium without the formal permission of the author.

When referring to this work, full bibliographic details including the author, title, awarding institution and date of the thesis must be given.

Efficiency of Chemical Free Cleaning for Fouling Control in Membrane Processes: Influence of Fouling Properties

Sorcha Daly

Submitted for the degree of Doctor of Philosophy at the University of
Edinburgh



2019

Declaration

This thesis has been completed by SORCHA DALY at the University of Edinburgh under the supervision of Dr. Andrea SEMIÃO. Full references are provided where other sources are used. This work has not been submitted for any other degree or personal qualification.

SORCHA DALY

Abstract

Dependence on membrane technology in seawater desalination and wastewater reclamation is increasing rapidly due to potable water shortages across the world. Nanofiltration (NF) and reverse osmosis (RO) are widely used membrane filtration techniques which use hydraulic pressure as the driving force for mass transport through the membrane. Interest is growing in use of forward osmosis (FO) membrane technology in wastewater reclamation and as a pre-step to low pressure reverse osmosis due to potential energy reductions. In FO, two liquids with different osmotic pressures are separated by a membrane and the osmotic pressure difference is the driving force for water permeation from the feed side to the draw side, eliminating the need for hydraulic pressure.

Membrane fouling is an unavoidable problem facing all membrane processes. The presence of contaminants such as organic waste and bacteria in the feed solution can lead to membrane fouling and to a reduction in performance. This study aims to research cleaning methods that don't involve the use of harmful chemicals for fouling control in FO and RO membrane processes. Cleaning efficiency is tested under varying physical and chemical conditions. Efficiency is determined in terms of both flux restoration and fouling layer removal as it has been determined in this study that significant flux restoration does not translate to complete fouling layer removal.

Feed solution chemistry, such as the quantity of Ca^{2+} in the feed and the operating pressure, and therefore initial flux greatly influence the rate and extent of fouling and therefore the efficiency of cleaning. Understanding fouling behaviour during operation and cleaning is important when optimising cleaning methods for RO and FO. For this reason, this study uses numerous visualisation and surface characterisation techniques to improve understanding of the fouling structure before and after cleaning.

The first aim of this study is to examine the efficiency of osmotic backwashing as a way of controlling organic fouling of BW30 membranes through both pure water flux measurements and membrane surface imaging. Confocal laser scanning microscopy is used to determine the thickness of the fouling layer before and after osmotic backwashing. Firstly, the influence of feed solution chemistry was examined. After 6.5 hours of organic fouling with alginic acid, the fouling layer thickness increased from 37 μm in the absence of calcium in the fouling solution to 179 μm in the presence of 2.5 mM CaCl_2 . This occurred

due to the formation of thick compact gel fouling layer as carboxyl groups present in alginate fouling form complexes with Ca^{2+} . One minute of backwashing with 0.7 M NaCl resulted in initial pure water flux restorations of 90% for the membrane fouled in the absence of CaCl_2 compared to 86% for the membrane fouled in the presence 2.5 mM CaCl_2 despite the fact that 31 μm and 141 μm of foulant remained on these membranes respectively.

As well as the feed solution chemistry, the impact of initial flux, on fouling and cleaning in RO was examined. As expected, higher initial fluxes resulted in thicker fouling layers with the layer increasing from 39 μm for an initial flux of 25 $\text{L/m}^2\text{h}$ to 270 μm for an initial flux of 100 $\text{L/m}^2\text{h}$. Although flux restorations of 100% were achieved for initial fluxes of 25 and 33 $\text{L/m}^2\text{h}$, foulant layers of 9 μm and 25 μm remained on the membrane surface respectively. This again shows that flux restoration alone cannot indicate cleaning efficiency as high values have been reported even when significant fouling remains on the membrane surface. Only 75% of the initial pure water flux was restored after fouling with an initial flux of 100 $\text{L/m}^2\text{h}$ showing that organic fouling at higher initial fluxes is largely irreversible due to the high hydraulic pressure applied to the fouling layer making it more dense and compact.

As the solution chemistry of the feed solution has a significant influence on the fouling layer characteristics, it is questioned whether the backwashing solution could alter the fouling layer characteristics during one minute of backwashing. In order to examine this, backwashing with a solution of 0.5 M CaCl_2 was tested. SEM-EDS measurements showed that the amount of elemental calcium on the membrane decreased by 19% after backwashing with NaCl but increased by 26% after backwashing with the same osmotic pressure of CaCl_2 . Atomic force microscopy was used to quantify the adhesion forces and elasticity of the fouling layers. The membrane backwashed with CaCl_2 displayed adhesion forces twice that of the virgin membrane due to the presence of Ca^{2+} ions forming complexes with carboxyl groups in the fouling layer. In terms of the elastic forces, the sample backwashed with NaCl displayed forces similar to that of a virgin membrane showing that the fouling layer is stiff and firm. This is because the layer becomes much thinner and closer to the membrane surface. The fouled membrane was the most flexible and “fluffy” however after backwashing with CaCl_2 the fouling layer remains flexible and

soft, again showing that Ca^{2+} forms complexes with the fouling layer. SEM was also used to compare the morphology of the fouling layer before and after backwashing.

Different backwashing trends are observed in osmotic backwashing of organically fouled forward osmosis membranes. In this case, the alginate fouling layer thickness increased from less than 33 μm , in the presence of 0 mM Ca^{2+} in the feed to 173 μm in the presence of 2.5 mM Ca^{2+} . One minute of backwashing removed almost 100% of the fouling layer in each case and restored 93% of the flux in the absence of calcium and 100% for the membrane fouled in the presence of 2.5 mM CaCl_2 . Backwashing became less effective as the initial membrane fouling flux was increased. This was increased by increasing the draw solution concentration. For a draw solution of 4 M NaCl the fouling layer decreased in thickness to 113 μm but backwashing with 0.7 M NaCl only removed 19% of the fouling layer showing that although it was thinner, the fouling layer was, in fact, more compact and dense. In this case, despite 90 μm of fouling remaining on the membrane surface, 100% of the flux was restored. As with the case of organic fouling with RO, this result shows that flux restoration alone cannot indicate how effective membrane cleaning is.

To test the true efficiency of backwashing in organic fouling of FO membranes, 5 consecutive fouling and backwashing cycles were performed. Even after 5 cycles, backwashing with 0.7 M NaCl can still remove the fouling layer and restore the initial pure water flux to 97%. This shows that backwashing is effective for the FO membranes subjected to organic fouling.

The limitations of backwashing in FO are evident in the context of initial bacteria adhesion on FO membranes. Initial adhesion of *Pseudomonas putida* on forward osmosis membranes was performed for 30 minutes resulting in an 18% membrane surface coverage of live bacteria cells. Backwashing with 0.7 M NaCl was ineffective while backwashing with 3 M NaCl offered a higher backwashing flux and therefore removed 93% of the adhered cells. After 60 minutes of bioadhesion under the same conditions, 3 M NaCl backwashing was not effective as 13% of the membrane surface remained covered in dead cells.

In order to test how the feed solution chemistry effects cell adhesion, varying concentrations of CaCl_2 were added to the feed resulting in an increase in live cell surface coverage from 18% in the absence of calcium to 27% in the presence of 5 mM CaCl_2 . This is due to a reduction in the cell-surface separation distance as the Ca^{2+} ions reduce the

repulsive force between the cells and membrane surface therefore increasing adhesion. This increase in adhesion resulted in a decrease in backwashing efficiency as the 3 M NaCl backwashing solution only removed 40% of the total bacteria. Backwashing with solutions of CaCl_2 was tested to determine if 1 minute of backwashing was enough time for Ca^{2+} ions to influence the cells on the membrane surface. As with organic fouling, the Ca^{2+} ions in the backwashing draw solution influenced the cells on the membrane surface resulting in a reduction in backwashing efficiency. Backwashing with 3 M CaCl_2 only removed 40% of the cell surface coverage compared to 93% for backwashing with 3 M NaCl.

This study shows that cleaning without the use of harmful chemicals in membrane processes depends strongly on the type of process, the type of fouling, the fouling feed solution chemistry and the initial membrane flux. It also shows that the type of backwashing draw solution is important as even 1 minute of backwashing is sufficient time for interactions to occur between the draw solution and the fouling layer. Finally, this study shows that flux restoration alone cannot indicate how effective membrane cleaning is and that the membrane surface must be examined either by imaging or another surface characterisation method (e.g. SEM-EDS) in order to get a complete picture of cleaning efficiency.

Lay summary

Potable water availability is an increasing problem facing global society despite the fact that water is the earth's most abundant resource. Attention is growing on seawater desalination and wastewater reclamation due to these potable water shortages across the world. In reverse osmosis (RO) membrane desalination, salt is removed from water using membranes (very fine filters) at very high pressures. Forward osmosis (FO) is another membrane technique. It can be implemented as a way of using wastewater to produce potable water with the aid of RO. In FO processes, two liquids of differing concentrations are separated by a membrane and water permeates from the liquid of low concentration (e.g. wastewater) to the liquid of high concentration (e.g. seawater) thus eliminating the need for applied pressure. Contaminants in the water begin to accumulate on the membrane surface. This is called fouling. RO membranes can become severely fouled and therefore need to be regularly cleaned leading to loss of production time and discharge of harmful cleaning chemicals to the environment. FO is also vulnerable to fouling although, due to lack of pressure needed, fouling in FO is less severe than RO.

This study aims to research alternative cleaning methods for fouling removal in FO and RO. Many fouling conditions will be tested to determine the efficiency of cleaning under different circumstances. Membrane flux is the flow of water through the membrane per unit area of membrane. Fouling results in the loss of membrane flux which results in higher energy requirements and costs. Cleaning efficiency is determined in terms of both how much the initial membrane flux can be restored and how much of the fouling layer can be removed. The cleaning methods used were surface flushing, which involves rinsing of the fouled membrane surface with pure water, and osmotic backwashing which involves reversing the flow of water through the membrane either by introducing a pulse of high concentration salt into the dilute side of the membrane, or by swapping the dilute solution and the concentrated solution which will reverse the flux through the membrane. It has been determined in this study that significant flux restoration does not translate to complete fouling layer removal. Microscopy was used to show that, in some cases, fouling still remains on the membrane surface despite complete restoration of flux.

The condition of the raw water to be treated, such as the type of contaminants present, the presence of elements such as calcium in the water and initial membrane flux have an effect on the extent of fouling and therefore the efficiency of cleaning. Understanding fouling mechanisms during both filtration and cleaning is important when optimising cleaning methods for RO and FO processes. For this reason, this study uses surface imaging and other characterisation techniques to improve understanding of the fouling layer before and after cleaning.

The first aim of this study is to examine how cleaning without the use of harmful chemicals can remove fouling due to organic contaminants on RO membranes. The cleaning technique used was osmotic backwashing with a sodium chloride (NaCl) solution for 1 minute. Microscopy was used to determine the thickness of the fouling layer before and after osmotic backwashing. The fouling solution was varied by adding different quantities of calcium to it. The fouling layer thickness increased as the amount of calcium in the fouling solution increased. This thickness increase occurred as calcium interacts with the organic foulant to form a thick compact gel fouling layer. Backwashing became less effective as the amount of calcium in the fouling solution increased. It was also found that the thickness of the fouling layer did not affect the backwashing efficiency.

In RO, the initial membrane flux is determined by the operating pressure. The impact of the initial flux on fouling and cleaning was examined. Higher fluxes resulted in denser fouling layers. At low fluxes, the membrane performance was completely restored by backwashing even though thin fouling layers remained on the surface. As the initial flux increased, backwashing became less efficient as the fouling layer became more dense and compact.

Backwashing with a calcium chloride (CaCl_2) solution was performed as it offers higher backwashing pressures than NaCl and therefore higher fluxes which could help remove the fouling layer. However, just as increasing calcium concentration in the fouling solution caused thicker fouling layers as it interacts with the organic foulant, backwashing with CaCl_2 for even just one minute resulted in interactions between the calcium and the fouling layer. These interactions could not be overcome by the high backwashing fluxes and therefore this backwashing method was not effective.

The second aim of this study is to examine alternative cleaning of FO membranes. Surface flushing of the fouled membrane for 1 minute was determined to be inefficient. Different

backwashing trends are observed in osmotic backwashing of forward osmosis membranes compared to RO membranes. The fouling layer thickness increased as the amount of calcium in the fouling solution increased, however backwashing restored the membrane performance regardless of the calcium concentration in FO, unlike in RO.

Similarly to RO, backwashing became less effective as the initial membrane fouling flux was increased. The fouling layer became more compact and dense and it could not be completely removed by backwashing. Despite this, the flux of the membrane was completely restored. As with the case of organic fouling with RO, this result shows that flux performance alone cannot indicate how effective membrane cleaning is and highlights the importance of surface imaging to obtain a true representation of cleaning efficiency. Backwashing with a calcium chloride (CaCl_2) solution was also performed on the FO membranes. However, as with RO, the calcium interacted with the organic fouling layer and therefore this backwashing method was not effective.

To test the true efficiency of backwashing of organic fouling of FO membranes, 5 consecutive fouling and backwashing cycles were performed. Even after 5 cycles, backwashing still removed virtually all of the fouling layer and restored the membrane performance. This shows that backwashing is effective for the FO membranes subjected to organic fouling at low fluxes.

Finally, FO membranes were subjected to fouling with bacteria for short durations to allow the bacteria to stick to the membrane. This initial attachment of bacteria on forward osmosis membranes was performed for 30 minutes. One minute of backwashing with a 0.7 M concentration of NaCl was ineffective while backwashing with 3 M NaCl offered a higher backwashing flux and therefore removed almost 100% of the bacteria from the membrane surface. After 60 minutes of attachment, 3 M NaCl backwashing was no longer effective as the bacteria were allowed to attach to the membrane for too long resulting in stronger bonds between the bacteria and the surface.

As with organic fouling, varying concentrations of CaCl_2 were added to the bacteria fouling solution resulting in an increase in fouling. This is because calcium reduces repulsive forces between the bacteria and membrane. This increase in attachment resulted in a decrease in backwashing efficiency as backwashing with 3 M of NaCl could not remove all of the attached bacteria.

Backwashing with calcium chloride (CaCl_2) solutions was performed. However, as with RO and FO, the calcium influenced the bacteria such that backwashing with solutions of CaCl_2 was not effective when compared with the 3 M NaCl.

This study shows that osmotic backwashing is an effective cleaning technique for organic fouling removal in FO processes and low pressure RO processes. Backwashing is also effective for initial bacteria attachment control under certain conditions. The efficiency of backwashing in membrane processes depends on the type of process, the type of contaminants present and the initial membrane flux. It also shows that the type of backwashing solution is important as interactions can occur between the backwashing solution and the fouling layer even after just 1 minute of backwashing. Finally this study shows that flux restoration alone cannot show how effective membrane cleaning is and that the membrane surface must be examined with imaging techniques in order to get a complete understanding of cleaning efficiency.

Acknowledgments

Thank you to everyone who has helped me produce my PhD. The best part of this experience has been meeting all the wonderful people who have helped me along the way.

Firstly, I acknowledge the support that I have received from The University of Edinburgh, School of Engineering. This has been a great place to work and study.

Thank you to my wonderful supervisor Dr Andrea Semião. I could not have done this without you. Thank you for all of your help and advice, your patience and understanding, your hard work, humour and brilliance. You'll never know how much you inspire me.

For all of your support and advice, thank you to Dr Filipe Teixeira-Dias and Prof Paolo Perona.

Thank you to my internal examiner Dr Santiago Romero-Vargas Castrillón and my external examiners Prof Eoin Casey and Prof Nigel Graham, for your comments, questions and corrections on my thesis and to Dr Thanasis Angeloudis for acting as non-examining chair.

Thank you everyone who helped me with the imaging techniques, Dr David Kelly, Dr Nicola Cayzer, Steve Mitchell and Kathryn Topham. Thank you to all of the technicians who helped me with the design, construction and testing of the crossflow systems and all of my lab work. Thank you particularly to Louise Hogg, Jim Hutcheson, Steve Gourlay, Chris Sturgeon, Kevin Tierney and Grant Gilfether.

To everyone in John Muir for making this a great place to work every day, from the amazing JM quiz team, who got to know my disturbing competitive side, to our "3.05" running team who did incredible at the Liverpool marathon festival (If you can't handle me at mile 1, you don't deserve me at mile 26, right?) to my wonderful office mates, particularly Mikey, Valentina and Zeyu, THANK YOU!

Thank you to my parents for your financial support particularly during my final year and always supporting me no matter what. Thank you to Niall, Elaine, Grainne, Enda and Lydia for your love and support. Thank you to Ruan, Tadhg, Ultan and Finn. You inspire me every day with your happiness, wonder, resilience, curiosity for learning and overall amazingness. Thank you to Meadhbh for your support, guidance, financial support, reassurance, hilarious jokes and friendship through all the highs and lows of this experience.

Table of Contents

Declaration.....	iii
Abstract.....	v
Lay summary	ix
Acknowledgments.....	xiii
Table of Contents.....	xv
List of figures.....	xix
List of tables	xxi
Chapter1: Introduction	23
Chapter 2: Literature review	27
2.1. Introduction	27
2.1.1 Water and Energy Crisis.....	28
2.1.2 Desalination Energy Demand.....	28
2.1.3 Wastewater treatment and reclamation	29
2.2 Membrane processes: Principles and applications.....	32
2.2.1 Pressure driven membranes	32
2.2.2 Forward Osmosis.....	33
2.2.3 Concentration polarisation	36
2.2.4 Reverse salt diffusion	40
2.3 Fouling.....	42
2.3.1. How solution chemistry influence organic fouling	43
2.3.2 Physical fouling conditions.....	46
2.3.3 Impact of hydraulic pressure on organic fouling	47
2.3.4 Bacteria adhesion and Biofouling	48
2.4 Cleaning.....	52
2.4.1 Membrane surface flushing	52
2.4.2 Osmotic backwashing	53
2.4.3 Salt interactions during osmotic backwashing	58
2.4.4 Further fouling of membranes after cleaning.....	59
2.5 Conclusion.....	61
Chapter 3: Materials and methods	63

3.1 Introduction.....	63
3.2 Design, construction and testing of the forward osmosis crossflow system	63
3.3 Design, construction and testing of the reverse osmosis crossflow system.....	69
3.4 Membranes	71
3.5 Fouling solutions	72
3.6 Operation of the FO crossflow system	73
3.7 Operation of the RO crossflow system.....	74
3.8 Cleaning	75
3.9 Total Organic Carbon (TOC) Analysis.....	76
3.10 Sample Staining	76
3.11 Microscopy	77
Chapter 4: Osmotic backwashing of organic fouling on reverse osmosis membranes:	
Influence of fouling and backwashing conditions on cleaning efficiency	81
4.1 Introduction.....	81
4.2 Chemical effect of feed solution chemistry on RO fouling and cleaning	84
4.3 Physical effect of feed solution chemistry on RO fouling and cleaning	90
4.4 Effect of backwashing flux on fouling removal of RO membranes	93
4.5 Effect of backwashing with Ca^{2+} ions on organic fouling removal of RO membranes .	96
4.6 Quantitative and qualitative focus on the membrane surface and fouling layer structure	99
4.6.1 SEM-EDS	100
4.6.2 SEM element mapping	101
4.6.3 Scanning electron cryomicroscopy.....	103
4.6.4 AFM Analysis	105
4.7 Flux decline during fouling	107
4.8 Conclusion	109
Chapter 5: Investigating chemical free cleaning of organic fouling on forward osmosis membranes: Effects of fouling and cleaning conditions	
5.1 Introduction.....	111
5.2 Chemical effect of feed solution chemistry on FO fouling and cleaning.....	113
5.3 Physical effects of permeate flux on FO fouling and cleaning	121
5.4 Fouling and cleaning cycles	125
5.5 Flux decline during fouling	128
5.6 Conclusion	130

Chapter 6: Factors effecting osmotic backwashing efficiency of forward osmosis membranes subjected to initial bacterial adhesion	131
6.1 Introduction	131
6.2 Effect of osmotic backwashing draw solution concentration on bacteria removal ..	134
6.3 Effect of bacteria adhesion time on osmotic backwashing efficiency	137
6.4 Effect of CaCl ₂ in the feed solution on adhesion and backwashing efficiency	140
6.5 Use of CaCl ₂ as an osmotic backwashing draw solution for bacteria removal	143
6.6 Conclusion.....	149
Chapter 7: Conclusions and future work	151
7.1 Conclusions	151
7.2 Future Work	156
Appendices.....	163
Appendix A: Materials and methods	163
Appendix B: Calibrations.....	167
Appendix C: Scanning electron microscopy images	171
Appendix D: Scanning electron microscopy energy-dispersive X-ray spectroscopy: Spectrums	173
Appendix E: Atomic force microscopy	175
References	177

List of figures

Figure 2.1 Pressure driven membrane processes.....	32
Figure 2. 2 Osmotic pressure driven membrane process	34
Figure 2. 3: SEM images of membrane cross section	35
Figure 2.4 Effects of concentration polarisation in forward osmosis	38
Figure 3. 1: Forward osmosis cross flow system.....	64
Figure 3. 2: Illustration of the forces experienced by the membrane	66
Figure 3.3: Proof of even flow on both sides of the membrane	67
Figure 3. 4: P&ID of the FO crossflow filtration system.	68
Figure 3. 5 P&ID of the FO crossflow filtration system after it was adapted to allow 2 cells.....	68
Figure 3. 6: Reverse osmosis crossflow system	69
Figure 3. 7: P&ID of the RO crossflow filtration system.	70
Figure 3. 8: SEM Images of the Aquaporin InsideTM membrane	71
Figure 3.10: Florescence microscopy representative images	80
Figure 4. 1: Chemical effects on backwashing efficiency in RO:	84
Figure 4.2: Representative confocal images of fouled and backwashed membranes.	85
Figure 4.3: Physical effects on fouling and backwashing in RO	90
Figure 4.4: Representative confocal images of fouled and cleaned membranes.....	91
Figure 4.5: Effect of osmotic pressure in RO:	94
Figure 4.7: Backwashing swollen fouling layers in RO	99
Figure 4.8: SEM mapping	102
Figure 4.9: Cryo SEM images of the surface of the fouled and backwashing membranes.	104
Figure 4.10: Chemical effects on fouling behaviour	107
Figure 4.11: Physical effects on fouling behaviour	108
Figure 5.1: Chemical effects of fouling and cleaning in FO:.....	114
Figure 5.2: Representative confocal images of fouled and cleaned membranes.....	115
Figure 5.3: Effect of backwashing draw solution in FO	118
Figure 5.4: Effect of backwashing salt type in FO:	120
Figure 5.5: Effect of initial flux on backwashing in FO	121
Figure 5.6: Representative confocal images of fouled and cleaned membranes.....	122
Figure 5.7: Flux decline of membranes subjected to five consecutive cycles of fouling and cleaning.....	125
Figure 5.8: Flux decline of membranes subjected to five consecutive cycles of fouling and cleaning under higher permeate flux rates.	127
Figure 5.9: Chemical effects on fouling behaviour in FO	128
Figure 5.10: Physical effects on fouling behaviour in FO	129
Figure 6.1: Effect of backwashing solution concentration for cell removal in FO:	135
Figure 6.2: Effect of adhesion time on backwashing efficiency.....	139
Figure 6.3: Effect of CaCl ₂ concentration in the feed on backwashing efficiency:	141
Figure 6.4: Effect of backwashing concentration of CaCl ₂ : Microscopy results of membrane samples subjected to bacteria adhesion	145
Figure 7.1: Illustration of how backwashing could be employed to restore flux	159
Figure 7.2: Flow diagram of how osmotic backwashing could be employed in a forward osmosis and low pressure osmosis hybrid system	160

Figure B.1: Calibration of thermocouples	167
Figure B.2: Calibration of flowmeters for FO crossflow	168
Figure B.3: Calibration of flowmeter for RO crossflow	168
Figure B.4: Calibration of pressure transducers for both FO and RO crossflow	169
Figure B.5: Calibration of the TOC analyser	170
Figure C.1: Cryo SEM images of the surface of the fouled and backwashing membranes..	171
Figure D.1: SEM EDS spectra for virgin, fouled and cleaned membranes.....	173
Figure E.1: Atomic force microscopy results showing the Young's modulus for each membrane sample	175

List of tables

Table 2. 1: FO membrane specification.	36
Table 2. 2: Adhesion force data of fouling with Ca^{2+} and K^{+} ions.....	44
Table 2. 3: Summary of results from the literature on the osmotic backwashing cleaning method.....	54
Table 4. 1: Flux decline due to CaCl_2 in the fouling solution in RO	86
Table 4. 2: Backwashing flux decline due to CaCl_2 in the fouling solution in RO. The backwashing flux was determined by weighing the feed solution during backwashing and dividing the weight change by the known membrane area.	87
Table 4.3: Flux decline in RO due to initial flux. The flux decline was determined by observing the initial flux and the final flux at the end of the experiment.....	92
Table 4.4: Corresponding backwashing flux and osmotic pressure for the given backwashing solutions in RO.	94
Table 4.5: SEM EDS results: Calcium concentration produced by Carl Zeiss SIGMA HD VP Field Emission SEM and Oxford AZtec ED X-ray analysis.	100
Table 4.6: AFM force measurements of fouling on RO membranes. The adhesive force is a measure of how sticky the membrane sample is and is determined by the “pull-off” force of the silicon nitride tip of 60 nm radius AFM probe. The elastic force is a measure of how stiff the membrane sample is.	106
Table 5.1: Flux decline due to increase in initial flux in FO.....	123
Table 6.1: Backwashing fluxes for increasing NaCl draw solution concentrations in FO	134
Table 6.2: Backwashing flux values for increasing draw solution concentrations and their corresponding osmotic pressures.....	144
Table A.1: Agreeability of the feed and draw solution weight changes (ΔW).	163
Table A.2: Pressure and flowrate of cell 1 and cell 2 on the draw side and the feed side. .	164
Table A.3: Membrane surface coverage. Experiment carried out 06/06/18 to 07/06/18. .	164
Table A.4: Difference in pressure between cell 1 and cell2 at 20 bar	165

Chapter1: Introduction

Moses is responsible for the first recorded instance of desalination, where, in Exodus 15, 22-25, he throws a piece of wood into seawater which then becomes fit to drink. Today, membrane desalination is a much more complicated process, which, although a good solution to the world's serious fresh water shortage, suffers from many drawbacks. Such drawbacks include, high energy requirements and costs, [1-3], the production of high volumes of concentrated brine which requires safe disposal, [4], the use of high volumes of chemicals which also require safe disposal, [5], and high fouling propensity which results in further energy requirements, [6-9], costs and further use and disposal of harmful cleaning chemicals, [5, 10]. To optimise desalination these drawbacks need to be overcome in a sustainable way which does not lead to further problems.

Thanks to desalination, the Earth's oceans now provide 1% the population with water, a number that will continue to grow as populations increase and fresh water sources diminish, [4]. However, chemical disposal from desalination harms the very oceans that provide the water in the first place. Cleaning chemicals in reverse osmosis (RO) desalination plants include acidic or alkaline solutions of detergents, complexing agents, such as EDTA, oxidants and biocides, [11]. Lattemann and Höpner, [12], describe how these chemicals are toxic to aquatic life and ecosystems. Desalination is a rapidly growing industry due to falling costs, [13], and reductions in energy demands, [3]. Further growth of desalination will only result in more discharge of harmful cleaning chemicals into the environment. Therefore more effort needs to be put on reducing the volume of chemical waste in order to make desalination more sustainable. One way of reducing chemical disposal is through development of alternative cleaning methods that do not require harmful chemicals and are both effective and sustainable.

Forward osmosis (FO) membrane technology is a growing area of research in desalination and wastewater reclamation. FO exploits the natural osmotic gradient between two solutions of differing osmotic pressures resulting in permeation of water from the more dilute solution (called the feed solution) into the higher concentration solution (the draw solution). This results in concentration of the feed solution and dilution of the draw solution. FO can be used to reclaim water from impaired water sources and to dilute seawater as a pre-step to RO which will then require lower pressures resulting in lower

energy requirements and costs, [14]. Unlike like RO, FO requires little to no pressure and therefore has a lower fouling tendency, [15]. As well as reducing energy requirements and costs, operating RO at lower pressures will potentially result in lower fouling rates. This lower fouling propensity means that fouling in FO and RO is potentially reversible without the use of harmful cleaning chemicals.

Research into alternative cleaning of membrane processes is growing, [16-20]. These cleaning methods include osmotic backwashing which involves reversing of the direction of flux through the membrane, [20, 21], and surface flushing which involves rinsing the fouled membrane with pure water, [18, 22]. Results vary from study to study and although a lot of research has been put into understanding fouling mechanisms in membrane processes, [23-31], factors effecting osmotic backwashing and surface flushing of membranes are not well understood due to a lack of comparable research in this area. This invites the development of a comparable study on the mechanisms of fouling that will in turn affect cleaning efficiency.

In this thesis, it is hypothesised that osmotic backwashing is an efficient and sustainable cleaning method to reverse the effects of fouling on RO and FO membranes. To prove this, the factors influencing organic fouling and biofouling and how these factors subsequently impact cleaning efficiency was investigated using tools such as surface imaging and flux measurements. To achieve this, the following objectives are outlined:

- To establish an understanding of how the organic fouling mechanisms of FO and RO membrane processes influence cleaning. Factors influencing organic fouling include feed solution chemistry and initial membrane flux, [24]. How these factors subsequently impact cleaning efficiency was investigated. The effects of feed solution chemistry was tested by varying the quantity of Ca^{2+} ions in the feed solution and the initial flux was tested by varying the draw solution concentration in FO and varying the applied pressure in RO. The efficiency of osmotic backwashing and pure water surface flushing was then examined for these various fouling conditions.
- To understand how factors effecting initial bacterial adhesion in FO influence osmotic backwashing. Different backwashing concentrations were tested to determine an optimal concentration that could remove the adhered bacteria from the membrane surface. The adhesion duration and the presence of CaCl_2 in the

feed have been shown to affect initial adhesion of bacteria, [32, 33]. How these parameters influence backwashing was tested by implementing the optimal backwashing concentration.

- To understand how the backwashing solution chemistry can influence backwashing efficiency. Different backwashing salts and ionic strengths were tested for both organic fouling and initial bacteria adhesion reversal to determine how they interact with the fouling layer and to determine if these interactions hinder or aid backwashing.

In order to achieve the objectives above, this thesis is presented in 7 chapters which are outlined below:

Chapter 1: Introduction

This is a brief introduction into the motivation behind this thesis and an outline of the main objectives and how they were achieved.

Chapter 2: Literature review

This is a more detailed introduction into the background and motivation of this thesis namely the world's water shortage and current drawbacks of desalination, and a review of the literature covering fouling and cleaning of membranes. This chapter identifies research areas which either require further understanding, such as backwashing of organic fouling layers, or are lacking entirely, such as backwashing of FO membranes subjected to initial adhesion of bacteria.

Chapter 3: Materials and Methods

This work was carried out using lab-based experiments. This chapter outlines all of the experimental work that was carried out including microscopy and the setup of the bench scale systems used to carry out these experiments. The various challenges that were met during the testing of these systems and how they were overcome are also outlined.

Chapter 4: Osmotic backwashing of organic fouling on reverse osmosis membranes: Influence of fouling and backwashing conditions on cleaning efficiency

In this chapter, osmotic backwashing with NaCl was performed on RO membranes which were fouled with alginic acid under different fouling conditions to assess cleaning efficiency. Backwashing was also carried out with CaCl₂ to identify how the presence of Ca²⁺

in the backwashing solution could affect fouling removal. SEM and AFM were used to obtain an understanding of the influence of Ca^{2+} ions in the backwashing solution on the fouling layer.

Chapter 5: Investigating chemical free cleaning of organic fouling on forward osmosis membranes: Effects of fouling and cleaning conditions

In this chapter, osmotic backwashing with NaCl and pure water surface flushing of organic fouling with alginate on FO membranes was tested under different fouling conditions to assess cleaning efficiency. Backwashing with CaCl_2 was also tested to determine how Ca^{2+} ions in the backwashing solution effect fouling layers formed in FO. Several fouling and cleaning cycles were performed to test the true efficiency of osmotic backwashing as a cleaning method in FO.

Chapter 6: Factors effecting osmotic backwashing efficiency of forward osmosis membranes subjected to initial bacterial adhesion

In this final experimental chapter, osmotic backwashing with NaCl was performed on FO membranes that were subjected to different initial bacterial adhesion conditions. Backwashing was also performed using CaCl_2 solutions to see how Ca^{2+} could affect bacteria removal during backwashing.

Chapter 7: Conclusions and Future Work

Finally, the main results and conclusions from this study are discussed in this chapter. Necessary further work is discussed for each chapter as well as discussion of future research to implement osmotic backwashing of membranes in real life.

Chapter 2: Literature review

2.1. Introduction

The use of membrane technology in water treatment (e.g. nanofiltration NF), seawater desalination (e.g. reverse osmosis RO and forward osmosis FO) and wastewater reclamation (e.g. NF, RO and FO) is progressing due to water shortages across the world. However the presence of contaminants such as organic waste and bacteria can lead to one of the largest problems associated with membrane processes: membrane fouling. Fouling is the deposition of suspended or dissolved contaminants on the membrane surface. In most cases, contaminants continuously deposit onto the surface until a certain point, [9, 34]. Biofouling involves initial disposition of bacteria onto the membrane surface followed by growth of the fouling layer, [35]. Fouling leads to a reduction in performance by reducing permeate flux (e.g. Tang et al, [36], reported an over 80% decrease in flux due to organic fouling in RO) and quality (e.g. Marshall et al, [37] showed that membrane selectivity decreases with time due to increased retention of contaminants) and increasing energy consumption; a reduction in membrane lifetime, leading to membrane replacement; and increased cleaning time losses. RO membrane replacements account for 11% of operation and maintenance costs in desalination, [10]. Therefore, cleaning of membranes is an advantageous approach to tackling membrane fouling. Research into fast and effective cleaning methods for fouling removal is needed, as current methods are inefficient. Understanding fouling behaviour during operation and cleaning is hence important when optimising cleaning methods for NF, RO and FO processes.

One of the main goals in membrane research is to improve and maintain membrane performance in terms of permeate flux. However, higher fluxes exacerbate the rate and extent of membrane fouling [24]. Therefore the need to investigate effective cleaning methods is more necessary than ever. Cleaning techniques involving the use of chemicals should be avoided as they suffer from serious drawbacks. For example, ETDA, a common cleaning agent, is not biodegradable and chlorine, another common cleaning chemical, damages the active layer of the membrane [3, 6, 38, 39]. For this reason, methods to clean the membrane surface without the use of harsh chemicals are being investigated. These include surface flushing with deionised water [18, 22, 40, 41], introducing air bubbles to the feed (called air scouring), [18, 41], and salt cleaning [42, 43]. These will be discussed further

in section 2.4 of this literature review. Another promising chemical free cleaning method is osmotic backwashing [21, 44, 45]. Osmotic backwashing works by reversing the flux direction through the membrane by reversing the osmotic pressure gradient across it. More discussion is provided in section 2.4 of this literature review.

This chapter is a review of the literature on organic fouling and biofouling and cleaning of RO and FO membrane processes with a particular focus on osmotic backwashing as a cleaning method. Current methods for determining backwashing efficiency will also be reviewed.

2.1.1 Water and Energy Crisis

Potable water availability is an increasing issue owing to the world's clean water scarcity. Water strained areas possess 41% of the population [3] , and 20% of the population cannot access safe drinking water, [46]. The rapid growth of the human population, industry and agriculture, makes this challenge even more urgent. With climate change decreasing our potable water supply, drinking water regulations becoming more stringent and the amount of wastewater from industry increasing, an effective method for water recovery is needed. The source of potable water has extended from groundwater, rivers and lakes. Today, desalination of seawater and treatment of wastewater from industry are being implemented to help resolve the problem. Seawater and saline aquifers are readily available making up 97.5% of all water on Earth, causing an increase in the use of membrane desalination for potable water production, [47]. Also seawater is easily accessible and abundant. Reverse osmosis desalination makes up 60% of all desalination processes, [48]. For this reason, research into the optimisation of reverse osmosis processes is imperative to protect the world's future water security.

2.1.2 Desalination Energy Demand

In the current environmental and economic climate, a desirable desalination process should be energy efficient and inexpensive as well as effective. Membrane desalination costs 40% less per cubic metre than thermal desalination, [49] and is therefore now the dominant desalination process worldwide.

Reverse osmosis (RO) is widely used in the desalination industry. The RO process uses hydraulic pressure that exceeds the osmotic pressure of seawater and the resistance of the

membrane and acts as a driving force for mass transport through the membrane. The use of RO in seawater desalination for potable use has increased because of decreasing costs and improving technology. Robust membranes and energy recovery systems have been developed to increase the reliability of the RO desalination process, [47].

However, desalination is currently an extremely energy intensive process. The required hydraulic pressures needed for RO water permeation result in high energy demands. Additional energy is needed to maintain the required flux by overcoming the elevated osmotic pressure along the membrane due to concentration of the feed and fouling on the membrane surface. Despite recent reductions of energy consumption in RO, [47], energy costs can make up 75% of the operational cost depending on energy prices, [1] and 30-44% of the total cost of water produced, [2]. RO plants typically use from 1.6 kWh to 2.5 kWh of electricity to produce 1 m³ of water even with the use of energy recovery systems, [3]. In comparison, sources quote that 0.28 kWh, [50], to 0.217 kWh, [51], of electricity is needed to produce 1 m³ of water for conventional freshwater treatment. For this reason, efforts are being made to research ways of reducing energy requirements in RO to optimise membrane desalination.

A key factor to consider when discussing energy demand in membrane desalination is membrane fouling. Fouling still remains a severe problem in this industry as it reduces water production and therefore increases energy demand. Also involved are energy and time losses that occur due to membrane cleaning. To help reduce fouling, the water needs to be pre-treated before it reaches the RO process. Microfiltration, ultrafiltration and membrane distillation are used as a pre-treatment step in RO processes, [47]. FO is now being investigated as a possible pre-treatment step in the RO desalination process, which is discussed in the next section.

2.1.3 Wastewater treatment and reclamation

Wastewater treatment is growing in importance for two main reasons. Firstly, wastewater discharge guidelines are becoming more stringent and secondly it is a valuable resource for producing water of potable standards [47, 52]. Public perception is one main barrier facing wastewater reclamation for potable reuse and therefore in order to implement it the

development of sophisticated, trustworthy, environmentally friendly, sustainable and affordable processes are very important.

An example of water reclamation is NEWater. NEWater is high grade water from secondary treated effluent, [53]. It is researched in Singapore to provide the electronics industry with water to be further treated as ultra-pure water. Qin et al, [53] studied a membrane bioreactor and reverse osmosis process (MBR-RO), to produce consistent, high quality effluent from domestic sewage in Singapore. They reported total dissolved solids and inorganic salt (Na, F, Cl, SO₄, CaCO₃, SiO₂ and Ca) rejections greater than 98.5%. This is a very encouraging result.

Valladares Linares et al, [52], studied the use of forward osmosis to recover water that can be further treated for fresh water production from municipal wastewater and reduce its volume. They reported a retention of the nutrients nitrogen and phosphate of 56% and 99%, respectively, and 99% retention of trace metals (Cr, Mn, Ni, Cu, Zn and Pb). This is important due to environmental concerns of these contaminants.

Wastewater reclamation can be carried out while also reducing energy requirements associated with RO. Among other factors, the ionic strength of the feed water affects the energy requirements in RO desalination, [54]. Reducing the concentration of the seawater could help reduce the energy required to overcome the osmotic pressure of the seawater and this could potentially lower the cost and fouling propensity of RO. Introducing an FO step before RO could be an effective way of reducing the concentration of the feed water for the RO step and therefore lower the RO energy requirements. A nearby impaired water source could be used as the feed solution and the volume of this impaired source would in turn be reduced during FO. It has been shown that using this type of FO/RO hybrid system can also increase product recovery by 46.5% and reduce sludge volume by 47% to 72%, depending on plant size, [55]. These results are encouraging for this type of water treatment however research is still limited and therefore further studies are needed.

In our current climate of water scarcity, wastewater is a valuable resource and can no longer be ignored as alternate ways of producing water are explored. These studies mentioned are important indicators of the value of wastewater and they will be important in improving public perception of wastewater reused for potable water. Knowing how various seawater and wastewater contaminants behave during fouling and cleaning of both RO and FO are

therefore very important in optimising membrane processes and will be examined further in this literature review.

2.2 Membrane processes: Principles and applications

In this section the mechanisms and applications of various membrane processes will be outlined. An effective membrane process should have a high permeate flux per unit pressure applied, high rejection of contaminants and it should be resilient to fouling and cleaning. It should also be energy efficient and inexpensive.

2.2.1 Pressure driven membranes

Pressure driven membrane processes work by applying hydraulic pressure to the feed side of the membrane, resulting in a transmembrane pressure gradient, ($\Delta P = P_{\text{feed}} - P_{\text{permeate}}$), across it, see figure 2.1. This is the driving force that causes the permeation of water. Ultrafiltration, microfiltration, nanofiltration and reverse osmosis membrane technologies use hydraulic pressure that exceeds the osmotic pressure of the seawater and acts as a driving force for mass transport through the membrane. Only nanofiltration and reverse osmosis membranes will be discussed in this review as they are more relevant to wastewater and seawater treatment.

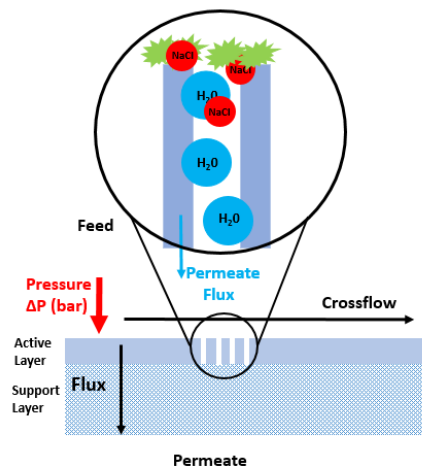


Figure 2.1 Pressure driven membrane processes

(Pore representation is for illustrative purposes)

Nanofiltration has a reported membrane pore size of $\leq 2\text{nm}$ and is used in the food and pharmaceutical industries to remove unwanted salts and organic compounds [56]. Reverse osmosis membranes are less permeable than NF membranes and have a reported pore size of 0.3 to 0.6 nm [57]. In reality membranes have a range of pore sizes, [58], and this pore

size can change with external factors such as pH, [59]. RO membrane technology is now the most widely applied water purification process for desalination and other water reclamation processes, [17]. RO technology currently dominates the desalination industry as over 60% of desalination plants are RO plants, [48]. RO can remove microorganisms and most dissolved substances from seawater and wastewater [60].

Membrane flux and rejection are defined by

$$J = L_p(\Delta P - \Delta \pi) \quad (2.1)$$

and

$$(\%)R = \left(1 - \frac{C_p}{C_f}\right) \quad (2.2)$$

Where J is the transmembrane flux, (L/m²h), L_p is the membrane permeability (L/m²hbar), ΔP is feed pressure - permeate pressure (Bar), $\Delta \pi$ is the osmotic pressure of the feed-permeate (Bar), R is the membrane rejection and C_p and C_f are the permeate and feed concentrations (M), respectively. The membrane flux equation does not account for concentration polarisation.

The most common types of NF and RO membranes are thin film composite membranes consisting of three layers, a dense polyamide active layer which is the selective layer and a porous support layer made from a polysulfone layer followed by a polyester layer which act as mechanical support for the membrane.

2.2.2 Forward Osmosis

The main downfall of NF and RO is that these processes require high pressures and therefore have high energy requirements (Recall, 1.6 kWh to 2.5 kWh of electricity is needed to produce 1 m³ of water) as well as high fouling tendencies (which are discussed in detail in section 2.3). Forward osmosis does not require the use of applied pressure for permeation. In FO, two liquids of differing osmotic pressures are separated by a water-permeable and salt-rejecting membrane. The osmotic pressure difference is the driving force for water permeation from the feed side (For example, wastewater) to the draw side (For example, seawater), eliminating the need for hydraulic pressure and thus making FO a low energy process. The solution on the draw side of the membrane is known as the draw solution (DS)

and the solution on the feed side is known as the feed solution (FS), see figure 2.2. FO can be carried out in two modes: The active layer facing the feed solution, called AL-FS mode, or the active layer facing the draw solution, called AL-DS mode.

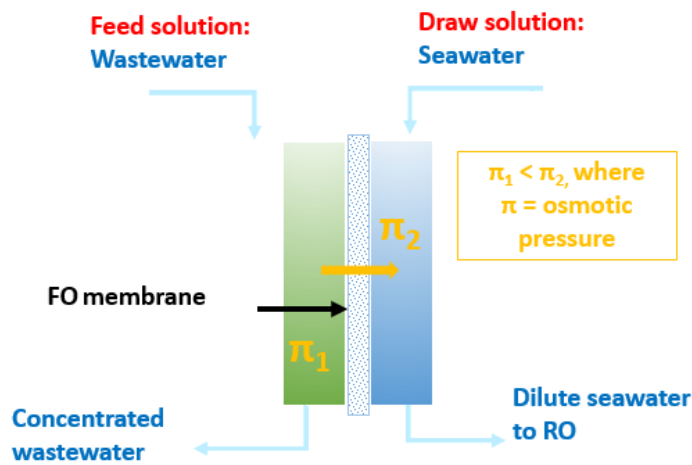


Figure 2. 2 Osmotic pressure driven membrane process

The lack of hydraulic pressure in FO compared to RO and NF suggests that the porous membrane support layer is not as important for functional support of the FO membrane. Thin film composite RO membranes can be used where a porous backing supports the polyamide active layer but membranes also exist where the polyester mesh support is embedded in the cellulose triacetate (CTA) active layer, [61], see figure 2.3. The membrane is therefore thinner and thus offers lower resistance to flux. However, the CTA membrane with the embedded support has not been shown to be superior to the traditional thin film composite membranes in terms of flux or solute rejection, (see table 2.1). Information on the CTA membrane is proprietary, but studies have shown that despite the fact that the support is embedded, the membrane is still asymmetric and therefore susceptible to concentration polarisation, (Concentration polarisation is discussed in section 2.2.3) which could explain why it is not superior, [62]. Also, results differ widely from varying sources.

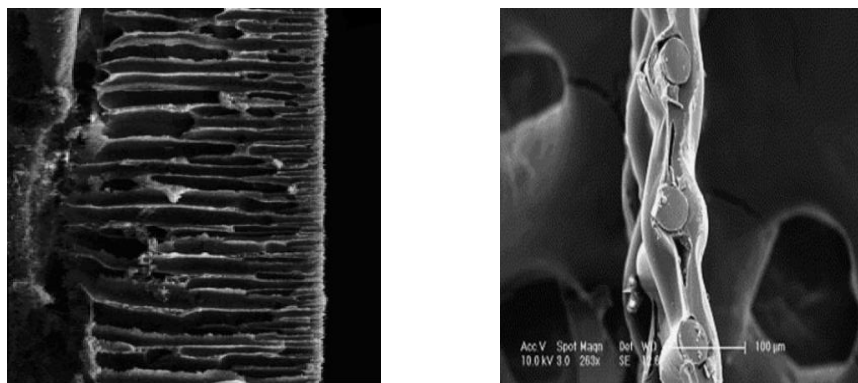


Figure 2. 3: SEM images of membrane cross section: SEM images of a dense, selective active layer and a porous support layer (left), [63], and a cellulose triacetate embedded polyester mesh support (right), [61]

Recently, the protein aquaporin has been embedded into membranes for FO. Embedding aquaporin proteins in forward osmosis membranes has been shown to improve their performance in terms of flux and rejection. A comparison between traditional membranes and aquaporin based membranes is shown in table 2.1. An investigation by Madsen et al, [64] found that aquaporin based membranes could produce a pure water flux 45% higher than traditional FO membranes and could reject over 97% of three trace organic contaminants (atrazine, 2,6-dichlorobenzamide BAM and desethyl-desisopropyl-atrazine). Although other results from the literature vary, aquaporin based membranes are shown to be competitive with traditional FO membranes, particularly the CTA membrane with embedded support. Differences in the flux and reverse salt flux measurements presented in table 2.1 are likely due to differences in experimental procedures such as temperature and crossflow velocity both of which effect flux and reverse salt flux, [65, 66]. Further research into these membranes in terms of fouling, cleaning and denaturation of the proteins in the membrane over time is necessary.

Table 2. 1: FO membrane specification. Results taken from the literature and the Aquaporin Inside™ manufacture's specifications. Results were obtained under similar conditions where the DS = NaCl. The osmotic pressure difference was 56 bar except for [67] where the osmotic pressure difference was 47.3 bar. For each test the feed solution was deionised water and the draw solution was 1 M NaCl except for [67] where the draw solution was 0.6 M NaCl.

Membrane	Flux (L/m ² h)	Reverse salt flux (L/m ² h)
Aquaporin (manufacture's specifications)	7	2.5
CTA TFC [65]	9.5	1
CTA embedded support [65]	5	2.7
CTA embedded support [67]	>9.5	5.58

FO can be used in a wide range of applications including concentration of industrial effluent, sludge liquids and landfill leachate, seawater desalination, water harvesting from municipal wastewater and the generation of osmotic power using pressure retarded osmosis, [52, 61]. FO has been proposed as a pre-treatment to the RO process to recover clean water from wastewater, simultaneously diluting seawater entering the RO step, [41]. This will lower the osmotic pressure of the seawater potentially reducing RO energy requirements. Lowering the pressure requirements of RO is also advantageous in terms of fouling. Operating at lower pressure has been shown to produce a less compact fouling layer that is easier to remove with chemical free cleaning methods, [18]. This will be discussed further in section 2.3.

Reverse salt diffusion is also an issue in FO. Draw solutions of divalent ions can lead to lower reverse salt flux, [67]. Reverse salt diffusion can affect fouling, cleaning and concentration polarisation.

2.2.3 Concentration polarisation

Concentration polarisation (CP) hinders membrane performance by reducing the flux. It occurs when the membrane active layer surface concentration differs to the bulk solution concentration such that the driving force is lower and therefore the flux is reduced, see figure 2.4. Types of concentration polarisation include, external and internal CP and cake enhanced CP.

Cake enhanced CP occurs when salts accumulate on the membrane active layer and a fouling cake layer hinders their back-diffusion to the bulk feed, [68]. This results in a higher salt concentration at the active layer surface. It causes a decrease in membrane rejection as salts go through the membrane. This was shown by Mahlangu et al, [68], who studied the effects of cake enhanced concentration polarisation on nanofiltration membranes. They reported a flux reduction of roughly 55% after 75 hours of fouling of NF270 membranes with a solution of Al_2O_3 (30 mg/L), CaCl_2 (0.5 mM) and alginate (at 20 mg/L). They reported reductions in salt rejection of over 30% due to cake enhanced CP for alginate fouling with latex in the presence of CaCl_2 . This shows the significance of cake enhanced CP with alginate fouling. Lee et al, [69], suggested that the increase in salt concentration at the membrane surface due to the fouling layer reduces the surface charge and therefore Donnan exclusion of the membrane. This therefore reduces the rejection significantly.

Forward osmosis is particularly vulnerable to CP because the concentrated draw solution is in contact with the porous support layer. In FO, internal concentration polarization (ICP) occurs in the membrane support where the solute concentration differs on the boundaries of the support layer (see figure 2.4). This reduces the osmotic pressure difference across the active layer and reduces the flux [70, 71]. Tang et al, [72], demonstrated how ICP can reduce flux in FO. A higher DS concentration will cause a higher osmotic pressure gradient and therefore a higher permeate flux, [72]. However salt accumulation in the permeate space will increase with higher DS concentrations and therefore the flux is highly non-linear with driving force due to ICP. ICP reduces the effective driving force and thus the flux. For a feed solution of 10 mM NaCl, (no foulant), draw solutions of 4 M NaCl and 0.5 M NaCl were compared. Although the initial flux was 70% higher for the 4 M NaCl draw solution, it experienced a 35 % decrease in flux over 8 hours compared to a 23% decrease in flux for the 0.5 M NaCl draw solution. The initial flux decline is controlled by the dilutive concentration polarization on the feed side, which, is controlled by the osmotic permeation rate. This means the higher draw solution becomes increasingly inefficient due to ICP, [67, 72].

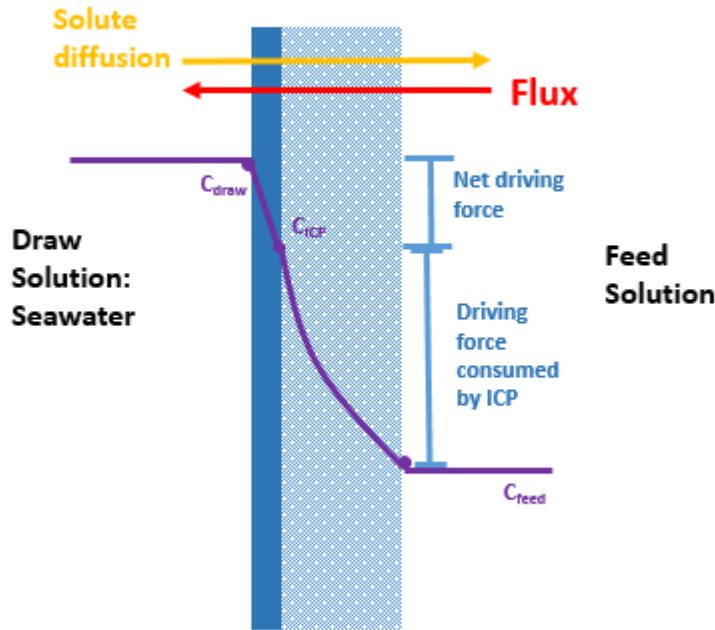


Figure 2.4 Effects of concentration polarisation in forward osmosis: The accumulation of salt in the active layer-surface layer interface decreases the overall driving force for permeate flux.

Possible methods for mitigating the effects of concentration polarisation include increasing crossflow rate on the membrane surface and increasing the solution temperature. Jin et al, [66], showed that the effects of concentration polarization decrease with increasing temperature as the solute diffusivity increases with temperature. They produced a model based on RO membranes at various temperatures. They produced a concentration polarisation factor, CP, of the membrane where

$$CP = \frac{\text{solute concentration in the membrane}}{\text{solute concentration in the feed}} \quad (2.3)$$

They found that CP decreased significantly with increasing temperature: the CP factor decreased from 3.03 to 2.17 when the temperature was increased from 15 to 35 °C. This is due to an increase in diffusivity of the solute ions at higher temperatures. However, increasing solution temperatures is not a feasible solution in water treatment as it will result in high energy demands and therefore increase costs. Increasing the crossflow rate will also help mitigate the effects of CP. This is because the extra shear force and turbulence across the membrane helps to equilibrate the salt concentration at the membrane surface, [36, 73]. Tang et al, [36], showed that the initial flux of ESPA3 membranes increased from 1.9 to 2.2 m/day when the crossflow rate was increased from

20 to 35 cm/s. As with increasing temperature, increasing crossflow velocities will require higher energies and therefore increase costs.

Increasing the temperature may not mitigate ICP in forward osmosis processes.

McCutcheon and Elimelech, [71], studied the influence of temperature on external and internal concentration polarisation experimentally in FO with NaCl feed and draw solutions. They showed that temperature did not mitigate the effects of ICP significantly. They increased the temperature of the FS and DS with the aim to increase the diffusivity of the solutions. At higher diffusivities, the salts can move in and out of the porous support more readily and so that the effect of ICP is less severe, [74]. However increasing the temperature also increased the flux and as ICP increases exponentially with flux, the effects of ICP prevailed and the temperature increase had a negligible effect in AL-DS mode.

As with CP in pressure driven processes, ICP in FO can be mitigated by increasing the crossflow rate on the membrane. Tang et al, .increased the initial flux of a reverse osmosis membrane, ESPA3, by 14% when the crossflow velocity was increased from 20 to 35 cm/s [36]. Hancock and Cath, [65] examined CP in FO and showed that the crossflow velocity on both sides of the membrane affects the external CP and the crossflow velocity in the DS affects the internal CP of the support layer which in turn affects the rate of reverse salt flux (Reverse salt flux is discussed in the next section). Higher crossflow velocities resulted in higher fluxes as increasing the FS velocity dilutes the reverse diffusing DS salts more rapidly and therefore decreasing the concentration at the feed boundary layer. This increases the chemical potential gradient across the membrane and therefore the flux increases. Also, lower feed crossflow velocity resulted in higher concentrative external CP effects. At the same time, when the DS velocity is low, the dilutive external CP in the support side is more severe and the flux is reduced.

It is therefore possible to reduce the effects of CP as much as possible by determining optimal crossflow rate and temperature.

2.2.4 Reverse salt diffusion

Bidirectional diffusion of solutes occurs in FO. The reverse diffusion of salts from the draw solution through the membrane to the feed side due to the concentration difference of solutes limits FO performance. For this reason it cannot be ignored when examining flux decline in FO processes. It is determined by Fick's law, [75]:

$$J_s = B\Delta c \quad (2.4)$$

Where J_s is the flux of an individual solute ($\text{mol/m}^2\text{h}$), B is the solute permeability coefficient, (m/h), and Δc is the trans-membrane concentration difference (mol/m^3).

Therefore reverse salt flux depends on the solution chemistries of both the FS and DS, the permeability and selectivity of the membrane and hydrodynamic conditions such as the crossflow velocity of both the FS and DS.

Lee et al, [15], reported cake-enhanced osmotic pressure (CEOP) due to reverse salt diffusion from draw solution to the feed is the prevailing factor affecting flux decline in FO rather than an increase in resistance due to fouling after conducting organic fouling experiments which compared FO and RO. This also means that the solutes lost from the DS will need replenishment and their presence in the FS may lead to environmental challenges during disposal, [65]. Also, in the case of substances containing polysaccharides in the FS, if the DS contains ions such as Ca^{2+} that can diffuse into the FS, cross linking will occur between Ca^{2+} ions and the alginate molecules on the membrane surface and this will worsen fouling, [30, 76].

Internal concentration polarisation and external concentration polarisation also affect reverse salt flux. In AL-DS mode, dilution in the porous support occurs and the solute concentration differential, the driving force for reverse salt flux, is reduced. It was shown that MgCl_2 is a weaker DS than NaCl and therefore MgCl_2 caused reverse salt flux 25-30% slower than NaCl , [65]. This is due to the higher viscosity, larger molecule size and lower diffusivity of MgCl_2 which make it harder for the solutes to diffuse in and out of the porous support and therefore the effects of ICP are lower, [73]. This results in lower reverse salt flux. However, as already stated, although the MgCl_2 salts will reverse diffuse at a lower rate, divalent salts will interact with organic fouling layer. Zou et al, [76], demonstrated how Mg^{2+} ions in their forward osmosis draw solution interacted with the algal biomass

fouling layer. They showed that fouling was more rapid with a draw solution of 0.5 M MgCl_2 compared to 2 M of NaCl .

Hancock et al, [65] showed that electrostatic effects also influence reverse salt flux. They tested a NaCl draw solution while varying the feed. Feed solutions used were MgSO_4 , CaSO_4 , K_2SO_4 , H_3BO_3 , NH_4HCO_3 and $\text{Ba}(\text{NO}_3)_2$. They found that for each feed solution the reverse diffusion of the sodium and chloride was equal-molar with the exception of the $\text{Ba}(\text{NO}_3)_2$ case where the chloride diffused much faster than the sodium. They conclude that as the small polar nitrate ion readily diffuses through the membrane, the larger barium ion diffuses much slower causing a charge imbalance that is restored by faster reverse diffusion of the Cl^- to maintain the charge balance of the two solutions. The bi-directional diffusion of the salts in the FS and DS is accompanied by the bi-directional diffusion of hydrogen ions (H^+) and hydroxide ions (OH^-), [65].

Hancock et al, [65] also studied the permeability and selectivity of the membrane and its effect on the reverse salt flux. They used two membranes; CTA-1 with a thin film composite structure and CTA-2 with a cellulose triacetate polymer and an embedded woven polymeric support mesh layer. Forward flux of calcium was 88% lower and reverse flux of NaCl was 82% lower with a CaSO_4 feed for CTA-1. CTA-1 was the less permeable, more selective membrane and therefore produced a lower rate of diffusion in both directions. Information on the CTA membranes are proprietary and therefore it not known if the different results for permeability and selectivity are due to the structure of the support or the thickness or porosity of the active layer, all of which can affect permeability.

Reverse salt flux also affects fouling reversibility. This was studied by Boo et al, [25] who compared the high reverse salt diffusion effects of NaCl draw solutions with low reverse salt diffusion effects of LaCl_3 draw solutions in colloidal fouling. For experiments performed with draw solutions of LaCl_3 , colloidal fouling was nearly 100% reversible. However, with the NaCl draw, the colloids combined in the high salt concentration due to reverse salt diffusion and the flux was not recovered. The reverse diffusion of NaCl resulted in destabilization/aggregation of the colloidal particles resulting in the formation of a cake layer that was more difficult to remove. Therefore reverse salt flux is a key factor that should be considered when optimising membrane cleaning. Choice of the draw solution should take into consideration the effects of reverse diffusing ions as they can exacerbate fouling.

2.3 Fouling

Where there is filtration, there is fouling. Membrane fouling is an unavoidable problem that affects all membrane processes involving any feed source. Fouling is unavoidable due to the presence of contaminants in freshwater, groundwater, wastewater and seawater. As already stated, fouling results in the reduction of permeate flux and product quality and increase in energy consumption and maintenance costs (membrane cleaning and replacement). The type of fouling depends on the water source but often includes mineral, colloidal, organic, inorganic and biofouling.

This literature review will focus on organic fouling and biofouling with particular focus on initial bacterial adhesion. Organic fouling includes polysaccharides, proteins, humic substances and fatty acids and are found in many wastewater sources such as the food industry [44] and produced water from the oil and gas industry [77]. Biofouling is fouling of a microbial gel-like cake layer with self-produced extracellular polymeric substances (EPS) which encase live and dead microbial cells. It is primarily composed of polysaccharides and proteins, [78].

A lot of research has been carried out on the different factors that contribute to organic fouling. Factors affecting organic fouling include the solution chemistry (e.g. monovalent and divalent ion concentration, pH, organic matter concentration) and the physical conditions under which fouling occurs (e.g. initial membrane flux, crossflow rate, applied transmembrane pressure, membrane materials, the presence and size of spacers or draw solution in FO processes). These key factors will be examined in this section.

Membrane biofouling has been recorded at length in the literature, [78-82] however in terms of initial membrane bioadhesion, little work has been done so far, [79, 83, 84]. This section will focus primarily on bioadhesion and the factors which influence it, which include cell surface hydrophobicity, [83], crossflow velocity, salt rejection, membrane surface roughness, free energy of adhesion, electrostatic double layer repulsion, [84], feed-water composition, permeate flux and conditioning layers, [79]. These will be studied in this section.

2.3.1. How solution chemistry influence organic fouling

Fouling initially occurs when the foulant adheres to the membrane surface (foulant-membrane energy of adhesion). The fouling develops further when foulants adhered to the membrane surface interact with foulants in the bulk feed solution (foulant-foulant energy of cohesion), [17]. It is the foulant-foulant interactions that are responsible for the characteristics of the fouling layer such as thickness and compactness, [30]. The solution chemistry of the feed can affect the intermolecular forces and adhesion forces governing the rate and extent of fouling, [30]. The characteristics of the fouling layer are important as they govern its impact on permeate flux, salt rejection, cake-enhanced concentration polarisation and its ability to be removed from the membrane surface.

Wastewater containing organic matter including polysaccharides and inorganic salts presents a huge problem in wastewater treatment. The presence of monovalent cations (such as K^+) and divalent cations (such as Ca^{2+}) in the wastewater worsen organic fouling and this has been shown numerous times in the literature [24, 30, 85, 86].

Lee and Elimelech, [30] studied alginate fouling of RO membranes and its relation to foulant-foulant adhesion forces. They found that for alginate fouling, the adhesion forces between the foulants on the membrane surface and the foulants in the bulk solution were highest in the presence of Ca^{2+} ions. Carboxyl groups present in alginate fouling form complexes with Ca^{2+} , forming what is known as the “egg box model”, neutralizing the negative charge of alginate molecules, resulting in a thick compact gel fouling layer on the surface of the membrane, [23, 34].

They found that the presence of divalent ions in the feed reduced the flux significantly and as the concentration of calcium was increased, the flux declined more. In the absence of divalent cations the flux reduced from 72 L/m²h to 68.4 L/m²h after 15 hours of fouling. A concentration of 0.05 mM $CaCl_2$ caused a flux decline of 25% (from 72 to less than 54 L/m²h). A concentration of 1 mM $CaCl_2$ caused a flux decline of 65% (from 72 to less than 25.2 L/m²h). Calcium ions had a much larger effect on the flux decline than the Mg^{2+} ions where the flux only decreased by 10% (72 L/m²h to 64.8 L/m²h). They found that this exacerbated fouling could be due to charge neutralization when the Ca^{2+} ions form complexes with alginate carboxyl groups and this results in a thick compact gel layer.

Research by de Kerchove and Elimelech, [85], also showed complexation of calcium ions with alginate, however they also studied how monovalent ions can govern fouling. In the presence of calcium, the alginate gel layer swelled (became thicker but weaker) with an increasing potassium (K^+) concentration. Without calcium, increasing the KCl concentration from 0 to 300 mM resulted in an increase in fouling layer thickness from 2.5 to 12.5 nm. In the presence of calcium, increasing the KCl concentration from 0 to 100 mM resulted in an increase in alginate layer thickness from 25 to > 150 nm. However when the KCl concentration was further increased from 100 to 300 mM the fouling layer thickness either did not change significantly (increased from 150 to 175 nm) or decreased from 150 nm to 50 nm. These experiments show the instability of the alginate fouling layer in the presence of calcium at high ionic strengths.

In terms of adhesion forces in the presence of calcium, alginic acid fouling displayed stronger adhesion forces at low ionic strength (3 mM KCl). As the concentration of KCl increased from 3 to 300 mM, forces decrease by 83%. The adhesion forces in this study were quantified with AFM and the results are summarised in table 2.2. Strong adhesion forces at low KCl concentration are due to Ca^{2+} ions forming complexes with alginate carboxyl groups. Increasing the KCl concentration increases competition between monovalent K^+ and divalent Ca^{2+} cations in the gel layer. Therefore the adhesion bonds are weaker. The ion exchange is responsible for gel “swelling” and therefore increase in gel thickness. This stretches and weakens the gel structure and could break up the fouling layer by the release of microscopic sheets, [16, 85]. This ion exchange is the basis for salt cleaning, (Outlined in section 4.3). This ion exchange needs to be considered when performing osmotic backwashing as monovalent cations come in contact with the fouling layer during backwashing. Backwashing is discussed in section 4.2.

Table 2. 2: Adhesion force data of fouling with Ca^{2+} and K^+ ions. Taken from [85].

Ca^{2+} concentration (mM)	K^+ concentration (mM)	Adhesion force (F/R) (mN/m)
0	3	-0.05
0	300	-0.05
1	3	-1
1	300	-0.03

The presence of divalent cations has a similar effect on humic acid (HA) fouling according to two studies by Tang et al [36, 86] and Lee and Elimelech [30]. Tang et al, [36], fouled RO and NF membranes with humic acid and used TEM to characterise the fouling. Permeate flux depended on humic acid concentration, operating pH, ionic strength, and calcium concentration. For NF270 membranes, increasing humic acid feed concentration from 2 mg/L to 5 mg/L resulted in a 19% greater flux decline over 96 hours. Increasing the Ca^{2+} concentration from 0 to 1 mM resulted in an increase in flux reduction from 35% to 85% over 96 hours. In a similar study, [86] the total amount of humic acid accumulated on the membrane surface was determined after fouling with and without Ca^{2+} ions. An increase in Ca^{2+} concentration from 0 to 1 mM resulted in an increase in HA fouling on the membrane surface of $30 \mu\text{g}/\text{cm}^2$ to $200 \mu\text{g}/\text{cm}^2$. Therefore the presence of Ca^{2+} ions in humic acid fouling also hinders membrane performance in terms of flux resulting from humic acid accumulation on the surface. This is because, as with alginic acid fouling, calcium binding occurs between the Ca^{2+} ions and the carboxyl groups among the humic molecules resulting in a cross linked fouling layer which inhibits flux, [34]. Lee and Elimelech, [30], observed that the presence of Ca^{2+} ions is worse in alginate solutions as they observed roughly 80% greater adhesion forces with alginate than with humic fouling. They attributed this to the larger size and stronger gel-forming tendency of alginate. It is believed that the stronger tendency to form gels is more common with hydrophilic organic molecules, such as the case of alginate molecules.

The feed solution pH also influences the adhesion and formation of the fouling layer such that decreasing the pH will worsen the effects of fouling, [30, 36, 86]. A lower feed pH results in higher foulant-membrane and foulant-foulant adhesion forces resulting in severe fouling, [30]. Tang et al, [36], observed a 37% greater flux decline when the feed solution pH was decreased from 8.5 to 4.5 over 96 hours of fouling with humic acid fouling. A decrease in pH from 7 to 4.5 resulted in an increase in HA accumulation on the membrane surface of $<25 \mu\text{g}/\text{cm}^2$ to $250 \mu\text{g}/\text{cm}^2$, [86]. Lee and Elimelech, [30], observed similar results with alginic acid fouling where a 15% greater flux decline was observed when the feed solution pH was decreased from 9 to 3. These results show that lowering the pH reduces the solution molecule charges therefore reducing electrostatic repulsion between molecules resulting in enhanced fouling.

Another important factor that can affect the chemistry of the fouling layer is reverse salt diffusion in FO processes. As already stated in section 2.4, divalent salts in the draw solution can reverse diffuse into the fouling layer and exacerbate fouling, [76]. Reverse salt diffusion can also change the pH of the feed solution. The bi-directional diffusion of the salts in the FS and DS is accompanied by the bi-directional diffusion of hydrogen ions (H^+) and hydroxide ions (OH^-), [65]. Hancock and Cath, [65] determined that the reverse flux of hydrogen ions and hydroxide ions from the DS to the FS did not occur at the same rate and therefore can result in a change in pH of these solutions. The pH of the FS decreased when it was made up of $MgSO_4$, $CaSO_4$ or K_2SO_4 solutions. This could mean that the H^+ ions diffused from the DS to the FS. Conversely, the pH of the FS increased when it was made up of boric acid or sodium silicate solutions. For this reason, in FO processes, the solution chemistry of the draw solution is also an influencer of fouling and cannot be ignored.

2.3.2 Physical fouling conditions

As well as solution chemistry, the physical aspects of fouling conditions, i.e. factors such as temperature, crossflow velocity and applied pressure, greatly influence the rate and extent of fouling in membrane processes.

Controlling operating temperatures in any large scale processes such as desalination and wastewater treatment is very difficult, costly and energy intensive. For this reason, the effects of temperature on membrane fouling is not widely researched. However, just as the solution temperature greatly influences the effects of concentration polarisation, as outlined in section 2.3, it also influences fouling. Jin et al, [66], studied humic acid fouling of nanofiltration membranes at temperature of 15, 25 and 35 °C. For an NF90 membrane, the flux decreased by 15% at 25 °C and 35 °C and by 25% at 15 °C, which may be explained by the colloidal size. They found that the size of humic acid colloids decreased with temperature and therefore the effects of fouling were higher. Interestingly, they also determined that the mass of humic acid deposited on the membrane remained relatively constant at around $1 \times 10^{-3} \text{ KgC/m}^2$ for all three temperatures tested. This suggests that the fouling layer became denser as the size of the colloids decreased and therefore the flux reduction was higher.

Crossflow velocity is a major influencer in membrane fouling as it affects both the initial flux and the fouling accumulation. Tang et al, [36], fouled RO and NF membranes with humic

acid and used TEM to characterise the fouling. ESPA3 membranes were fouled with humic acid at two different crossflow rates: 20 cm/s and 35 cm/s. The initial flux was 14% higher for the cross-flow rate of 35 cm/s. After 96 hours of fouling, the flux decreased by around 10% for both crossflow rates. The increase in initial flux is due to the reduction in concentration polarization at the higher cross-flow rate, (see section 2.3), this should result in a higher fouling rate due to higher permeation drag but the increase in the shear rate mitigates the fouling effects by reducing build-up on the membrane. Seidel and Elimelech, [87], showed how increasing the crossflow rate will reduce organic fouling in nanofiltration. For a constant initial flux of 16.9 $\mu\text{m/s}$ a flux decline of over 70% was reported for a crossflow rate of 4 cm/s compared to a flux decline of 50% for a crossflow rate of 40.4 cm/s under the same conditions. This shows that the higher crossflow rate results in a higher shear rate that can help slow fouling on the membrane surface.

Seidel and Elimelech, [87], also showed how increasing the initial flux will increase the fouling rate. For a constant crossflow velocity of 4 cm/s, an initial flux of 16.6 $\mu\text{m/s}$ resulted in a flux decline of almost 80% compared to an initial flux of 5.6 $\mu\text{m/s}$ which resulted in a flux decline of less than 20% under the same organic fouling conditions. A higher initial flux will result in a high fouling rate as the permeation drag perpendicular to the membrane is higher and therefore can overcome the electrostatic repulsion between the organic foulant and the membrane surface.

Mi and Elimelech, [24] studied organic fouling in FO with alginic acid, humic acid and bovine serum albumin. They found that, before a fouling layer is formed, both chemical and physical conditions affect fouling. However, once the fouling layer has developed, further changes in chemical and hydrodynamic conditions no longer affect it. Applied pressure can further enhance the organic fouling layers and this is outlined in the next section.

2.3.3 Impact of hydraulic pressure on organic fouling

Operating pressures have a high impact on organic fouling. Lower operating pressures lead to less compact, thicker fouling layers that may be easier to remove (this will be outlined in section 2.4). At higher applied pressures, organic fouling layers have been shown to be more compact, [87].

As to whether osmotic pressure will produce different fouling properties to applied pressure, experiments by Mi and Elimelech [18] showed that fouling occurs at similar rates

in the presence of hydraulic or osmotic pressure. They applied 28 bar across two cellulose membranes, one using hydraulic pressure and the other using osmotic pressure (i.e. DS = 4 M NaCl). The initial flux and the rate of membrane flux decline was similar in the two modes. In RO mode the flux decreased from 29 L/m²h to < 15 L/m²h. In FO mode the flux decreased from 29 L/m²h to < 12 L/m²h. However, the fouling layer characteristics varied between the two pressure modes. For FO processes, no applied pressure is required and therefore the fouling layer structure was loose and less compact than the thin, dense fouling layer formed in hydraulic pressure driven processes, [15, 18]. The actual difference in thickness has not yet been quantified in the literature, however Mi and Elimelech, [18], used adhesion force data to prove that the fouling layer formed in FO is easier to remove using shear force (outlined in section 2.4).

In the case of RO and NF technology, the applied pressure greatly affects the initial flux and the rate of fouling, [36]. Tang et al, [36], fouled NF270 membranes with humic acid for 96 hours and compared applied pressures of 13.8 bar and 6.9 bar. The pressure of 13.8 bar yielded an initial flux of 200 L/m²h and a flux reduction of 33% over 96 hours. The pressure of 6.9 bar yielded an initial flux of only 95 L/m²h however the flux reduction was negligible. These results are expected as the higher flux will lead to a faster rate of fouling.

By increasing the flux, and therefore the drag force, foulant-membrane and foulant-foulant interaction forces can be overcome resulting in significant fouling, [86]. This is reported by Tang et al, [86] who fouled BW30 with humic acid. They reported that an increase in initial flux from 1.17 to 2.16 m/day resulted in an increase in humic acid accumulation from 8 to 23.6 µg/cm³ due to the higher drag force.

The results discussed in this section show that higher fluxes are not always advantageous as they lead to higher rates of fouling and therefore cleaning time losses will increase. Balancing energy requirements and costs as well as cleaning costs and time losses is necessary for optimal membrane performance.

2.3.4 Bacteria adhesion and Biofouling

The accumulation and growth of bacteria and other microorganisms in the membrane, known as biofouling, is particularly severe due to the strong adhesion of the microorganisms to each other and to the membrane surface and the excretion of exopolymeric substances (EPS) resulting in the formation of a biofilm, see figure 2.5, [8, 88].

EPS is made up of polysaccharides, proteins, nucleic acids, lipids, and other polymeric compounds, [89]. The biofilm coats the membrane surface, resulting in greater resistance to flux and therefore disrupting the membrane performance.

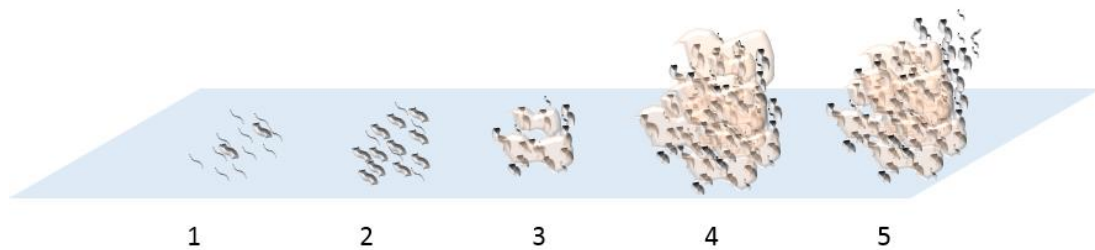


Figure 2.5: Illustration of bacteria attachment and biofilm maturation on a surface adapted from, [90]. 1: Initial bacterial adhesion. 2: Cells aggregate forming micro colonies and EPS. Here adhesion becomes irreversible. 3: Biofilm is formed in multi-layered clusters. 4: Further maturation and protection of the biofilm. 5: The biofilm reaches a critical mass and starts to colonize further.

As with organic fouling, the extent of biofouling will depend on both chemical and physical factors such as permeate flux, temperature, crossflow rate, solution chemistry and pH. The effects of permeate flux and solution chemistry will be discussed in this review.

In terms of initial adhesion of bacteria, some important factors that influence adhesion are, the membrane properties, [79, 91, 92], the initial membrane flux, [93], the feed solution chemistry, [33, 94] and the properties of the cells themselves, [95]. Semião et al, [93], showed that increasing the flux of BW30 membranes from 5 to 20 L/m²h resulted in an increase in adhesion as the membrane surface coverage increased from less than 5% to greater than 25% with adhesion of *Pseudomonas fluorescens*. van Loosdrecht et al, [95], showed that that hydrophobic cells had higher adhesion rates than hydrophilic cells. These factors may affect the further biofouling.

Although effects of biofouling in forward osmosis have been reported, research so far is quite limited, particularly work on initial adhesion. Kwan, et al, [80], reported a 10% flux decline for FO membranes biofouled with 2x10⁶ CRU/ml *Pseudomonas aeruginosa* for 18 hours. Yoon et al, [81], reported a 20% reduction in flux due to biofouling for 55 hours with 10⁷ CRU/ml of the same bacteria. Zhang et al, [82], reported an over 45% flux decline due to biofouling of a forward osmosis membrane bioreactor due to a combination of organic fouling and biofouling.

Kwan, et al, [80], compared biofouling under applied pressure and osmotic pressure. Their experiments were carried out under the same conditions and resulted on a 10% flux decline for FO which was significantly lower than a 30% flux decline for RO. They showed that FO biofilm layers were loose, thick and “mushroom-shaped”, while RO biofilms were tight layers with larger amounts of EPS per cell. The compact RO biofilms resulted in greater osmotic pressure and hydraulic resistance than FO, resulting in the higher flux decline. Yoon et al, [81] also compared biofouling in FO and RO. Under identical conditions, biofouling in FO resulted in a 20% decrease in flux compared to a 50% decrease in flux for RO. This shows that different driving forces i.e. osmotic pressure for FO and hydraulic pressure for RO has a significant impact on biofouling. These experiments were carried out at the same permeate flux showing that it is the pressure and not the flux that effects the fouling layer. Kwan et al, [80], suggest that the high pressures involved in RO generate a pressure gradient across the biofilm. This pressure gradient causes the biofilm structure to compact into a tight structure of shrunken channels and pores. This does not occur in FO due to the lack of pressure.

As well as the physical effects of pressure, the solution chemistry will have a profound effect on the rate and extent of initial adhesion and biofouling. Calcium ions have been shown to affect *Pseudomonas putida* and *Pseudomonas fluorescens* biofilms, [33, 96]. Safari et al, [33], reported a 61% increase in bio volume of *P. fluorescens* biofilm formed in the presence of 15 mM of CaCl_2 compared to no CaCl_2 . Fetcher, [97], reported that the addition of cations decreased the cell-surface separation distance as the cations reduce the repulsive force between the negatively charged cells and the negatively charged membrane surface therefore increasing adhesion. It is not just the physicochemical interactions that influence adhesion but also the function of the bacteria cells. Ca^{2+} has been shown to bind with the protein LapF, a key protein for the initial attachment secreted by *Pseudomonas putida*, and form large aggregates in biofouling, [96].

Martínez-Gil et al, [96], reported that the influence of Ca^{2+} on *P. Putida* attachment was time dependant and noted that it took 24 hours to observe significant influence of calcium on the bacteria. This suggests therefore that it is the decrease in repulsive negative forces between the cells and the membrane surface that a causes the increase in adhesion as it was only carried out for 30 minutes.

These results prompt the need for more research into bacteria adhesion and biofouling in forward osmosis and also into the development of efficient and cost effective cleaning techniques to restore membrane performance and prolong membrane life.

2.4 Cleaning

As already shown, fouling is an inevitable limitation in membrane processes and therefore fouling control is a worthwhile way of optimising the process. The development of cleaning techniques for membrane processes is needed to remove the fouling layer and reverse its effects. Currently, various methods of cleaning are carried out and both chemical and chemical free cleaning methods exist. These include chemical cleaning with chlorine and detergent solutions, [29, 40, 42, 98], physical cleaning by increasing the cross flow rate, air scouring and rinsing the membrane with deionised water, [18, 25, 41, 99] and osmotic backwashing, [19, 21, 52, 100, 101]. As already stated, chemical cleaning can harm the environment and damage the membrane [3, 38]. Therefore mainly chemical free cleaning methods will be reviewed further.

2.4.1 Membrane surface flushing

Physical cleaning efficiency by surface flushing either by increasing crossflow rate or flushing with deionised water varies widely with the type of process (RO or FO) and the type of fouling (Organic or biofouling).

Experiments by Mi and Elimelech [18] showed that fouling occurs at similar rates in both RO and FO fouled membranes. However due to the difference in fouling layer characteristics, the cleaning efficiency of alginate fouled membranes in the presence of calcium ions varied widely between RO and FO fouling modes. They used surface flushing with deionised water and recovered 98% of the initial flux of forward osmosis membranes and 70% of the initial flux of RO fouled membranes. The fouling reversibility of FO was attributed to the less compact organic fouling layer formed in FO mode. Due to the lack of hydraulic pressure, the fouling layer formed during FO operation is less dense than that formed during RO and therefore much easier to remove. This shows that the surface flushing cleaning method is much more suitable for FO processes. Surface flushing combined with another cleaning method may reverse fouling in RO.

Zhang et al, [82] who reported an over 45% flux decline due to biofouling of a forward osmosis membrane bioreactor alleviated fouling using surface flushing. They used intervals of 15 minutes of tap water rinsing to mitigate the biofouling but after approximately 70 hours of fouling this method was no longer effective. This shows that other cleaning

methods deemed effective after short fouling durations may need to be tested after longer durations to determine if/when they become ineffective. Mi and Elimelech, [18], only performed fouling for 20 to 24 hours and therefore longer fouling durations may have resulted in fouling that could not be reversed by surface flushing. Several fouling and cycles necessary to test the true efficiency of a given cleaning method.

Physical cleaning by simply increasing the crossflow velocity experiments were performed by Lee et al [15]. They restored only 70% of the initial flux of RO membranes fouled with alginic acid in the presence of Ca^{2+} . They report that this is due to the compact dense structure of the fouling layer caused by the hydraulic pressure applied to the membrane during fouling. Yoon et al, [81], fouled FO membranes with 10^7 CRU/ml of *Pseudomonas aeruginosa* in the presence of 10 mM NaCl and 1 mM CaCl_2 . They also used physical stress with increased crossflow rate from 4 to 33 cm/s. However this method did not work and the flux was not restored.

The literature presented on surface flushing is not comparable from study to study and therefore it is difficult to determine the factors affecting it and whether it is truly efficient or not. This invites further studying on surface flushing as a potential cleaning method or membrane processes.

2.4.2 Osmotic backwashing

Osmotic backwashing is another promising way of reversing membrane fouling while potentially avoiding the environmental issues and membrane damage associated with chemical cleaning. With osmotic backwashing, the flux is reversed from the draw side to the feed side either by switching the circulating solutions or by injecting a pulse of high salt concentration to the feed side. This minimizes discharge of cleaning chemicals to the environment and potentially allows for full recovery of the initial flux.

The method of osmotic backwashing has been investigated in RO, [19, 21, 42, 45, 102] and in FO, [17, 25, 44, 77, 99, 103, 104]. In both RO and FO, the results of osmotic backwashing methods to remove fouling and restore flux have been inconsistent and are summarised in table 2.3.

Table 2. 3: Summary of results from the literature on the osmotic backwashing cleaning method

Reference	Feed Solution	RO/FO	BW Duration (minutes)	% of initial flux restored
[102]	Artificial wastewater with <i>Pseudomonas aeruginosa</i>	RO	50-60 second pulse	80 – 90%
[43]	Alginate and Pectin	RO	15 to 60 minutes	90 - 110%
[42]	Sodium alginate	RO	15 minutes	80%
[19]	Alginic acid	RO	10 minute pulse	93-97%
[52]	Synthetic Wastewater	FO	12 hours	0%
[99]	SWWE from the city of Jeddah	FO	-	0%
[100]	CaCl ₂ (3.88 g/l), Na ₂ SO ₄ (2.84 g/l) and NaCl (1.11 g/l) with 130% saturated CaSO ₄	FO	60	0%
[77]	Drilling wastewater	FO	30	100%
[104]	Filtered centrate	FO	10	81% for cycles 1 and 2
[17]	Alginate NaCl, CaCl ₂ , and MgCl ₂	FO	15	100%, 99% and 93% for cycles 1, 2, 3
[103]	5 g/L meat extract, 1 g/L C ₆ H ₁₂ O ₆ , 0.6 g/L (NH ₄) ₂ SO ₄ , and 0.14 g/L K ₂ HPO ₄ . Between 1 and 2 g/L NaHCO ₃	FO	60	90%
[105]	Concentrate from RO desalters	FO	20	94% and 84% for cycles 2 and 3 (cycle 1 was cleaning with EDTA)
[44]	Olive Mill Wastewater	FO	30	95%
[106]	Hydraulic fracking flowback	FO	30	95% CTA membrane 82% TFC membrane 78% TFC membrane

The different fouling layer structures and effects of ICP mean that backwashing efficiency differs between RO and FO and depends on the feed solution composition.

In RO, osmotic backwashing can be induced by introducing a pulse of high concentration solution to the feed side causing the osmotic pressure on the feed side to exceed the hydraulic pressure applied to the membrane and thus the permeate flow is reversed. Ramon, Nguyen et al, [19] did this to examine the use of osmotic backwashing to clean RO membranes. Backwashing compared well with chemical cleaning. Backwashing restored 93% to 97% of the flux depending on the pH and cleaning with EDTA restored 100% of the flux. Both methods restored more flux than physical cleaning with deionised water (66%). The combination of chemical and physical cleaning is an effective removal method. Chemical cleaning loosens the foulant layer, and physical cleaning removes it by shear force.

Tow et al, [16] fouled SW30HR RO membranes with alginic acid and 1 mM CaCl_2 and used backwashing and an increase in crossflow velocity to remove the fouling layer. This restored 80% of the initial flux but the amount of fouling remaining on the membrane surface was not quantified. The efficiency of backwashing alone without increasing crossflow was not tested and therefore it is not known if backwashing individually was as efficient and to what extent the increase in crossflow improved backwashing efficiency.

Lee and Elimelech, [43], found that cleaning organic fouled RO membranes with a 100 mM solution of NaCl for 15 minutes at a crossflow of 42cm/s restored 90% of the flux. Ang et al, [42], also discussed salt cleaning in organic fouled RO membranes and reported similar results. They used 500 mM NaCl for 15 minutes to remove a fouling layer of alginate molecules in the presence of 0.5 mM Ca^{2+} . This restored over 80% of the initial flux. When DI water was used, only 19% of the flux was recovered. This is because the compact gel linked network in the fouling layer is strong enough to withstand the shear force of the DI water flow.

Valladares Linares, Li et al, [99], identified from LC–OCD chromatographs that backwashing effectively removed an alginate fouling layer from the membrane however it did not restore the flux. After hollow fibre membrane fouling experiments with a feed solution of synthetic municipal wastewater, they soaked the membrane in 4% NaCl while recirculating deionised water before performing backwashing. However, the flux did not improve in either AL-FS or AL-DS modes. This could be due to the diffusion of salt into the FO membrane during fouling and osmotic backwashing. The diffused salt remaining inside the membrane leads to differing solute concentrations at the boundaries of the support layer.

This causes internal concentration polarisation and reduces the osmotic driving force. In AL-FS mode, dilutive ICP occurs and in AL-DS mode concentrative ICP occurs, [73]. This means that there are also potential CP effects during cleaning that might hinder flux restoration, and not the fouling itself, which is why it is important to use visualisation techniques as well as flux measurements when testing backwashing efficiency.

Arkhangelsky et al, [100], also studied osmotic backwashing in hollow fibre FO membranes and compared it to hydraulic backwashing. The FO membranes were scaled with CaCl_2 (3.88 g/L), Na_2SO_4 (2.84 g/L) and NaCl (1.11 g/L) with 130% saturated CaSO_4 in AL-DS mode. After the flux decreased by about 30%, they reversed the orientation of the membrane for the osmotic backwash step. Like Valladares Linares, Li et al, [99] they concluded that osmotic backwashing in FO was ineffective at restoring flux due to reverse salt flux where the salt from the DS accumulated inside the pores of the support layer during cleaning.

In contrast to these studies, Hickenbottom, et al, [77], effectively used osmotic backwashing to reverse the effects of fouling in FO. They used drilling waste water from a shale gas field as a feed solution and NaCl as a draw solution. After fouling in AL-FS mode, the diluted DS was replaced with deionised water, while the FS remained unchanged. After osmotic backwashing, the FS was flushed with clean water. This successfully restored the water flux and removed the fouling layer from the surface.

Holloway, et al, [104], also showed that backwashing is effective. They studied the use of FO in concentration of anaerobic digester centrate. The FS was raw centrate or filtered centrate and the DS was 70 g/L NaCl. The membrane was in AL-FS mode. Osmotic backwashing was then performed with 50 g/L NaCl as the FS and DI water as the DS. Four fouling experiment cycles and three cleaning cycles were performed. The initial flux was $10.5 \text{ L/m}^2\text{h}$ and at the start of the second cycle it had fallen to $9 \text{ L/m}^2\text{h}$. Cleaning by osmotic backwashing was then performed after cycle 2 and the flux was returned to $9 \text{ L/m}^2\text{h}$. Flux decline was much slower following the backwashing cycles than after no cleaning. An increase in backwashing time did not improve flux. They suggest that, during osmotic backwashing, foulants in the pores of the support layer are removed while the cake layer may partially remain on the active layer. When the fouling is resumed, the cake layer blocks the recurrence of pore plugging which results in a slower flux decline after osmotic backwashing.

Achilli, et al, [103], studied backwashing in FO, its influence on flux recovery and reverse salt transport in a novel osmotic membrane bioreactor. They fouled the membrane with meat extract and background electrolytes in AL-FS mode. To implement backwashing, the FS was replaced with 5 g/L NaCl and the DS was replaced with double deionised water. The DS was 50 g/L NaCl. They found that backwashing was effective in restoring only 50% of the lost flux. Backwashing did not have a significant influence on reverse salt transport. For a new membrane, the reverse salt transport was 7.7 g/m²h and for a used membrane that had been backwashed the reverse salt transport was 6.3 g/Lm²h. This reduction is due to any fouling that remains on the membrane after cleaning which resists the reverse salt flux, [103].

It is necessary to foul and clean the same membrane numerous times to determine the true efficiency of a cleaning method. Motsa, et al, [17] used osmotic backwashing to clean organically fouled membranes where divalent cations were present. To implement this, the DS (NaCl of varying concentration) was replaced with ultrapure water. The FS contained varying concentrations of sodium alginate, Mg²⁺ and Ca²⁺. Like Hickenbottom, Hancock et al, [77], they found that backwashing could restore the flux by effectively removing the gel fouling layer. Backwashing restored 100%, 99% and 93% of the flux after cleaning cycles 1, 2, and 3 respectively. They also reported reversing the CP profile and restoring the membrane charge.

Limited information is provided on osmotic backwashing of biofouled membranes in the literature. Yoon et al, [81], who fouled FO membranes with 10⁷ CRU/ml of *Pseudomonas aeruginosa* in the presence of 10 mM NaCl and 1 mM CaCl₂, induced osmotic backwashing by replacing the feed with 4 M NaCl and the draw with deionised water but as with tap water flushing, the flux was not restored.

These studies show that osmotic backwashing restores the initial flux to varying extents in FO due to concentration polarisation and fouling layer characteristics. All experiments vary widely from study to study and therefore a fundamental understanding is needed. These results invite a systematic study on conditions affecting osmotic backwashing of fouled membranes such as hydrodynamics and feed and draw solution characteristics using comparable conditions. Understanding these effects could advance the optimisation of osmotic backwashing in membrane processes.

2.4.3 Salt interactions during osmotic backwashing

It is worth discussing salt interactions when discussing osmotic backwashing. During osmotic backwashing, the salts of the draw solution come into contact with the fouling layer giving rise to the conditions under which salt cleaning occurs. The mechanisms behind salt cleaning with a monovalent solution (e.g. NaCl or KCl) involve membrane swelling and ion exchange between the Ca^{2+} ions in the alginate layer and the Na^+ or K^+ which will break up the calcium bridging between the foulant molecules that strengthen the fouling layer. These structural changes to the fouling layer make it easier to physically remove as the alginate molecules are freed from the swelled gel layer, [43]. This occurs in backwashing and coupled with the reverse permeate drag can make for a very effective cleaning method depending on the feed solution and cleaning parameters.

Mi and Elimelech [18] investigated salt cleaning and surface flushing for FO fouled membranes. They compared the cleaning efficiency of DI water and a 50 mM NaCl solution. Both resulted in almost 100% flux recovery, showing that ionic strength does not affect the cleaning efficiency in FO but it is the physical removal of the fouling layer. This is because in FO the alginate layer on the membrane is less compact than that in RO and shear force can effectively remove the fouling and therefore ion exchange to weaken the fouling layer may not be necessary. However, the feed solution only contained 0.5 mM CaCl_2 . The amount of Ca^{2+} ions present greatly affects the structure of the fouling layer. The higher the Ca^{2+} concentration, the stronger the fouling layer is due to more severe gel networks and it is more difficult to remove, [30]. Therefore, at higher Ca^{2+} concentrations, the use of DI water alone may not be enough to effectively remove the fouling layer and salt cleaning may be more effective.

The influence of salt cleaning on alginate fouling in FO was investigated by Motsa et al [17]. The FS contained varying concentrations of sodium alginate, Mg^{2+} and Ca^{2+} and the DS contained NaCl of varying concentration. They flushed NaCl and CaCl_2 solutions on both sides of the membrane after fouling (therefore preventing backwash), this achieved 88%, 81% and 81% flux recovery in fouling cleaning cycles 1, 2 and 3 respectively. When both sides of the membrane were flushed with deionised water, (no salts), 98%, 93% and 91% flux recovery was achieved for cycles 1, 2 and 3 respectively. This agrees with [18] as it shows that while salt cleaning could improve flux, it was clearly the physical removal of the

fouling layer by the shear force of the cross flow fluid that restored the flux and not the ion exchange reaction.

This suggests that during backwashing in FO, it is the reverse permeate drag that is the prevailing factor, affecting the backwashing efficiency however the choice of backwashing salt and its strength could have a significant impact on the fouling layer due to interactions in the fouling layer.

2.4.4 Further fouling of membranes after cleaning

How well the membrane is cleaned will determine the fouling behaviour in subsequent fouling of the membrane, [18, 44, 106]. Mi and Elimelech [18] used AFM to compare cellulose acetate and polyamide membranes and proved that the composition of the membrane surface is extremely important in determining fouling behaviour. Adhesion force data showed that even a small percentage of adhesive sites on the membrane surface can increase membrane fouling potential and decrease cleaning efficiency. The cellulose acetate membrane had a maximum adhesion force of 1.2 mN/m. However the adhesion data of the polyamide membrane was higher with 18% of the adhesion forces distributed in the range of 1.2–2.0 mN/m. For this reason initial fouling rates were 14% higher for the polyamide membrane, (The flux decrease by 45% in the first 4 hours of fouling).

This result is very important when considering how cleaning efficiency can affect further membrane fouling. Any organic matter not removed from the membrane surface during cleaning may aggravate subsequent fouling. As shown by Lee and Elimelech, [30], adhesion forces are proportional to fouling rate, (Section 2.3.1). Mi and Elimelech [24] also found that the rate and extent of organic fouling depends heavily on foulant-foulant interactions (Section 2.3.2). The average foulant-membrane adhesion force was 0.35 mN/m (between a carboxylate modified latex probe and a clean FO membrane (CTA, HTI)) while the average foulant-foulant adhesion force was 0.66 mN/m (for alginate fouling with 200mg/L alginic acid in the presence of 0.5mM Ca^{2+}). This suggests that any foulant not removed from the membrane surface by cleaning will exacerbate further fouling.

For this reason, restoration of pure water flux alone is not enough to prove that the performance of the membrane has been restored. Images of the “cleaned” membrane surface, and quantification of the adhesion forces of the “cleaned” membrane are also necessary to prove if the membrane performance has been restored. Subsequent fouling

and cleaning tests must be carried out to determine if fouling remaining on the surface will lead to worsened fouling effects.

2.5 Conclusion

As the earth's population faces a huge water crisis, sustainable and environmentally responsible processes to produce potable water need to be developed as a matter of urgency. Membrane desalination can offer this but efforts are still needed to reduce energy consumption and costs. In an attempt to do this, membrane fouling has been examined in order to understand its mechanisms and develop ways to reduce it and remove it effectively. A sustainable cleaning method for RO and FO membrane processes is needed to improve performance and extend membrane life.

Organic fouling of RO, and recently FO, membranes has been studied by many in order to understand the mechanisms behind it and the chemical and physical operational parameters affecting it. The operational pressure and also the type of pressure (osmotic or applied) will affect the fouling layer structure in terms compactness and thickness, [15, 18, 36, 87]. Also the feed solution chemistry, particularly the presence and strength of divalent ions such as Ca^{2+} due to cross linkage with alginates, will have a great influence on the rate and extent of fouling, [24, 30, 85, 86].

Research into biofouling and particularly bioadhesion is very limited in FO, [79, 80, 107]. It has been shown that Ca^{2+} ions influence biofilms and therefore the presence of CaCl_2 in the feed solution will greatly influence fouling behaviour, [33, 96]. Magnitude and type of pressure also greatly affects biofouling, [108], but little is known about how it affects initial adhesion in FO, and hence even less on the impact on cleaning, namely backwashing.

While extensive research has been carried out in RO membrane fouling, cleaning via backwashing is still limited, [16, 19, 42, 43, 102]. Investigations into FO fouling has increased in the past number of years and although its more reversible fouling layer has resulted in a lot of research in chemical free cleaning, the methods used and therefore the results vary widely, as summarised in table 2.3. Research into backwashing of bioadhesion in both membrane processes remains extremely limited, [81]. Studies on numerous fouling and cleaning cycles are also limited, [18, 44, 106]. These types of studies are a very effective way of determining the true efficiency of cleaning.

The current studies on membrane cleaning are not comparable and therefore the factors that influence cleaning are not easily identified. Differences between studies such as the membrane type, fouling duration, fouling solution chemistry, membrane flux, cleaning

duration and cleaning method mean that it is difficult to get an understanding of what makes a cleaning method effective or ineffective.

An area that lacks research is the use of multiple fouling and cleaning cycles to verify cleaning efficiency. This research is important as in real membrane processes, fouling reversibility will need to be sustained for numerous fouling and cleaning cycles in order to prolong the life of the membrane and reduce replacement time losses and costs.

An area even more lacking in research is the reversal of initial bacteria adhesion on membranes. Biofouling is notoriously difficult to remove even with the use of cleaning chemicals, [109]. Therefore implementing cleaning methods before biofouling has a chance to develop may be an effective way of keeping biofouling at bay.

Under the right conditions, osmotic backwashing has great potential in the control of both RO and FO processes. In order for this to be effective, investigations using consistent experiments are necessary to examine backwashing efficiency. The structure of the fouling layer, the pressure (applied or osmotic) of the operation, the duration of fouling, the duration of backwashing, how backwashing salts affect the fouling layer are all important factors that will affect the cleaning efficiency.

Chapter 3: Materials and methods

3.1 Introduction

In order to examine the efficiency of osmotic backwashing in forward osmosis and reverse osmosis membrane processes, several types of membranes, filtration equipment, analytical instruments and microscopes were used. Determining of the backwashing efficiency was based on both pure water flux measurements and quantitative measurements of fouling layer characteristics before and after fouling and cleaning. This chapter outlines the various analytical equipment used, the experimental protocols employed and the design, construction and testing of the bench scale cross flow systems.

In order to carry out the experiments, custom forward osmosis and reverse osmosis bench scale rigs were designed, constructed and tested. Designs were based on bench scale setups reported in the literature, [34, 107, 110] and optimised based on extensive pre-testing that was carried out to ensure consistent and reproducible results could be obtained. Both the RO and FO membranes used were commercial membranes purchased from Filmtech™ and Aquaporin Inisde™ respectively.

Optical, electron and atomic force microscopy was used for both qualitative and quantitative analysis of the membranes and the fouling layer structure and behaviour. Total organic carbon analysis and ion chromatography were also used to analyse the product water.

3.2 Design, construction and testing of the forward osmosis crossflow system

All forward osmosis experiments were carried out in a custom built forward osmosis bench scale rig, as shown in figure 3.1.

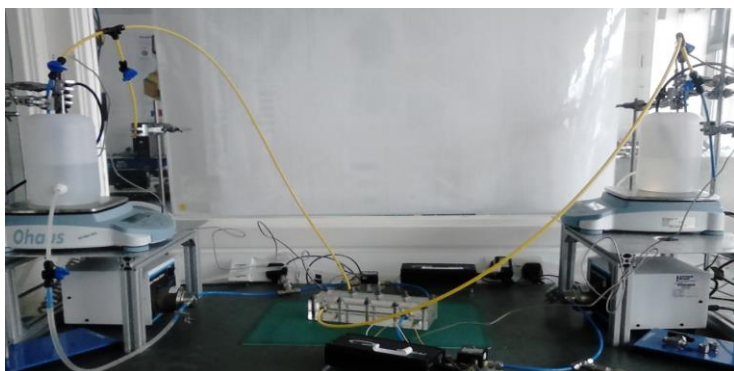


Figure 3. 1: Forward osmosis cross flow system

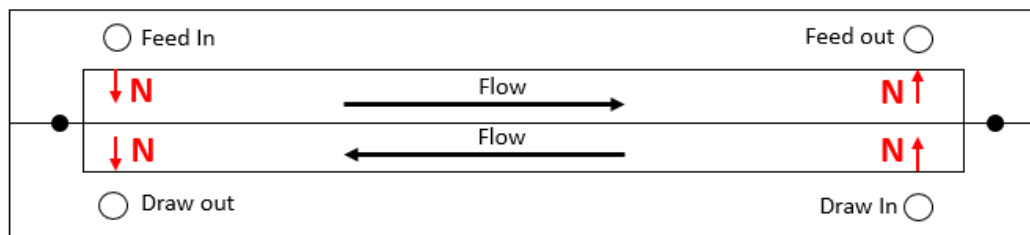
There were several key factors to consider when designing the FO crossflow rig. The flux is recorded by weighing the draw solution. This involves weighing a tank that is attached to the rest of the rig which poses difficulties as it is challenging to achieve an accurate recording. This is because an accurate weight of an object can only be recorded when the object is completely isolated from external forces like vibrations which is not possible with this set-up. One method employed in the literature is the use of an overflow system where, as the draw solution volume increases, it overflows into a separate beaker which is weighed on a balance [104, 105]. This method is, however, also imprecise as the transmembrane flux is not enough to overcome the high surface tension of the water and the overflow is sporadic and slow. Therefore the increase in weight of the overflow beaker over time is not accurate.

Elsewhere in the literature, in order to measure the flux, some studies measure the weight change of the feed solution [17, 100] and others the draw [52, 77, 103]. Measuring the weight loss of the feed means weighing both the weight of the water that has permeated the membrane and the fouling layer that has deposited on the membrane surface. This is therefore an inaccurate representation of flux and therefore should not be used. Therefore, in this study, the weight gain of the draw solution was used to measure flux as it is more accurate than measuring the weight loss of the feed solution.

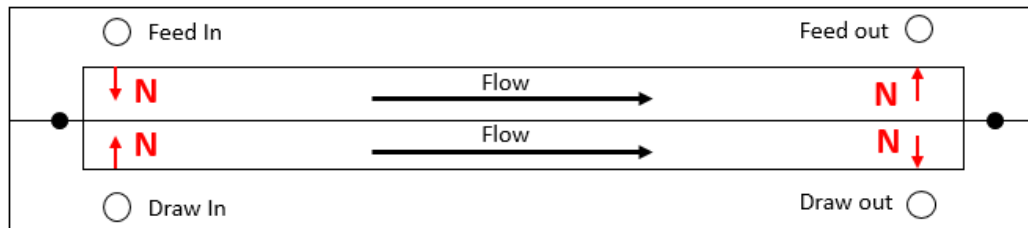
Once it was established that weighing the draw solution is the best approach to measure flux, it was necessary to overcome the inaccuracy of weighing the draw solution tank which is subjected to the external vibrations of the rig. It was determined that an effective way to do this is by isolating the tank as much as possible, i.e. not allowing any tube or measuring device to come into contact with the tank by using clamps. The outlet however was

attached to the tank and it was determined that using a rigid outlet tube attached to a flexible tube instead of an entirely rigid tube resulted in more accurate results due to fewer vibration effects, see figure 3.1. Both the feed and the draw solutions were measured during pure water flux tests. This means that weight loss due to fouling build-up would not occur. It was found that the weight loss of the draw and the weight gain of the feed were within 5% of each other, therefore showing that this method is accurate. Results are shown in Appendix A. The entire rig was set up on a marble slab to reduce any external vibrations.

Another factor to consider is whether to use co-current or counter-current flow, see figure 3.2. In co-current mode, both the feed and draw solution enter the membrane cell from the same end, figure 3.2.B. In counter-current mode, they enter at opposite ends, Figure 3.2.A. The counter current mode is theoretically more efficient as the osmotic pressure change remains constant along the membrane cell [111]. This orientation therefore has been applied in the literature [17, 104]. However, in practice the counter-current flow orientation posed challenges. This is illustrated in figure 3.2.A. As both liquids enter the cell the force of the flow causes the membrane to become strained and comes in contact with the channel wall therefore reducing the effective membrane area. Motsa et al. [17] combatted this by using a shorter channel length and therefore reducing the membrane area. However, a smaller membrane area will result in a lower permeate rate and therefore less accurate results. Co-current flow is widely reported in the literature [24, 77, 110] as it decreases the stress on the membrane in the cell, illustrated in figure 3.2.B.



A Force on membrane = $2N$



B Force on membrane = 0

Figure 3. 2: Illustration of the forces experienced by the membrane in counter-current (A) and co-current (B) flow orientation. The image shown is a cross section of the elevation of the membrane cell.

To further show that even flow was delivered on both sides of the membrane humic acid was used to visually observe that the membrane was not forced against the channel wall in co-current flow, as shown in figure 3.3.

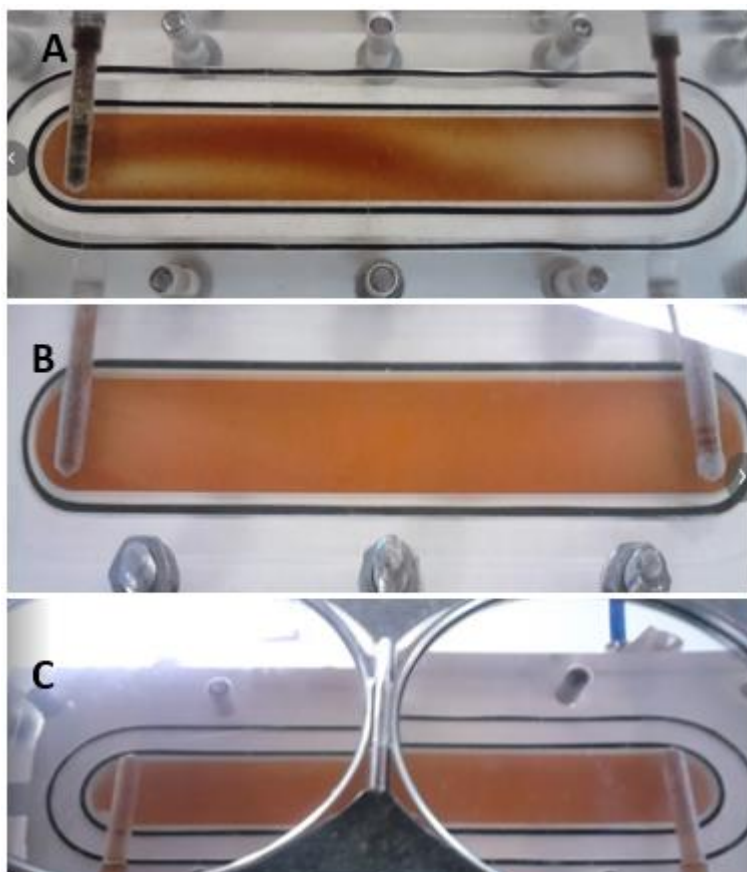


Figure 3.3: Proof of even flow on both sides of the membrane. The humic acid fouling solution shows that counter-current flow (A) puts the membrane under strain at the inlet and outlet as the flow is uneven. Co-current flow delivers even flow across the channel (B). B shows the feed side and C illustrates the draw side of the cell underneath. This shows that there is even flow on both sides of the membrane (B & C).

Two variable speed gear pumps (Cole Parmer, Vernon Hills, IL) delivered constant flow from two reservoirs for feed and draw solutions and backwashing solutions to a custom built Perspex membrane cell. Later this system was adapted to accommodate two membrane cells in parallel, as shown in figure 3.5. The gear pumps were used to control the crossflow rate and delivered a constant crossflow for the duration of each experiment. To ensure the flow split evenly and both cells were delivering even flow, the flowrate and pressure of both the inlet and outlet lines of both the feed and draw sides were tested. Calculations (Appendix A) showed that the flowrate in both lines were within 6% of each other and the pressure in each tube was within 1% of each other, hence showing that the flow divided evenly to produce accurate results. Bioadhesion tests were also carried out where both cells were fouled with *Pseudomonas putida* for 30 minutes. The surface coverage was determined to be the same for both cells showing even distribution of the flow. These

results are shown in Appendix A. Piping and instrumentation diagrams of the FO systems are shown in figures 3.4 and 3.5.

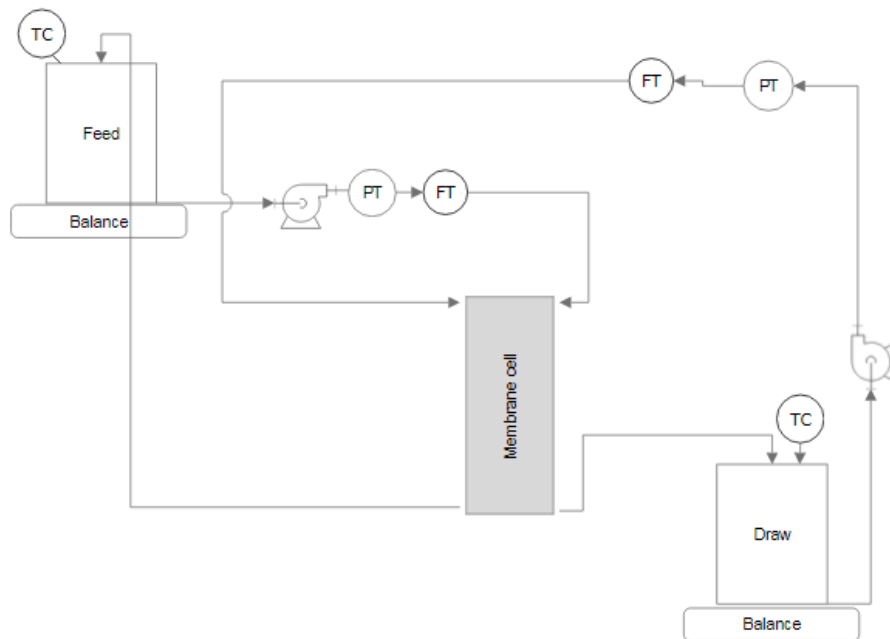


Figure 3. 4: P&ID of the FO crossflow filtration system.

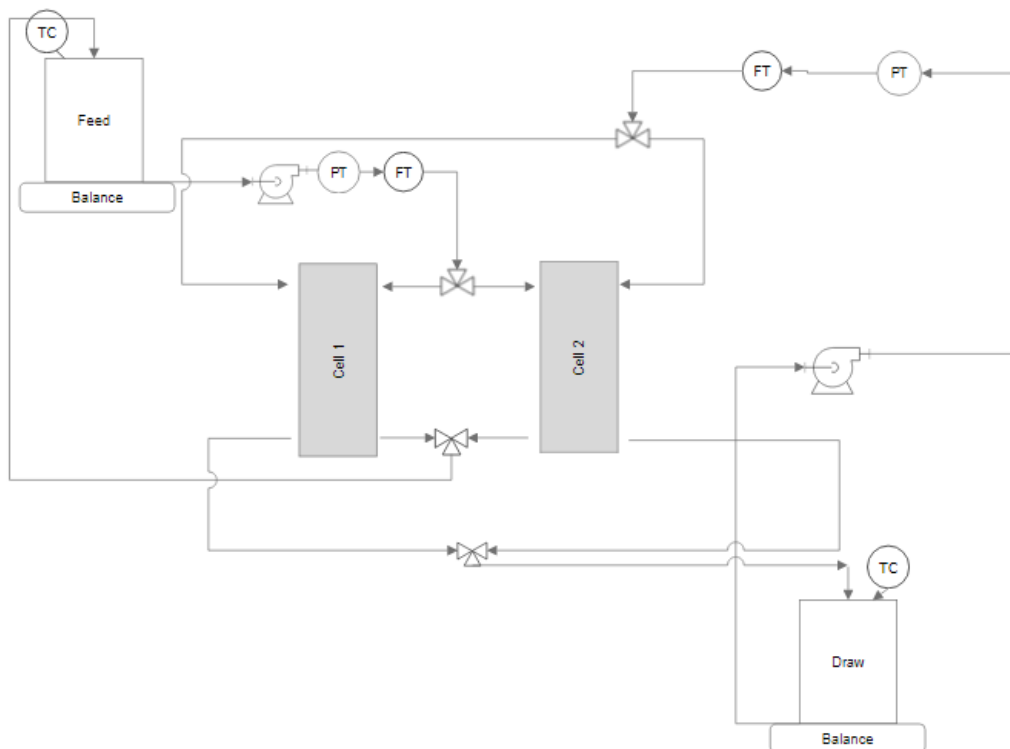


Figure 3. 5 P&ID of the FO crossflow filtration system after it was adapted to allow 2 cells.

The temperature was maintained at $20 \pm 1^\circ\text{C}$ by a cooling bath. The operating temperature can affect the fouling of the membrane (see Chapter 2) and also evaporation needs to be avoided as it will result in inaccurate weight (and therefore flux) measurements. The FO membrane cell had an effective membrane area of 0.0048 m^2 (width 25 mm, length 191 mm) and the membrane was placed between two 3 mm channels for the draw and feed solutions. Each line was fitted with one flowmeter and one pressure transducer to monitor flow conditions. Each tank contained one thermocouple to monitor temperature and one conductivity meter to measure reverse salt flux. These measuring devices were all calibrated (see Appendix B). The conductivity, temperature, pressure and flowrate of the feed and draw solutions were logged with a DAQ 54 Omega data logger (Omega, UK).

3.3 Design, construction and testing of the reverse osmosis crossflow system

All reverse osmosis experiments were carried out in a custom built, stainless steel reverse osmosis bench scale rig, as shown in figure 3.6.

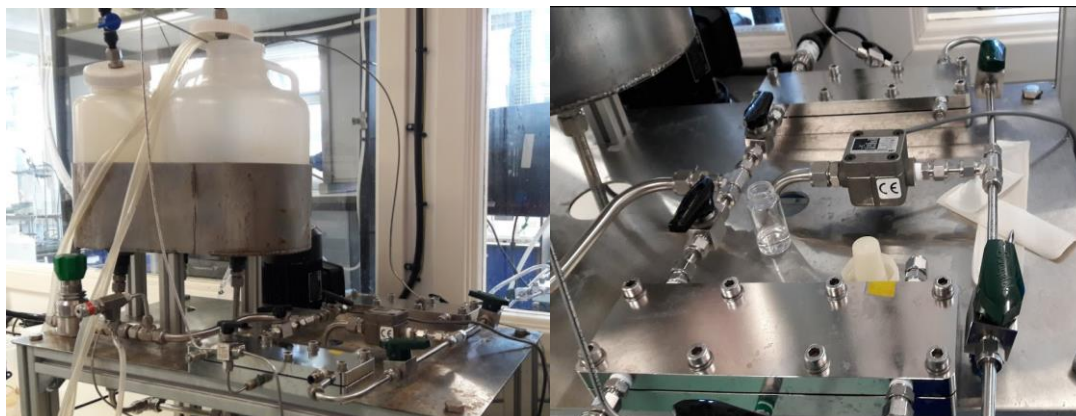


Figure 3. 6: Reverse osmosis crossflow system. Left: View of fouling and backwashing tank. Right: View of membrane cells.

One diaphragm pump delivered constant flow from three reservoirs for feed solutions, backwashing draw solutions and deionised water to two stainless steel membrane cells in parallel. The crossflow rate could be controlled by the pump and delivered a constant flowrate throughout the fouling experiment. A piping and instrumentation diagram of the system is shown in figure 3.7.

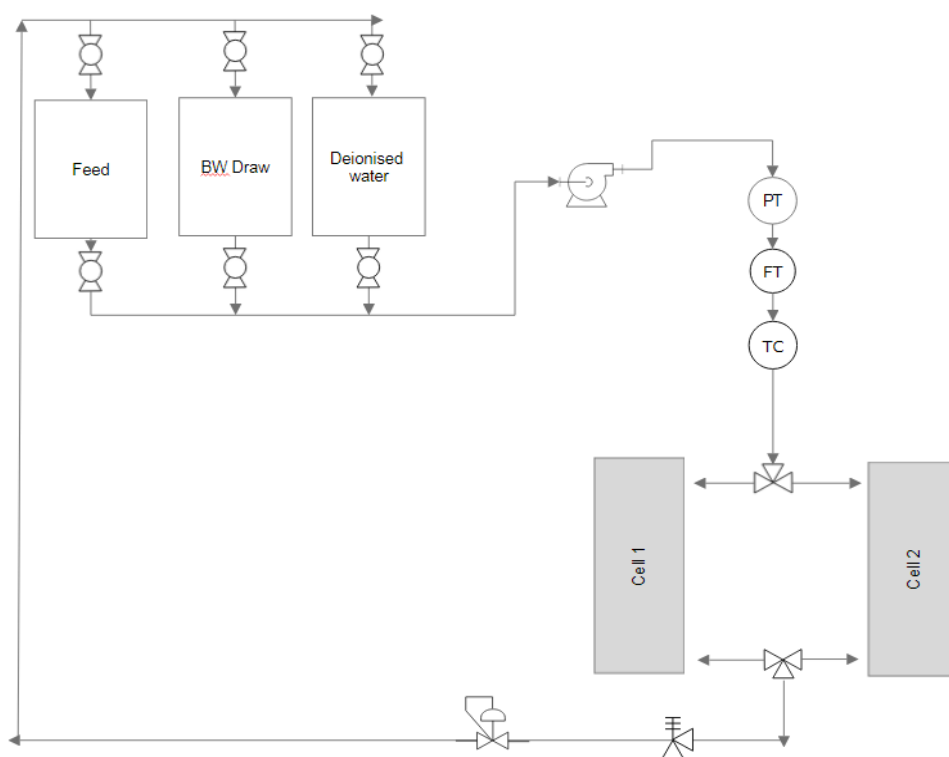


Figure 3. 7: P&ID of the RO crossflow filtration system.

The cross flow was maintained at 0.9 L/min/cell. To ensure the flow was split evenly between the two cells, one pressure transducer was placed on each cell. Calculations (Appendix A) showed that the pressure in both cells were within 3% of each other hence showing that the flow divided evenly to produce accurate results.

A back pressure regulator (Swagelok, UK) was used to vary the pressure applied to the membrane. The temperature was maintained at $20 \pm 1^\circ\text{C}$ by a cooling bath. Each RO membrane cell had an effective membrane area of 0.0048 m^2 (width 25 mm, length 191 mm) and a channel height of 3 mm. The rig was fitted with one flowmeter, one thermocouple and one pressure transducer to monitor flow conditions. Each tank contained one conductivity meter to measure reverse salt flux and the pH of the feed solution was tested before and after each fouling run. As with the FO system, these measuring devices were all calibrated (see Appendix B). The temperature, pressure and flowrate of the feed and draw solutions were logged with a DAQ 55 Omega data logger (Omega, UK).

A pressure relief valve (Swagelok, UK) was fitted before the back pressure regulator to prevent over pressure.

3.4 Membranes

Forward osmosis membrane: Aquaporin Inside™

For all forward osmosis experiments, a commercial, aquaporin based membrane was used, (Aquaporin Inside™, Denmark). This is a thin-film composite membrane, consisting of a polyamide active layer containing aquaporin proteins, an intermediary polyester layer, and a non-woven polyester support layer. It is approximately 4-5 mm thick. SEM images of the dense active layer and porous support layer are shown in figure 3.8.

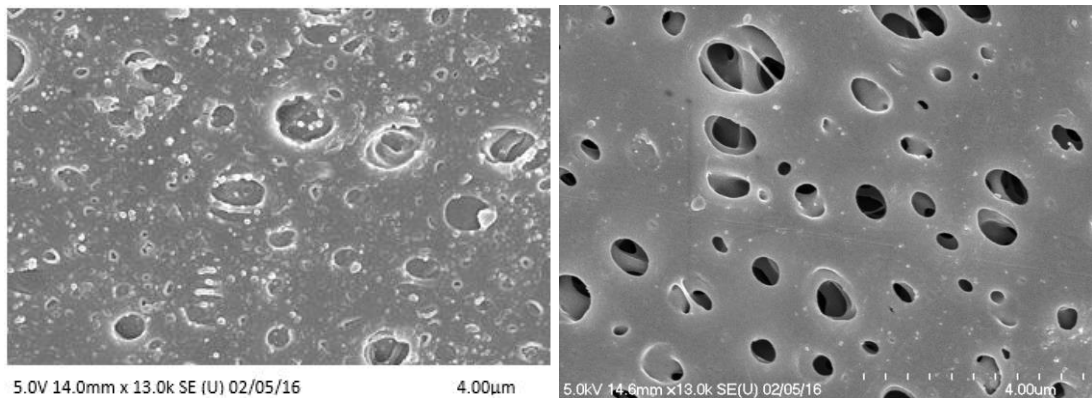


Figure 3. 8: SEM Images of the Aquaporin Inside™ membrane. Active layer (left) and support layer (right) of the aquaporin based membrane.

Aquaporin proteins are selective water channel forming proteins added to the membrane to enhance its flux [112]. Water molecules are transferred through the aquaporin protein pore and ionic species are rejected. Investigations have determined a pure water flux of $> 9 \text{ L}/(\text{m}^2\text{h})$ for aquaporin based membranes compared to $< 8 \text{ L}/(\text{m}^2\text{h})$ for conventional cellulose triacetate based FO membranes tested under the same conditions [64].

This membrane was stored wet at 4°C . The membrane was cut to fit the cell before use.

Reverse osmosis membrane: BW30

The flat sheet reverse osmosis membrane BW30 was used in the study. The BW30 membrane is a thin film composite (TFC) membrane with aromatic polyamide on polysulphone. BW has a permeability of $6.1 \text{ L}/(\text{m}^2\text{hbar})$ and a NaCl rejection of 94% at 0.1 M.

The membranes were stored dry at room temperature. They were then cut to fit the membrane cell and stored in deionised water overnight at 4°C before use.

3.5 Fouling solutions

Organic Fouling Solutions

Organic fouling was implemented with alginic acid (AA) sodium salt from brown algae (Sigma Aldrich, UK). Alginic acid was chosen as the model foulant as it is widely available and most suitable for use with the chosen imaging techniques. Fouling with alginic acid results in the formation of a thick gel layer, it is easy to image with confocal microscopy. As fouling solutions were made from a 2 g/L AA stock. Upon initial preparation, this stock was stirred overnight to ensure the alginic acid was dissolved completely.

For both the forward osmosis and reverse osmosis experiments a fouling solution of 200 mg/L AA was prepared with a background electrolyte solution of 1 mM NaHCO_3 buffer, 20 mM NaCl. CaCl_2 was added to the background electrolyte at varying concentrations for each experiment. The final fouling solution was then stirred overnight to ensure complete mixing also.

Model bacteria strain and media

Pseudomonas putida was the bacteria strain used. *P. putida* is a rod shaped, gram negative, non-spore forming organism that is found in soil and water and uses organic compounds for carbon and energy [113]. *P. putida* was chosen as a model bacteria strain in this study as previous work observed its strong adhesion to reverse osmosis and nanofiltration membranes [83, 84].

Cultures were obtained by inoculating 100 mL King's B broth supplemented with tetracycline at a final concentration of 10 $\mu\text{g}/\text{ml}$ using single colonies of *P. putida*.

The King's B broth was prepared as follows: 20 g of peptone, 10 g of glycerol, 1.5 g of K_2HPO_4 and 1.5 g of $\text{MgSO}_4 \cdot 7\text{H}_2\text{O}$ were added to 1 litre of deionised water. This was mixed thoroughly and then autoclaved. This was then stored at room temperature.

Tetracycline was prepared as 40 mg/ml and stored frozen. 100 μl was added to the culture before incubation.

The single bacteria colonies were isolated by streaking on a King's B agar plate and incubating at 28°C for 48 hours. Once grown they were stored at 4°C.

The culture was incubated at 28°C with shaking at 75 rpm and left to grow overnight to mid exponential stage, corresponding to an optical density of 0.8. Next the culture was centrifuged at 5000 rpm for 10 minutes. The supernatant was decanted and the pellet was re-suspended in 0.1 M NaCl using a vortex shaker. Next, 200 ml of this culture was added to the feed solution. This ensured a standardised inoculum of 10^8 cells/mL in every experiment.

Deionised water

Pure water ($18.2 \mu\Omega/\text{cm}$) was obtained from Triple Red Alto™ Ultrapure Water Polisher (Triple Red now known as Advidity, UK).

3.6 Operation of the FO crossflow system

The membranes were placed in the cells and taped in using double sided tape to ensure that the membrane was inflexible inside the cell. The pure water flux (PWF) of the membrane was tested with a feed of deionised water. The draw solution used for PWF was the same as the draw intended for fouling, usually 0.7 M NaCl was used to simulate seawater similar to experiments carried out in the literature, [34, 52, 107, 110]. PWF was carried out for 30 minutes. Next, in order to implement fouling, the feed solution was changed to the chosen fouling solution and the draw was also renewed so that the initial draw concentration was accurate. For organic fouling, tests typically lasted from 18 to 20 hours depending on the experiment. For bacterial adhesion, experiments lasted from 15 to 60 minutes depending on the experiment.

Backwashing was carried out immediately after fouling. In order to implement backwashing firstly the flow was stopped. One cell was isolated by turning of the inlet and outlet valves. This was brought to the microscope as the fouled membrane. The draw and feed solutions were changed in order to reverse the flow of water through the membrane. During backwashing the feed used was deionised water. The BW draw was changed depending on the experiment. Backwashing was carried out for 1 minute. During backwashing the flux was again measured by weighing the draw solution.

After backwashing the flow was stopped and the feed and draw solutions were again changed in order to determine the pure water flux of the membrane after backwashing to

see if the membrane performance improved. The feed and draw solutions used were identical to those used for the initial PWF measurements.

While PWF and fouling tests were carried out the draw solution weight was logged using LABVIEW software. The conductivity of both feed and draw solutions was recorded using a Cond 340i meter (WTW, Germany) throughout each stage of the experiment. The weight of the draw solution was logged at known intervals throughout the experiment. The weight changes throughout each experiment could then be calculated and thus the flux could be calculated by dividing by the known area of the membrane.

After the experiment the membranes were removed to be sent to the microscope and the crossflow system was cleaned.

3.7 Operation of the RO crossflow system

The membranes were first cut to fit the cell from a dry flat sheet stored at room temperature. These membranes were then soaked in deionised water at 4°C overnight to remove their preservative layer. The membranes were then rinsed placed in the cells.

The membranes were compacted overnight at 25 bar with deionised water. Membrane compaction is the compression of the membrane layers under applied pressure which results in a reduction in membrane flux. It is therefore necessary to pre-compact the membranes before fouling to ensure that the loss in flux is due to fouling alone and not membrane compaction. To ensure the membranes are fully compacted, the flux was taken initially at the start of compaction. It was then taken again after approximately 18 hours and then again after another 30 minutes to ensure the flux had stopped decreasing. The flux was determined by collecting permeate from a valve on the permeate line over a known time, such as for example 30 seconds. The amount collected was then weighed and so the flux could then be calculated from the collection time and weight obtained.

After compaction, the pure water flux of the membranes was tested with a feed of deionised water at a pressure of 20 bar for 30 minutes and the flux was recorded every 15 minutes. Next, the system was stabilised with the background electrolyte solution at the desired initial flux (this depended on the experiment) for 30 minutes and again the flux was recorded every 15 minutes. The pressure used was determined by the desired initial flux of each experiment. Next, the AA foulant was added and the fouling was continued for 6.5

hours. The permeate flux was tested every 20 minutes for the first hour and then every hour for the remaining time.

As with the FO experiments, after fouling, one cell was isolated from the system by closing the inlet and outlet valves. Backwashing was then implemented in the other cell by reducing the pressure to ambient and exposing the fouling layer to a high salinity solution (0.7, 4 M NaCl, 2, 3 M CaCl₂) for 1 minute. A feed solution of deionised water was used. During backwashing the flux was measured by weighing the weight loss of the feed solution.

After backwashing the pure water flux was retested at 20 bar for 30 minutes. Again, the flux was recorded every 15 minutes. The membranes were then removed from the cells and observed under the microscope, and the crossflow system was then cleaned. In some cases, the pure water flux was not retested after backwashing in order to determine if the pure water effected the fouling layer.

The flux was measured by measuring the weight change of the permeate over a fixed time period, (usually 30 seconds). On the bench scale rig, the permeate line was fixed with a valve that allowed collection of the permeate. The permeate was collected for 30 seconds, 3 times at known periods throughout each experiment. This was then weighed and the flux could be calculated by dividing by the known area of the membrane. The change in flux throughout the experiment could then be known.

3.8 Cleaning

Both RO and FO rigs were cleaned using the same method. After each experiment the membranes were removed from the cells and observed under the microscope. The entire rig including the membrane cells was rinsed with deionised water. Then 0.1 M NaOH was recirculated in the rig for 30 minutes. This was then neutralised with HCl and the rig was again rinsed with deionised water. For bacterial adhesion tests an extra ethanol recirculation was carried out for 30 minutes before NaOH was used.

3.9 Total Organic Carbon (TOC) Analysis

High levels of TOC in water can react in the disinfection process resulting in the formation of dangerous disinfection by-products [114]. An effective water treatment process therefore should eliminate or drastically reduce the TOC content of the water. For the organic fouling and cleaning experiments, levels of TOC in permeate and feed samples were measured using a total organic carbon analyser (TOC-V CPH) in non-purgeable organic carbon (NPOC) mode (Shimadzu, Milton Keynes, UK).

For FO experiments 10 ml samples for TOC analysis were taken from the feed and draw solutions at the start and end of the experiments and at least 4 more samples were taken throughout. For RO experiments, samples were taken at the start, every 20 minutes for the first hour and then every hour until one final sample was taken at the end. The level of TOC in the samples can be used to indicate the quantity of fouling accumulated on the membrane surface. By examining the TOC in the feed solution and draw solutions at the start and end of each experiment the amount of carbon accumulated on the membrane surface can be approximated by a mass balance of carbon in the system. Note that this mass balance assumes that the amount of carbon accumulated elsewhere in the system is negligible.

Prior to analysis the samples were acidified using 2 M HCl and sparged for 1.5 minutes with N₂ to remove inorganic carbon (for calibration, see Appendix B). During analysis, a known 10 ppm standard of potassium hydrogen phthalate (PHP) was used to ensure results were accurate.

3.10 Sample Staining

Organic Fouling

The fouled and backwashed membrane samples were stained with concanavalin A (Con A). Con A is a widely used lectin which binds to mannose residues of glycoproteins. Con A Alexa Fluor™ 488 Conjugate (ThermoFisher Scientific) which exhibits bright green fluorescence was used in this study. Staining was carried out in the following way: at least 3 samples of 20 mm by 20 mm were cut from the centre of the fouled membrane, which were then placed directly on top of a glass slide. Stock solutions of Con A (1 mg/ml) were prepared and stored frozen in 100 µl volumes. Prior to use, 50 µl of thawed Con A solution were

carefully applied directly on top of the fouling layer using a micropipette. Samples were allowed to incubate in the dark for 30 minutes.

Next an adapted washer was made from double sided tape was placed around the sample. A glass coverslip was then placed on top of the O-ring. The purpose of the O-ring placed in between the glass coverslip and the glass slide is to prevent the coverslip from compressing the gel-like fouling layer which could lead to inaccurate thickness values.

Experiments were performed without Con A and these showed that the Con A could not stain the membrane which has natural fluorescence and this background fluorescence of the membrane had no effect on the overall results.

Sample Staining: Bioadhesion

After the adhesion and backwashing, the membranes were removed from the cells underwater. To do this, the pump was stopped and all inlet and outlet valves around the membrane cells were closed. The cells were then removed and submerged in a bath containing 4 L of the feed solution background electrolyte 0.1 M NaCl. Under the solution, the membranes were carefully removed from the cells, cut into samples of 20 mm by 20 mm and placed into petri-dishes of 3 cm diameter.

The samples were then stained with 4 ppm propidium iodide and left to incubate for 15 minutes under laminar flow, at room temperature, in the dark. Propidium iodide is a commonly used counterstain used to detect dead or injured cells in red fluorescence. It only penetrates cells with disrupted membranes and cannot enter live cells. It is therefore possible to differentiate between live and dead *P. putida* cells using microscopy. After staining excess stain was removed by gently washing the samples in 0.1 M NaCl. The membrane samples were then brought to a Widefield Nikon TE2000 microscope for analysis.

3.11 Microscopy

Confocal Laser Scanning Microscopy (CLSM)

The membrane sample was observed under a Zeiss LSM 880 with Fast Airyscan microscope. At least 3 images of each sample were taken. The system consisted of a laser scanning module that was mounted on an inverted microscope (Zeiss) and an argon laser. Images were recorded at an excitation wavelength of 488 nm and digital images were produced by

obtaining z-stacks of the fouling layer. This microscope provides lateral resolution to 200 nm for 2D and 3D z stacks and 500 to 600 nm axial resolution for z-stacks. The smallest increment quantified by the microscope is < 25 nm.

Image analysis was performed with Imaris™ software. This was used to precisely visualize and measure the fouling layer thickness. As shown in figure 4.2, the surface coverage of the fouling layer remained even for each fouling condition and therefore the heterogeneity of the fouling layer was not considered in this study. The fouling layer thickness shown in this study are based on averages determined from at least 3 measurements.

Scanning Electron Microscopy

Scanning electron microscopy was used to produce images of the virgin Aquaporin membrane. A Hitachi S4700 Scanning Electron Microscope equipped with an 8k x 8k CMOS sensor was used.

Cryo Scanning Electron Microscopy

Scanning electron cryomicroscopy (Cryo SEM) was used to visually observe and compare the surface morphology of the fouled and backwashed membranes. A Hitachi S4700 Scanning Electron Microscope equipped with an 8k x 8k CMOS sensor was used. First the wet samples were mounted onto a metal stub and “cryo-fixed” by submerging them into sub-cooled nitrogen (nitrogen slush) at -210°C using controlled environment freezing apparatus (Vitrobot™). The samples were then quickly moved into the cold-stage of the SEM cryo-preparation chamber, which is under vacuum. Next, the samples were sputter coated with gold before being transferred into the SEM chamber for imaging.

All the samples were mounted onto the same metal stub together to ensure they underwent identical cryo-fixing and sputter coating conditions and therefore the results were consistent and accurate for each sample.

Scanning Electron Microscopy (Energy Dispersive X-Ray Spectroscopy)

Scanning Electron Microscopy / Energy Dispersive X-Ray Spectroscopy (SEM-EDS) was used for elemental analysis of the fouled and backwashed membranes and to map the surface of membrane samples to observe the distribution of element on the surface. A Carl Zeiss SIGMA HD VP Field Emission SEM and Oxford AZtec ED X-ray analysis software was used.

The samples were coated with carbon overnight before being placed under vacuum in the SEM.

Maps and spectra were recorded using an accelerating voltage of 10 kV, an aperture size of 80 μm , and a working distance of 7 ± 1 mm.

Atomic Force Microscopy

This section was performed by a microscope technician under my observation. The Young's modulus (elastic modulus) and adhesive force of the fouled and backwashed membranes were determined by examining indentation and retraction curves obtained using atomic force microscopy (AFM). Force measurements were performed using a Veeco Multimode/Nanoscope IIIa AFM, (Veeco, Santa Barbara, CA) and a Hamamatsu 1394 ORCE-ERA camera.

A commercial silicon nitride cantilever with a sharp triangular silicon nitride tip of 60 nm radius (DNP-10, C type, Bruker, UK) with a spring constant of 0.142 N/m was used in this study. The raw data was analysed using the Hertz model fitting with PUNIAS software with a constant Poisson ratio of 0.5.

At least 50 measurements of each sample were taken to get average measurements. The measurements were carried out on the membranes whilst they remained submerged in the relevant alginate acid fouling solution. Samples of the virgin membrane were also taken for reference.

Before measuring each sample the spring constant was determined by the AFM first using a glass slide to determine the inverse optical lever sensitivity (INVOLS) and then the spring constant.

Widefield Fluorescence Microscopy

A Widefield Nikon TE2000 microscope was used to image the bioadhered membranes. Live cells were imaged in the green FITC filter while dead cells were imaged in the Texas red filter. The magnification used was X40. Threshold analysis was used to determine the total area of live and dead cells using ImageJ software. At least 10 images of both the live and dead cells were taken to determine an average surface layer coverage. Below are representative images of membranes containing live and dead cells:

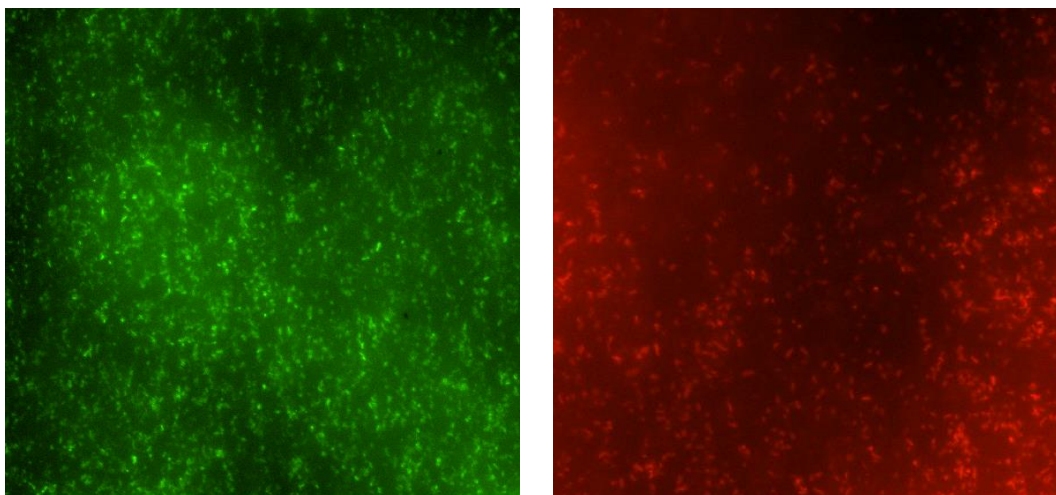


Figure 3.10: Florescence microscopy representative images of live (green) and dead (red) cells. The live cells represent a surface coverage of approximately 12%. The dead cells represent a surface coverage of approximately 5%.

Chapter 4: Osmotic backwashing of organic fouling on reverse osmosis membranes: Influence of fouling and backwashing conditions on cleaning efficiency

4.1 Introduction

By 2025, 60% of the world's population will live in water stressed areas [3], yet seawater is the earth's most abundant resource. For this reason, seawater desalination is a good solution to this urgent water crisis. Membrane technology is now the most widely applied water purification process for desalination and other water reclamation processes, [17]. The use of RO in seawater desalination for potable use has increased because of decreasing costs and improving technology. However NF and RO technologies still suffer many drawbacks, most notably membrane fouling.

Fouling leads to permeability losses and therefore drives up costs in RO desalination. Organic fouling is amongst the many potential foulants that are widespread in natural and waste waters and seawater RO plants are mainly fouled by organic material, [115]. Organic fouling in reverse osmosis (RO) processes has been widely reported in the literature, [36, 60, 86, 116]. Lee and Elimelech, [30] studied alginate fouling of RO membranes and found that, in the presence of 1 mM CaCl_2 , the flux declined by 65% after 15 hours. Similarly Tang et al, [36] fouled RO and NF membranes with humic acid. They subjected NF270 membranes to humic acid fouling in the presence of 1 mM CaCl_2 for 96 hours and reported an 85% reduction in membrane flux. Fouling is unavoidable and therefore effective cleaning strategies should be a fundamental part of membrane process.

RO membrane replacement costs due to fouling account for 11% of operation and maintenance costs in desalination, [10]. Various cleaning methods have been tested as a way to mitigate membrane fouling with varying results. The most prevalent form of cleaning is currently chemical cleaning. Ang et al, [38] used numerous combinations of chemicals to clean LFC-1 membranes that were fouled with wastewater effluent from a municipal treatment plant. A combination of ethylenediaminetetraacetic acid (EDTA) and NaOH restored 92.8% of the initial pure water membrane flux, (PWF). In a similar study, LFC-1 was fouled with sodium alginate, Suwannee River natural organic matter, bovine

serum albumin, and octanoic acid (25 mg/L of each) in the presence of 0.5 mM Ca^{2+} [42]. They used 0.5 mM EDTA at pH 11 to restore 91% of the initial pure water flux. However these cleaning agents are harmful to the environment, [12] and damage the surface of the membrane, reducing its selectivity, [3, 18]. Therefore, it is necessary to limit their use where possible and explore chemical free cleaning methods for RO and NF membranes.

Some work has been performed on chemical free cleaning in reverse osmosis with widely varying results [15, 16, 19, 21, 45, 102]. Physical cleaning experiments by increasing the crossflow velocity were performed by Lee et al, [15]. This cleaning method did not restore the flux of RO membranes fouled with alginic acid in the presence of Ca^{2+} . They report that this is due to the compact, dense structure of the fouling layer caused by the hydraulic pressure applied to the membrane during fouling. No further attempts were made to restore the RO flux in this study. More work is needed to fully understand chemical free cleaning in RO in order to optimise it.

Physical cleaning by osmotic backwashing has been reported, [16, 19, 102]. Backwashing is implemented by reversing the membrane flux direction from the permeate side to the feed side either by switching the feed and permeate solutions (under ambient pressure) or by injecting a pulse of high salt concentration to the feed side where the osmotic pressure difference between the feed and permeate sides overcomes the applied hydraulic pressure and according to equation (1.1) the permeate flux is reversed. This reverse in flux direction can potentially remove the fouling layer that has accumulated on the membrane surface. Ramon et al, [19] examined the use of osmotic backwashing to clean SW30HR-LE RO membranes that were fouled with alginic acid. Backwashing with a 10 minute pulse of 96 g/L NaCl restored 93% of the initial flux and outperformed physical cleaning with deionized water which only restored 66% of the initial flux. However, they did not perform any surface imaging to confirm the quantity of fouling remaining on the surface after backwashing. Although the addition of NaOH increased the backwashing efficiency to 97%, no further attempts were made to optimise backwashing without the use of chemicals in this study. Tow et al, [16] fouled SW30HR RO membranes with alginic acid and 1 mM CaCl_2 and used backwashing and an increase in crossflow velocity to remove the fouling layer. This restored 80% of the initial flux but again the amount of fouling remaining on the membrane surface was not quantified. There is a clear lack of understanding between fouling layer characteristics and efficiency of backwashing. In previous research into

alginate fouling, some studies achieve backwashing efficiencies of over 90%, [19, 43], while for other backwashing is not as effective, [16, 42], see table 2.3 in the literature review section. More research is therefore needed to understand how the fouling layer characteristics can influence backwashing.

Factors that affect fouling will in turn affect backwashing. Solution chemistry, such as the quantity of Ca^{2+} in the feed and the operating pressure, and therefore initial flux have already been shown to greatly influence the rate and extent of fouling, [30, 36, 85], but no work has shown how these parameters effect backwashing. The influence of the magnitude of the fouling layer in terms of thickness on the efficiency of backwashing has not been reported. It is expected that a higher thickness will result in a greater resistance to backwashing but the effects of fouling layer characteristics on backwashing flux have never been reported. Knowing these influences can lead to optimisation of the backwashing process through, for example, higher backwashing fluxes or longer backwashing durations.

There is a wide variation of backwashing duration in the literature, from an injection lasting 50 to 60 seconds, [102], to 10 minutes, [19], to even 1 hour, [43]. The shorter the backwashing duration, the less time will be lost during cleaning and less backwashing solution will be needed. Therefore a backwashing duration of 1 minute is used in this study. As the solution chemistry of the feed solution has a significant influence on the fouling layer characteristics, it is questioned whether the characteristics of the backwashing solution could alter the fouling layer during backwashing even during a contact time of just 1 minute. This will be shown in this study.

Previous studies demonstrate that backwashing restores the initial flux from 80%, [16], to over 100%, [43], in RO and yet little has been done to quantify the amount of fouling remaining on the membrane surface after backwashing, as well as backwashing optimization and influence of fouling characteristics on the backwashing efficiency. Therefore the aim of this study is to examine the efficiency of osmotic backwashing as a way of removing organic fouling from RO membranes through both flux measurements and surface imaging. As limited information is provided on fouling layer properties after backwashing in the literature, in this study, surface imaging and atomic force microscopy will be performed to obtain an improved understanding of the fouling layer structure. Confocal microscopy is used to determine the thickness of the fouling layer before and after osmotic backwashing. Atomic force microscopy is used to quantify the adhesion

forces and elasticity of the fouling layers. SEM is also used to examine the fouling layer morphology both before and after backwashing.

4.2 Chemical effect of feed solution chemistry on RO fouling and cleaning

The presence of CaCl_2 in the fouling solution has a significant effect on the rate and extent of RO fouling, [30, 36]. Lee and Elimelech, [30], reported a 75% increase in flux reduction when RO membranes were fouled with alginic acid in the presence of 1 mM CaCl_2 compared to the absence of calcium. This stark increase in fouling should in turn have an effect on cleaning efficiency but to what extent is not yet known. In order to examine how feed solution chemistry during fouling effects cleaning efficiency, osmotic backwashing was applied to membranes fouled under various solution chemistries.

Osmotic backwashing with 0.7 M NaCl was applied to membranes fouled with 200 mg/L alginic acid. The initial flux was set to 80 $\text{L/m}^2\text{h}$. The membranes were fouled with different feed characteristics through the variation of CaCl_2 concentration in the feed and their efficiency on cleaning was assessed through flux measurements and surface imaging with confocal microscopy. This is shown in figure 4.1.

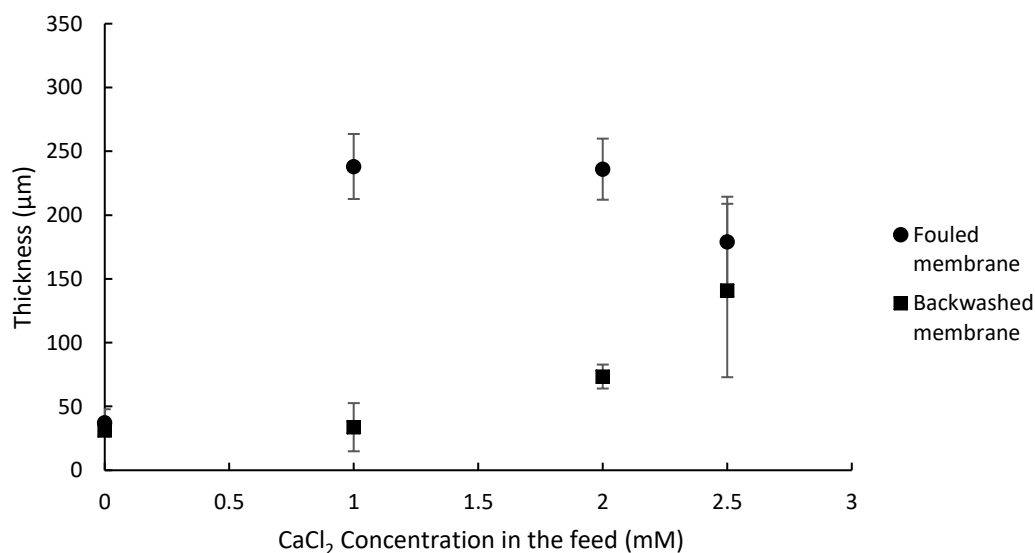


Figure 4. 1: Chemical effects on backwashing efficiency in RO: Confocal microscopy results of membrane samples subjected to fouling in cross-flow showing the thickness of the fouling layer. Membrane = BW30. Mode = AL-FS. Fouling conditions: Feed solution = 200 mg/L AA. Initial flux = 80 $\text{L/m}^2\text{h}$. Fouling duration = 6.5 hours. Backwashing duration = 1 minute. Backwashing draw solution = 0.7 M NaCl. Backwashing feed solution = deionised water. Error bars show standard deviation of repeated experiments.

Figure 4.2 below shows representative confocal images of fouled and cleaned membranes.

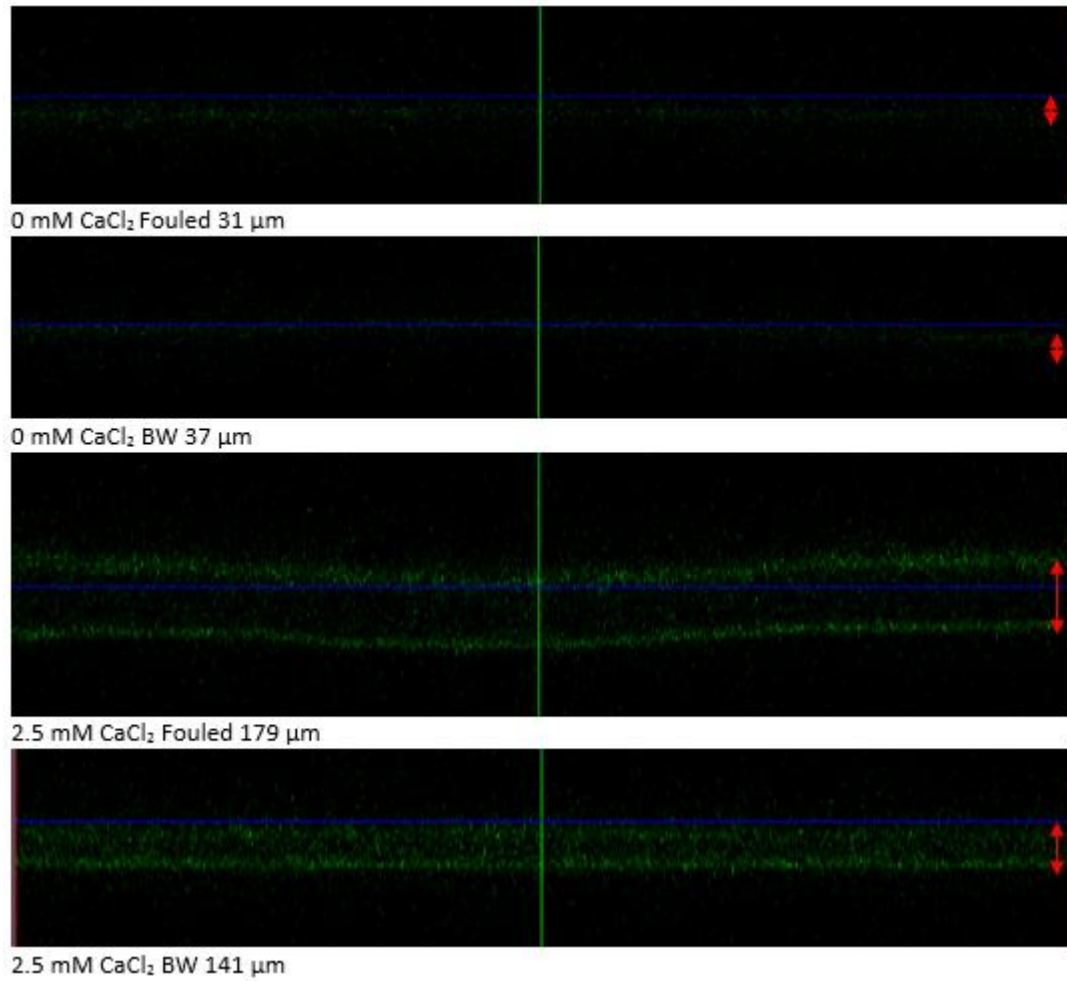


Figure 4.2: Representative confocal images of fouled and backwashed membranes. Membranes were fouled with 200 mg/L alginate acid fouling solutions with varying CaCl_2 concentration as shown.

The thickness of the clean membrane was determined to be $33 \pm 2.5 \mu\text{m}$ from several measurements of the surface using confocal microscopy. This was then subtracted from the determined thickness values of the fouled membranes to obtain the net fouling layer thickness.

Carboxyl groups present in alginate fouling form complexes with Ca^{2+} present in the feed neutralizing the negative charge of alginate molecules, resulting in a thick compact cross-linked gel fouling layer on the surface of the membrane, this is known as the “egg box model” [23, 34]. The egg box model is called as such due to the way that the Ca^{2+} ions (the eggs) are arranged in the structure of the long carboxyl groups (the box). This explains the sharp increase in fouling layer thickness as calcium is introduced to the feed in figure 4.1.

The fouling layer thickness increased from 37 μm in the absence of calcium to 238 μm in the presence of 1 mM CaCl_2 , figure 4.1. This increase in fouling layer thickness resulted in increasing flux losses. There is a pronounced flux decline when calcium is present compared to the absence of calcium presented in table 4.1 below.

Table 4. 1: Flux decline due to CaCl_2 in the fouling solution in RO

CaCl_2 Concentration (mM)	% Flux decline
0	10
1	57
2	66
2.5	69

As the CaCl_2 concentration increased from 0 to 1 mM the thicker fouling layer offered greater resistance to flux and therefore a stark flux decline occurred, see table 4.1. From figure 4.1, as the concentration of CaCl_2 increases from 1 to 2 mM the fouling layer thickness remains relatively unchanged (actually decreases by 2 μm) yet the flux decline is greater for 2 mM CaCl_2 (see table 4.1). This suggests that the fouling layer becomes denser as the concentration of CaCl_2 increases and further cross linkage of carboxyl groups and Ca^{2+} ion occurs. Also as the concentration of CaCl_2 increases from 2 to 2.5 mM the gel layer thickness decreased by 57.28 μm yet the flux continued to decline. This greater resistance to flux, despite the thinner fouling layer, suggests that the layer has become more compact and saturated with CaCl_2 . Total organic carbon analysis was used to determine that amount of carbon deposited on the membrane during fouling. The amount of carbon remained constant for each experiment at 21.3 ± 2 mg/L. The slight decrease in fouling layer thickness, figure 4.1, suggests that the layer is becoming denser with the increase in calcium in the fouling solution.

Hong and Elimelech, [23], also reported a pronounced reduction in flux (39%) after the addition of calcium in organic fouled nanofiltration membranes after 25 hours of fouling. They explained this is due to the denser organic fouling layer after the addition of calcium. Similarly, Li and Elimelech [34] examined organic fouling of nanofiltration membranes and reported that the addition of calcium in the feed resulted in a 50% decrease in flux compared to just 10% in the absence of calcium after 240 hours of fouling. Again, they

explained that this is due to the highly compacted fouling layer formed in the presence of calcium resulting in a higher resistance to flux.

It has been reported that membrane rejection decreases during fouling due to cake enhanced osmotic pressure, [68, 69]. This occurs as the salt concentration at the membrane surface increases due to back diffusion to the feed being prevented by the fouling layer. Lee et al, [69], reported a 10% decrease in rejection of RO membranes due to colloidal fouling. However, in this study, the level of fouling had no effect on rejection which remained above 96% in each fouling case. This could be due to the fact that the gel layer potentially does not simply hinder back diffusion of salts and instead, this microenvironment of increased salt concentration leads to an enhanced fouling layer due to sequestration of Ca^{2+} ions at the membrane surface. This was reported by Seidel and Elimelech, [87], who reported that rejected Ca^{2+} ions increase in concentration at the membrane surface and therefore enhance natural organic matter fouling.

In order to remove the fouling layer, osmotic backwashing was applied by reversing the flow of water through the membrane. In order to implement this, the pressure was reduced to ambient and the feed solution was replaced with a 0.7 M NaCl solution, known as the draw solution. This created an osmotic pressure difference across the membrane that acted as a driving force for reversing the flow across the membrane (backwashing). More details of how backwashing is performed are given in the materials and methods section of this thesis. The CaCl_2 concentration used in the feed during fouling has an influence on the backwashing flux efficiency, as shown in table 4.2 below. Increasing the CaCl_2 concentration in the feed from 0 mM to 2.5 mM decreases the backwashing flux from 23.12 $\text{L/m}^2\text{h}$ to 16.4 $\text{L/m}^2\text{h}$.

Table 4. 2: Backwashing flux decline due to CaCl_2 in the fouling solution in RO. The backwashing flux was determined by weighing the feed solution during backwashing and dividing the weight change by the known membrane area.

CaCl_2 feed concentration (mM)	Backwashing flux ($\text{L/m}^2\text{h}$)
0	23.1
1	26.4
2	18.6
2.5	16.4

From table 4.2, it can be shown that the increase in thickness of the fouling layer does not necessarily offer extra resistance to backwashing flux. As the CaCl_2 concentration increases from 0 to 1 mM, the fouling layer thickness increases by 201 μm , however, the backwashing flux increases by over 3 $\text{L/m}^2\text{h}$ showing that the thicker fouling layer offered no extra resistance to backwashing flux. The question arises as to how the fouling layer thickness can increase flux resistance during fouling but not during backwashing. This is because, during backwashing, the pressure is reduced to ambient and the direction of the flux is reversed. The pure water permeate is now the feed solution and the draw solution is now a high salinity solution. The fouling layer is a high salinity gel and therefore does not necessarily resist the driving force for flux unlike during fouling where it acts as an extra barrier to permeation.

It is evident that increasing the CaCl_2 concentration further from 1 mM to 2 mM and 2.5 mM will begin to hinder backwashing flux, see table 4.2. The backwashing flux decreased from 23 $\text{L/m}^2\text{h}$ for the membrane fouled in the absence of calcium to 16.4 $\text{L/m}^2\text{h}$ when fouled with 2.5 mM CaCl_2 . This is potentially due to extra resistance provided by the more compact fouling layer produced with 2.5 mM CaCl_2 in the feed as the fouling thickness does not increase, see figure 4.1. As the fouling layer becomes denser with CaCl_2 it offers high adhesion to the membrane surface and high cohesion between fouling layers, [85].

Hong and Elimelech, [23], studied humic acid fouling of NF membranes and reported a 60% decrease in flux in the presence of 1 mM CaCl_2 , compared to a less than 10% decrease in the absence of calcium. They hypothesised that this was due to the formation of a highly compact, dense fouling layer. Mi and Elimelech, [24], studied adhesion forces of alginate fouling layers in FO and used AFM to determine that the average adhesion force of the alginate fouling increased twofold in the presence of 0.5 mM Ca^{2+} compared to the absence of calcium. As well as this, Lee and Elimelech, [30], also used AFM to show how the adhesion forces increase with increasing calcium concentration. They should that increasing the calcium concentration from 0 mM to 1 mM resulted in a fourfold increase in the maximum adhesion force which will result in a thicker, more compact fouling layer. This increase in adhesion results in less efficient backwashing and the fouling layer is therefore not removed, see figure 4.1, where the amount of fouling remaining on the membrane increases from 34 μm to 141 μm as the CaCl_2 concentration increases from 1 mM to 2.5

mM. It is therefore the fouling layer density, caused by the increase in adhesion forces, and not the thickness that influences backwashing efficiency.

For CaCl_2 concentrations of 0 mM and 1 mM, osmotic backwashing was ineffective at completely removing the fouling layer with 31 μm and 34 μm of foulant remaining on the membrane surface respectively. As the Ca^{2+} concentration in the feed increases further, backwashing becomes less efficient and the amount of fouling remaining on the membrane after backwashing increases, see figure 4.1. The fouling layer thickness after backwashing increased from 34 μm to 73 μm to 141 μm as the CaCl_2 concentration in the feed increased from 1 mM to 2 mM to 2.5 mM respectively. Again this is due to the higher energy of adhesion between the fouling layer and the membrane surface as well as the higher energy of cohesion between the fouling layers due to the higher Ca^{2+} ion concentrations resulting in a denser fouling layer that is thus more difficult to remove.

This shows that backwashing with 0.7 M NaCl is not sufficient at completely removing the fouling layer for membranes fouled with an initial flux of 80 $\text{L}/\text{m}^2\text{h}$ where even at low CaCl_2 concentrations. In the literature, studies rely on flux restoration alone to determine backwashing efficiency in organic fouling, [19], but that is not sufficient. In this study, despite the fact that the fouling layer could not be removed completely, the level of flux restoration was significant. The initial pure water flux was restored by 90% in the absence of CaCl_2 . In the presence of 1 mM and 2 mM CaCl_2 , 92% of the flux was restored despite the fact that the fouling layer remaining on the membrane surface was 40 μm thicker for the 2 mM CaCl_2 feed. Finally, 86% of the flux was restored for the membrane fouled with 2.5 mM CaCl_2 . These results show that a high flux restoration alone cannot confirm significant fouling removal has occurred in RO and highlights the importance of surface imaging to examine true cleaning efficiency. The high flux restoration despite the incomplete fouling layer removal is due to the dilute nature of the fouling layer. Alginate is hygroscopic, meaning it can hold several times its weight in water, [117], and therefore although a fouling layer is present after cleaning, it is not dense enough to have a large effect on the membrane flux.

Flux alone is not an adequate measure of cleaning efficiency as fouling that remains on the membrane surface will exacerbate subsequent fouling. Motsa, et al, [17], showed that surface flushing with ultra-pure water could restore 98%, 93% and 91% of the flux for three consecutive fouling cycles in forward osmosis operation. Cleaning loses efficiency after

subsequent fouling cycles as the fouling layer becomes more difficult to remove due to the accumulation of fouling from cycle to cycle. For this reason, surface imaging is necessary in order to get a true cleaning efficiency.

4.3 Physical effect of feed solution chemistry on RO fouling and cleaning

The rate and extent of fouling is dependent on the initial flux of the membrane and this has been shown in the literature for RO and NF membranes, [23, 28, 86, 87, 108]. Tang et al, [36], showed that initial fluxes of 0.6, 1.2, and 2.2 m/day corresponded to flux reductions of 2%, 4%, and 9%, respectively after 4 days of fouling BW30 membranes with humic acid. This increase in fouling will therefore impact the backwashing efficiency. This impact be examined in this section.

Osmotic backwashing with 0.7 M NaCl was applied to membranes fouled with 200 mg/L alginic acid and 2.5 mM CaCl₂ and with varying initial fluxes by varying the applied pressure, and their efficiency on cleaning was assessed. This is shown in figure 4.3 below.

Representative confocal images are shown in figure 4.4.

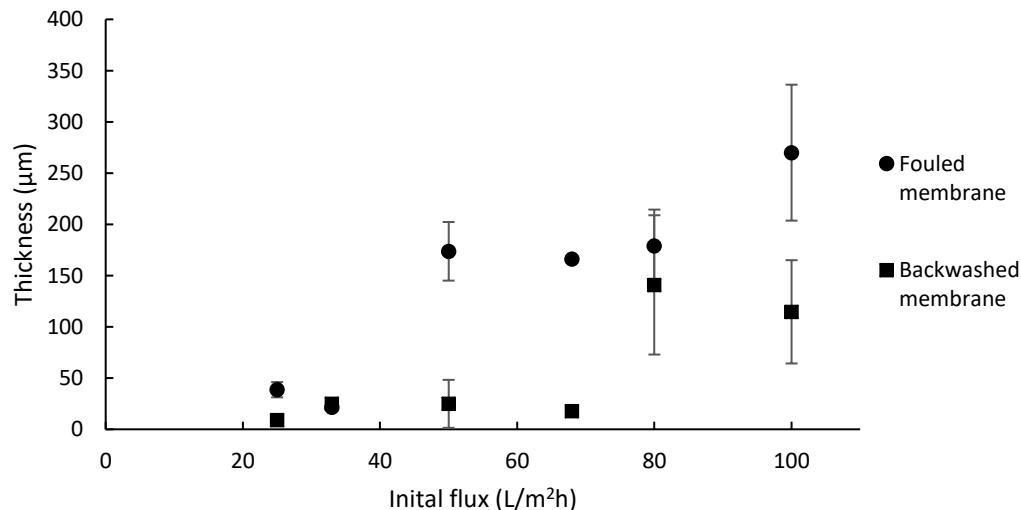
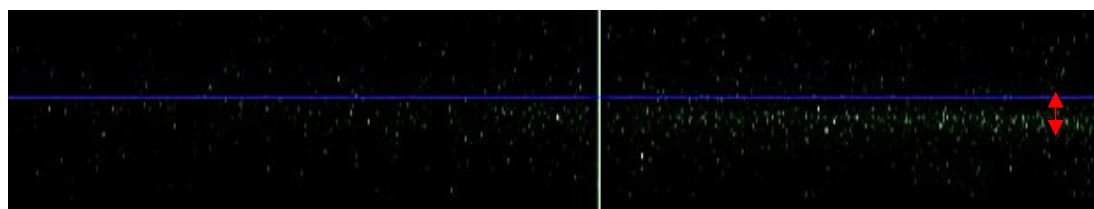
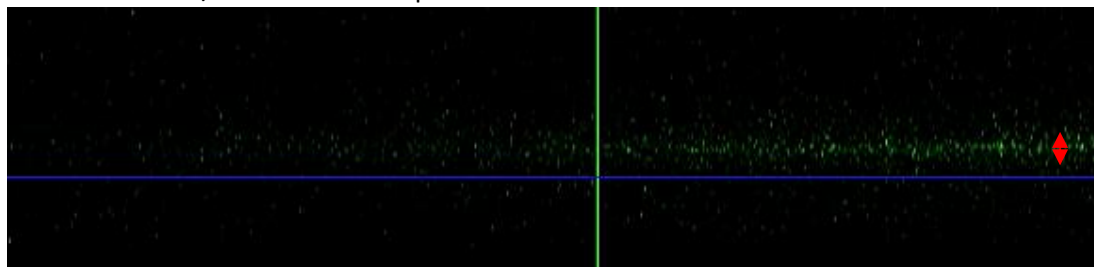


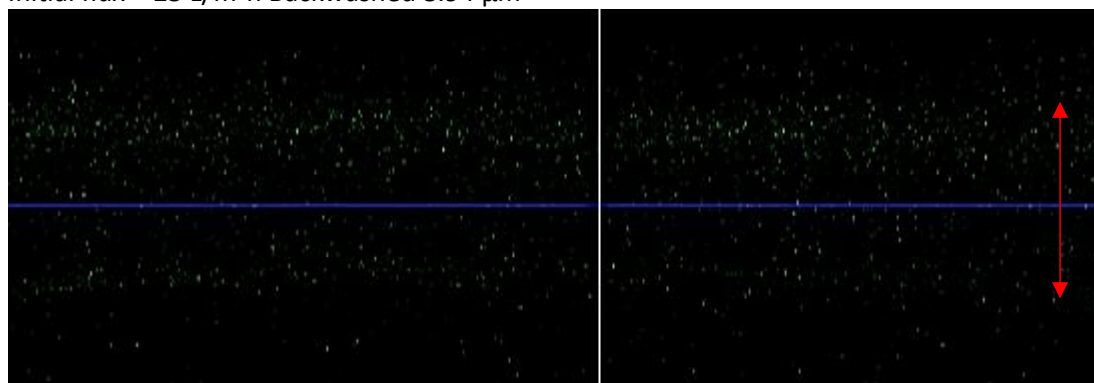
Figure 4.3: Physical effects on fouling and backwashing in RO: Confocal microscopy results of membrane samples subjected to fouling in cross-flow showing the thickness of the fouling layer. Fouling conditions: Feed solution = 200 mg/L AA 2.5 mM CaCl₂. Fouling duration = 6.5 hours. Backwashing = 1 minute. Backwashing draw solution = 0.7 M NaCl. Backwashing feed solution = deionised water. Membrane = BW30. Mode = AL-FS. Error bars show standard deviation



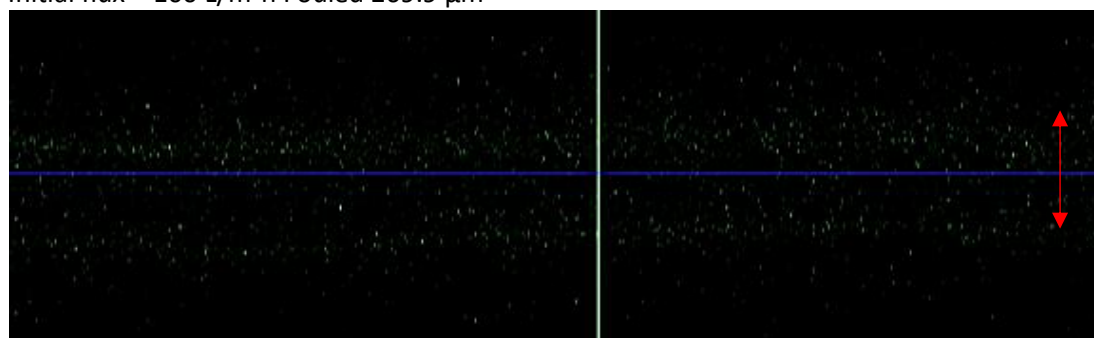
Initial flux = 25 L/m²h Fouled 38.6 μ m



Initial flux = 25 L/m²h Backwashed 8.94 μ m



Initial flux = 100 L/m²h Fouled 269.9 μ m



Initial flux = 100 L/m²h Backwashed 114.3 μ m

Figure 4.4: Representative confocal images of fouled and cleaned membranes. Membranes were fouled with 200 mg/L alginic acid fouling solutions with 2.5 mM CaCl₂ at initial fluxes shown.

As expected, higher initial fluxes resulted in thicker fouling layers with the layer increasing from 39 μ m for a flux of 25 L/m²h to 270 μ m for a flux of 100 L/m²h. This is due to the foulants experiencing a hydrodynamic drag force towards the surface of the membrane due to the permeate flux. By increasing the flux, and therefore the drag force, foulant-membrane and foulant-foulant interaction forces can be overcome resulting in significant fouling, [86]. This is reported by Tang et al, [86] who fouled BW30 with humic acid. They

reported that an increase in initial flux from 1.17 m/day to 2.16 m/day resulted in an increase in humic acid accumulation from 8 $\mu\text{g}/\text{cm}^3$ to 23.6 $\mu\text{g}/\text{cm}^3$ due to the higher drag force.

Higher initial fluxes resulted in larger reductions in flux, see table 4.3 below.

Table 4.3: Flux decline in RO due to initial flux. The flux decline was determined by observing the initial flux and the final flux at the end of the experiment.

Initial flux ($\text{L}/\text{m}^2\text{h}$)	Flux reduction (%)	Rejection (%)
25	19	95.1
33	26	95.2
50	49	95.9
68	60	96.3
80	69	97.3
100	75	97.3

As the initial flux increases from 25 to 100 $\text{L}/\text{m}^2\text{h}$, the flux reduction increases from 19% to 75% after 6.5 hours of fouling. This higher rate of fouling is expected due to the higher perpendicular force on the membrane. Overall, the rejection increased slightly with increased fouling. This increase in rejection could be due to the thicker fouling layer acting as an extra barrier to salt permeation. During the course of fouling for 6.5 hours, any changes in rejection were negligible (averaging 0.018%) showing that cake enhanced osmotic pressure due to salts getting trapped at the membrane surface by the fouling layer did not occur.

Recalling that from section 4.2, where, as the CaCl_2 concentration was increased from 0 mM to 1 mM, the fouling layer thickness increased by 201 μm but this increase in thickness did not have an effect on the backwashing flux and therefore showing that a thicker fouling layer will not necessarily offer greater resistance to flux. This is also evident in this study. The initial flux of 25 $\text{L}/\text{m}^2\text{h}$ resulted in a fouling layer of 39 μm thickness and a backwashing flux of 13 $\text{L}/\text{m}^2\text{h}$ was observed. An initial flux of 100 $\text{L}/\text{m}^2\text{h}$ resulted in a fouling layer of 270 μm thickness and a backwashing flux of 20 $\text{L}/\text{m}^2\text{h}$ was observed. Again the increase in flux is potentially due to the increase in concentration at the membrane surface and therefore a

higher driving force for backwashing flux. As already stated in the above section, it is in fact the density of the fouling layer that influences backwashing flux, not the thickness.

In terms of backwashing effects on fouling layer thickness, as seen in section 4.2, as the thickness increases, it becomes more difficult to remove, increasing from 9 μm to 155 μm as the initial flux increased from 25 to 100 $\text{L}/\text{m}^2\text{h}$. Organic fouling at higher pressures is largely irreversible due to the hydraulic pressure applied to the fouling layer making it dense and compact, [118]. This shows that the backwashing flux is not enough to remove the compact fouling layer produced at higher pressures.

The effects of pressure on fouling are extremely evident when initial membrane fluxes of 50 and 80 $\text{L}/\text{m}^2\text{h}$ are examined. They produce similar fouling layer thickness at 174 μm and 179 μm respectively and similar backwashing fluxes and 17.4 $\text{L}/\text{m}^2\text{h}$ and 16.4 $\text{L}/\text{m}^2\text{h}$, respectively. However backwashing is ineffective for the 80 $\text{L}/\text{m}^2\text{h}$ case. It only removed 18% of the fouling layer compared to a 72% removal for 50 $\text{L}/\text{m}^2\text{h}$. This was accompanied by an 81% pure water flux restoration for 80 $\text{L}/\text{m}^2\text{h}$ compared to a 90% restoration for 50 $\text{L}/\text{m}^2\text{h}$. This shows that although the same thickness, the layer is denser and stronger due to the higher permeate drag applied due to the high pressure. The denser membrane is therefore more difficult to remove and requires further cleaning.

The restoration of initial pure water flux is directly proportional to the initial fouling flux. At lower initial fluxes, the pure water flux of the membrane was much easier to restore with this method of backwashing. The PWF was 100% restored for initial fluxes of 25 and 33 $\text{L}/\text{m}^2\text{h}$. The backwashing efficiency then decreased as the initial fouling flux was increased as the membrane pure water flux was restored by 90%, 85%, 81% and 70% for initial fluxes of 50, 68, 80 and 100 $\text{L}/\text{m}^2\text{h}$ respectively. Therefore, for higher applied pressures resulting in higher initial fluxes, a different approach to backwashing, for example through increasing BW flux, cross-flow or BW duration, is necessary.

4.4 Effect of backwashing flux on fouling removal of RO membranes

In order to examine if higher backwashing fluxes could improve cleaning efficiency, osmotic backwashing with different draw solution osmotic pressures, and hence higher

backwashing permeate fluxes, was applied to membranes fouled with 200 mg/L alginate acid and 2.5 mM CaCl_2 at an initial flux of 80 $\text{L/m}^2\text{h}$.

Increasing the draw solution osmotic pressure will increase the backwashing flux resulting in a higher drag force to remove the fouling layer. The corresponding osmotic pressures and backwashing fluxes of the different backwashing draw solutions are provided in the table below, table 4.4.

Table 4.4: Corresponding backwashing flux and osmotic pressure for the given backwashing solutions in RO. The osmotic pressure was calculated using data obtained from Cath el al, which was calculated using OLI Stream Analyzer 2.0, [61].

Backwashing solution	Backwashing Flux ($\text{L/m}^2\text{h}$)	Osmotic Pressure (atm)
0.7 M NaCl	16.40	41
4M NaCl	27.27	240
3M CaCl_2	48.31	410

The cleaning efficiency was examined by determining the fouling layer thickness after fouling and after backwashing followed by PWF testing. This is shown in figure 4.5.

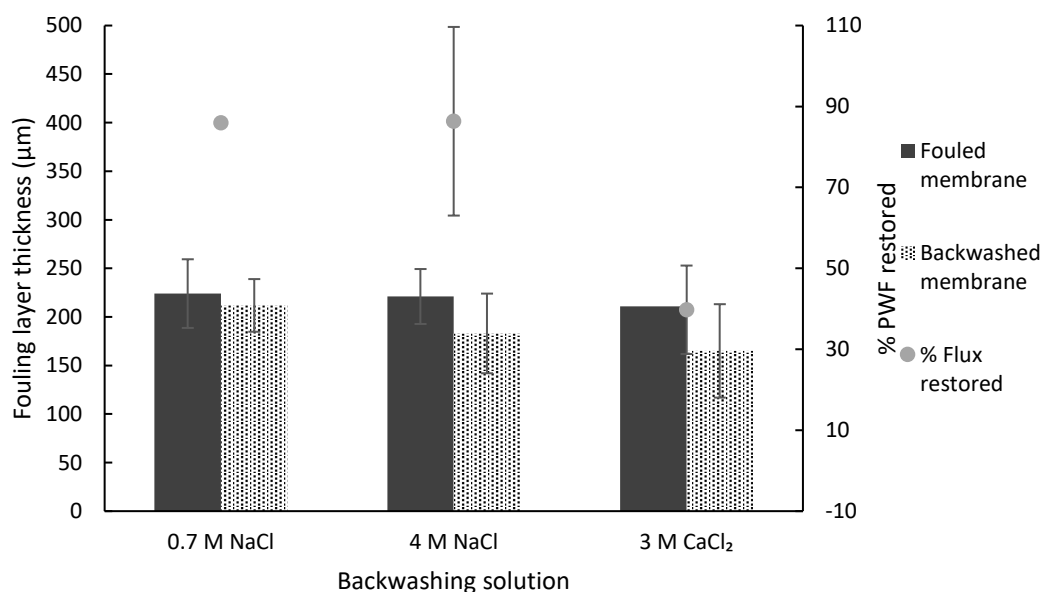


Figure 4.5: Effect of osmotic pressure in RO: Confocal microscopy results determining the fouling layer thickness before and after backwashing and PWF testing and corresponding PWF values after cleaning: Feed solution = 200 mg/L AA 2.5 mM CaCl_2 . Initial flux = 80 $\text{L/m}^2\text{h}$. Fouling duration = 6.5 hours. Backwashing = 1 minute. Backwashing draw solution is shown on graph. Backwashing feed solution = deionised water. Membrane = BW30. Mode = AL-FS. Error bars show standard deviation. T-tests were carried out on these results and a P value of 0.44 was determined showing that these results are statistically significant.

The osmotic pressure difference is the driving force for flux and therefore as it increases, backwashing flux increases and more of the fouling layer is removed. The average initial fouling layer thickness for the above three experiments is 219 μm . After backwashing, the remaining fouling layer decreases from 211 to 165 μm as the backwashing flux increases from 16.4 to 48 $\text{L}/\text{m}^2\text{h}$ (from table 4.4). This is due to the higher permeate drag force available to remove the fouling from the membrane surface.

In terms of flux restoration, the backwashing fluxes of 0.7 M and 4 M NaCl restored 85.9% and 86.3% of the initial pure water flux, respectively, despite the low removal of the fouling layer. This reinforces the conclusion from sections 4.2 and 4.3 that flux restoration alone is not a good indicator of efficient membrane cleaning and should be accompanied by membrane surface observations.

In order to achieve the backwashing flux of 48 $\text{L}/\text{m}^2\text{h}$, a backwashing solution of calcium chloride was used. Despite this higher backwashing flux, the performance of the membrane reduces after backwashing as the initial pure water flux cannot be restored. Despite being superior in terms of fouling layer removal, backwashing with 3 M CaCl_2 with a BW flux of 48.31 $\text{L}/\text{m}^2\text{h}$, was less efficient than 4 M NaCl with a BW flux of 27.3 $\text{L}/\text{m}^2\text{h}$. Backwashing with 3 M of CaCl_2 resulted in only 40% of the initial PWF being restored despite the smaller fouling layer thickness. However, as already stated in section 4.2, it is not the thickness but the density of the fouling layer that influences pure water flux restoration.

As explained in the literature review, bidirectional diffusion of solutes occurs during osmotic cleaning where the concentration difference causes salts to diffuse in the opposite direction to the water flux. The results in table 4.4 suggest that the Ca^{2+} ions in the backwashing solution interfere with the fouling layer by diffusing towards the alginate fouling layer and forming complexes with the carboxyl groups in it. This makes it denser despite only being exposed to the fouling layer for 1 minute. Motsa et al, [17] studied the relationship between alginate and Ca^{2+} ions in FO fouling and found that once the surface is covered with foulant, the fouling depends more on the foulant-foulant interactions than hydrodynamic conditions such as permeation drag. This could be a potential reason why CaCl_2 is not an effective backwashing solution as the permeate drag is not enough to overcome the strong bonds caused by the Ca^{2+} ions in the fouling layer.

In order to further examine the interference of Ca^{2+} ions with the alginate fouling layer during backwashing, a direct comparison between backwashing with CaCl_2 and NaCl was made and this is outlined in the next section.

4.5 Effect of backwashing with Ca^{2+} ions on organic fouling removal of RO membranes

To directly compare the backwashing with NaCl and CaCl_2 , backwashing with both solutions was tested with the same osmotic pressure, and hence creating the same backwashing flux. Backwashing was applied to membranes fouled with 200 mg/L alginic acid and 2.5 mM CaCl_2 at an initial flux of 80 $\text{L/m}^2\text{h}$. In addition to examining the fouling layer thickness before cleaning, and after backwashing and PWF testing, the membrane was brought to the microscope immediately after backwashing i.e. without checking the final PWF of the membrane. The fouling thickness was examined and this is shown in figure 4.6.

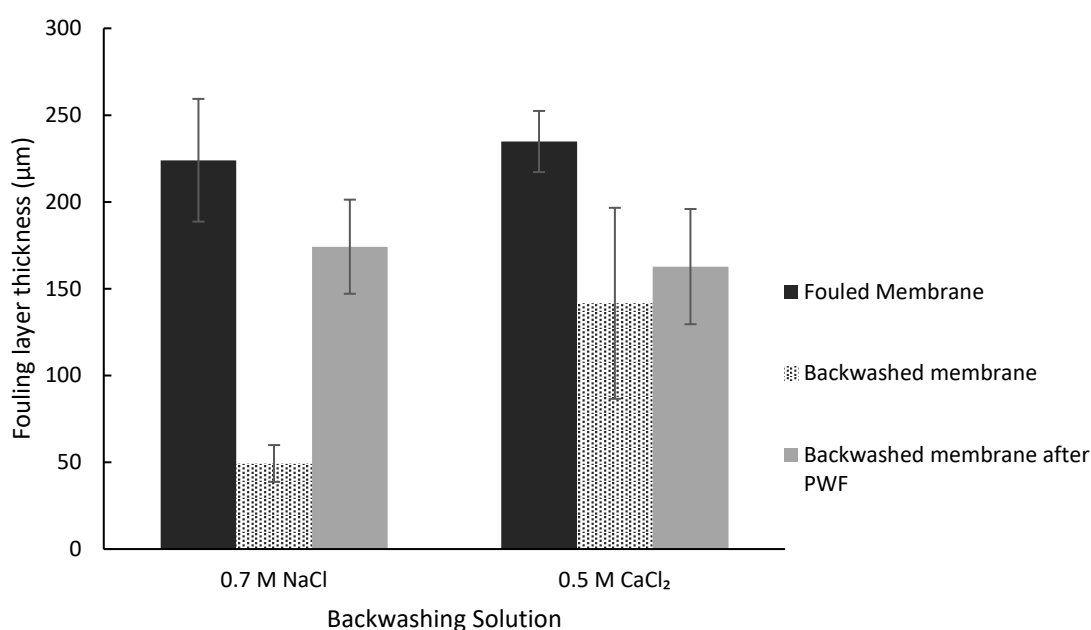


Figure 4.6: Fouling layer swelling in RO. Confocal microscopy results for fouling layer thickness, before and after backwashing and after the second PWF test. FS = 200 mg/L AA 2.5 mM CaCl_2 . Initial flux = 80 $\text{L/m}^2\text{h}$. Fouling duration = 6.5 hours. Backwashing = 1 minute. Backwashing draw solution is shown on graph. Backwashing feed solution = deionised water. Membrane = BW30. Mode = AL-FS. Error bars show standard deviation

Both membranes were fouled under identical conditions. The backwashing solutions of NaCl and CaCl_2 both offered the same osmotic pressure (41 and 40 atm respectively).

Therefore, it is unexpected that 142 μm of fouling remains on the surface compared to 49 μm for backwashing with NaCl. The 0.5 M CaCl_2 backwashing solution removes 35% of the fouling layer and only restores 52% the initial flux compared to 0.7 M NaCl which removed 78% of the fouling layer and restored 86% of the flux. This shows the Ca^{2+} ions in the backwashing solution are interfering with the fouling layer during cleaning by forming complexes with the carboxyl groups present in the fouling layer and making it worse despite the fact cleaning is only carried out for one minute. It is clear that 1 minute is enough time for complexes to form between the Ca^{2+} ions in the backwashing solution and the alginates in the fouling layer resulting in a denser layer that hinders flux recovery.

Another glaring observation is that the backwashed fouling layer can swell when exposed to deionised water. Usually after the membranes are fouled and backwashed, the pure water flux of the membrane is recorded by observing the flux with a feed of deionised water. Then the membrane is removed from the cell and imaged under the microscope. There is a significant difference in the fouling layer thickness before and after the PWF test is implemented after backwashing with 0.7 M NaCl. Figure 4.6 shows that the fouling layer after backwashing with NaCl swelled to 3.5 times its thickness after the pure water flux test. In comparison, the layer after backwashing with CaCl_2 swelled by only 13% during the PWF test.

Swelling of the alginate fouling layer when the concentration of the surrounding monovalent solution (e.g. NaCl) is decreased has been previously discussed in other studies [16, 85, 119]. This occurs when the operation switches from backwashing to pure water flux testing. Moe et al, [120], explain that the swelling of the alginate gel is due to both the osmotic pressure and elasticity of the gel. The gel has a high osmotic pressure due to its high ion concentration. When in contact with deionised water (for example during PWF tests), this osmotic pressure acts as a driving force for water to enter the gel layer, thus causing it to swell. However this does not occur with solutions of CaCl_2 . They show that alginate gels in calcium chloride (divalent) solutions shrink when the solution concentration is increased (e.g. during backwashing) but they exhibit hysteresis and do not release bound Ca^{2+} ions and therefore do not re-swell when the concentration is decreased (during pure water flux). Tow et al, [16] noted this swelling phenomenon when cleaning RO and FO membranes and they proposed it could prompt removal of the gel from the membrane surface and lower the energy barrier for removal. They cleaned alginate fouled RO

membranes by first allowing the fouling layer to swell by simply reducing the pressure to ambient and the crossflow to 0 cm/s for 1.5 minutes and then gradually increasing the crossflow to a final crossflow of 25 cm/s for 10 minutes. This method resulted in a flux restoration of only 80%. The amount of foulant remaining on the membrane surface was not quantified.

de Kerchove and Elimelech, [85], showed that increasing the ionic strength of the fouling solution reduces the electrostatic repulsive forces in polygalacturonic acid layers resulting in a more compact layer compared to layers formed at low ionic strengths which were more swollen. However they showed that this did not occur with AA layers, as increasing the fouling solution concentration increased the gel layer thickness. It was suggested that this swelling was due to the ion-exchange process and the change in conformation of the polysaccharides.

This fouling layer swelling after backwashing may cause inaccurate fouling layer thickness results. This swelling occurrence could explain why the flux cannot be restored after cleaning with CaCl_2 despite the fact the fouling layer after PWF testing appears to be similar in thickness as that cleaned with NaCl.

To determine if the lower removal energy barrier of the swollen gel layer could be exploited to improve backwashing, a final backwashing step was applied once more after exposing the fouling layer to deionised water. Membranes were fouled with 200 mg/L alginic acid and 2.5 mM CaCl_2 at an initial flux of 80 L/m²h, then backwashed with 0.7 M NaCl, then exposed to deionised water for 30 minutes (PWF test) and then a final 1 minute backwash with 0.7 M NaCl was performed on the swollen fouling layer. The final fouling thickness was then examined and this is shown in figure 4.7.

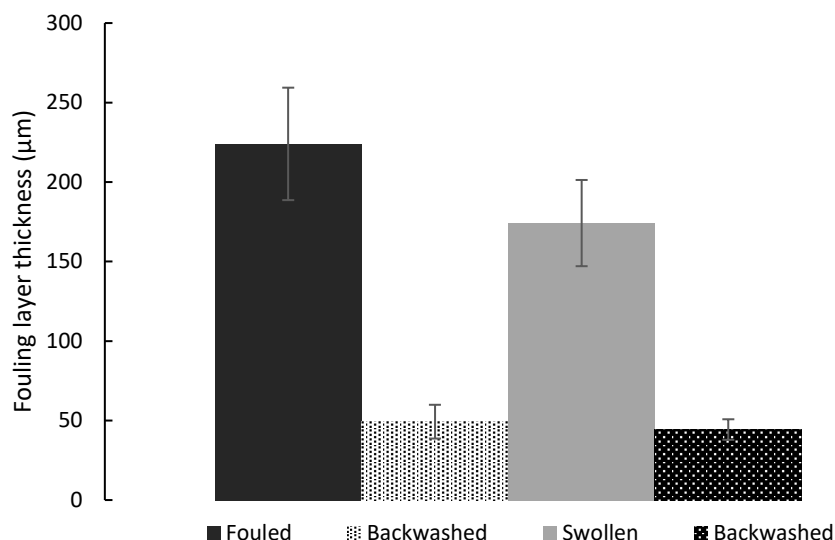


Figure 4.7: Backwashing swollen fouling layers in RO .Confocal microscopy results for fouling layer thickness, before and after backwashing, after the second PWF test and after a final backwashing test. FS = 200 mg/L AA 2.5 mM CaCl₂. Initial flux = 80 L/m²h. Fouling duration = 6.5 hours. Backwashing = 1 minute. Backwashing draw solution = 0.7 M NaCl. Backwashing feed solution = deionised water. PWF = 30 minutes. Final backwash = 1 minute. Membrane = BW30. Mode = AL-FS. Error bars show standard deviation

From figure 4.7 above it is clear that the final backwashing step has a negligible effect on the fouling layer thickness. The fouling layer only decreases from 49 μm after the first backwash to 41 μm after the second backwash. Despite the gel swelling resulting in a less dense fouling layer, backwashing with 0.7 M NaCl is not enough to overcome even this lower energy barrier of removal. It is proposed that the energy of adhesion of the swollen fouling layer formed under these conditions is still too high for 1 minute of backwashing. The extent of swelling and subsequent removal of the fouling layer depends on the thickness and adhesion energy of the layer, [121]. This cleaning method could be effective under different fouling conditions, e.g. lower initial flux, lower CaCl₂ concentration, or a different membrane.

To further confirm this fouling layer swelling phenomenon, various observation techniques were used to examine the fouling layer and membrane surface. This is outlined in the next section.

4.6 Quantitative and qualitative focus on the membrane surface and fouling layer structure

4.6.1 SEM-EDS

Scanning electron microscopy energy dispersive x-ray spectroscopy (SEM EDS) imaging, was used to determine the quantity of calcium on the surface of each membrane. The surfaces examined were the virgin membrane, the membrane fouled with 200 mg/L alginic acid and 2.5 mM CaCl_2 at an initial flux of 80 L/m²h, the membrane backwashed with 0.7 M NaCl, the membrane backwashed with 0.5 M CaCl_2 , and the membranes that underwent PWF testing after NaCl and CaCl_2 backwashing (See figure 4.6). The results are displayed in table 4.5 below. Spectra for these membranes are available in appendix D.

Table 4.5: SEM EDS results: Calcium concentration produced by Carl Zeiss SIGMA HD VP Field Emission SEM and Oxford AZtec ED X-ray analysis.

Sample	Apparent Ca Concentration
Virgin membrane	0
Fouled	7.69 ± 0.49
BW 0.7 M NaCl	6.24 ± 0.11
BW 0.5 M CaCl_2	10.37 ± 0.59
BW 0.7 M NaCl + PWF	0
BW 0.5 M CaCl_2 + PWF	8.8 ± 0.32

Comparing the amount of calcium on each membrane shows that calcium does interact with the fouling layer during cleaning. The virgin membrane does not contain any calcium. The membrane was fouled with 2.5 mM of calcium which diffused into and bound with the alginate layer. The quantity of calcium decreases from 7.69 for the fouled membrane to 6.24 after backwashing with NaCl. This slight reduction of calcium concentration is due to the ion exchange that occurs during backwashing due to increased competition between the Na^+ ions in the backwashing solution and Ca^{2+} ions in the fouling layer as discussed by Lee and Elimelech, [43], who explain that ion-exchange reactions between Na^+ and Ca^{2+} results in the breakup of the alginate gel network, hence the fouling thickness after cleaning, figure 4.6. After backwashing with calcium chloride, instead of decreasing, the quantity of calcium on the membrane surface increased to 10.97. This further shows that calcium binding occurs within the alginate layer during the 1 minute backwash.

The pure water flux testing stage further reduced the calcium concentration in the fouling layer. For the fouling layer backwashed with NaCl, the calcium concentration was reduced to 0. This could be due to the osmotic pressure caused by the calcium ions in the fouling layer. Just as the water molecules enter the layer causing it to swell, the calcium ions diffuse out of the layer in the opposite direction. For the fouling layer backwashed with CaCl_2 , as predicted from figure 4.6, only slight swelling occurs and therefore the amount of calcium in the fouling layer only reduced to 8.8 as the bound Ca^{2+} ions are not released. This data shows that calcium does interfere with the fouling layer and the resulting layer has low swelling potential compared to fouling layers exposed to NaCl solutions.

4.6.2 SEM element mapping

SEM mapping is used to produce images showing the distribution of different elements on a sample. SEM mapping was used to image the surface of the fouled and backwashing membranes and the results are presented below.

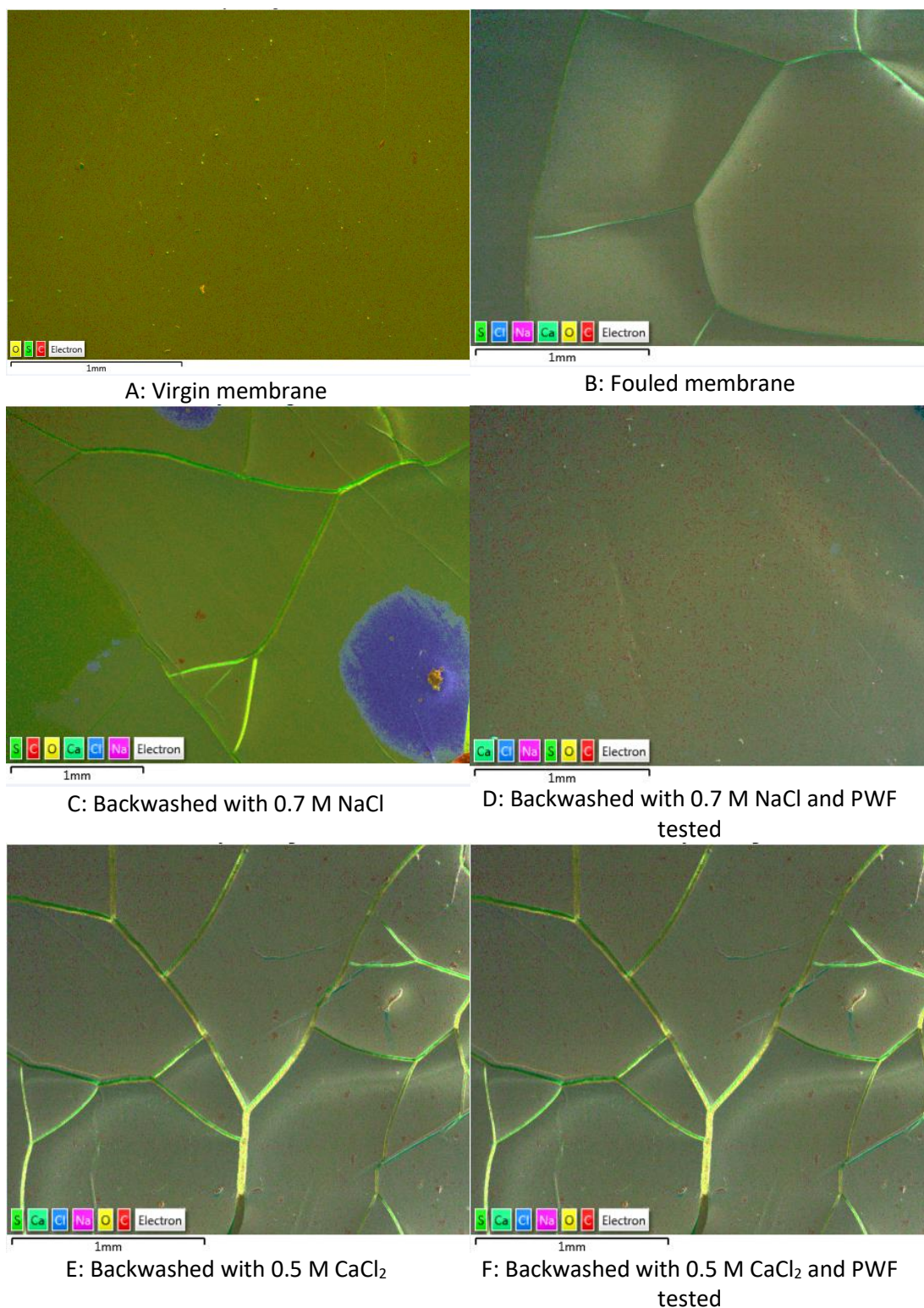


Figure 4.8: SEM mapping used to image the surface of the fouled and backwashing membranes. Note: The fouled membrane samples were left to dry and then coated overnight with carbon. This resulted in cracking of some of the fouling layers.

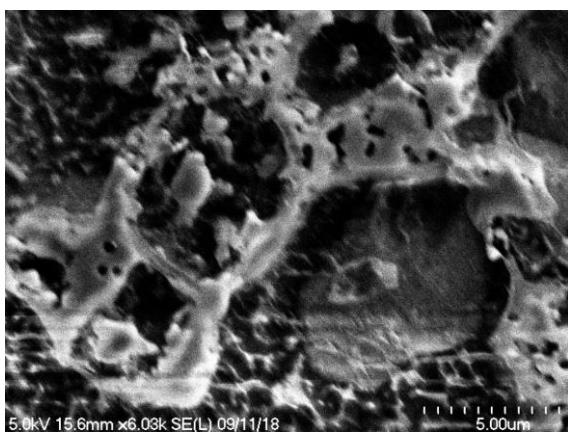
The fouled membrane (Figure 4.8.B) presents an even distribution of the elements throughout the layer. Figure 4.8.E shows that the fouling layer was evenly distributed after

the Ca^{2+} ions in the backwashing solution diffused into the fouling layer and bound with the alginate layer and after the fouling layer was exposed to deionised water (Figure 4.8.F).

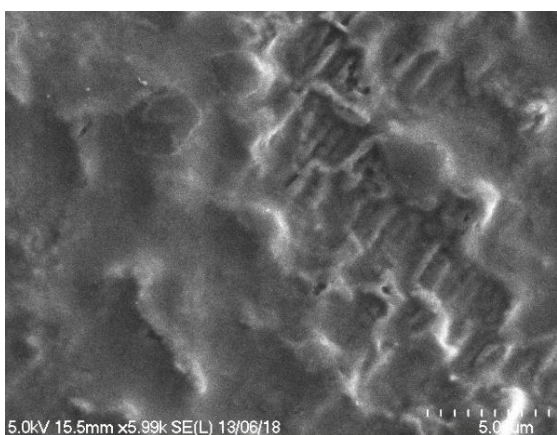
The most notable finding from elemental mapping is the element pattern on the membrane backwashed with 0.7 M NaCl (Figure 4.8.C). Localised chlorine concentration is evident, (blue patches) and the membrane surface is more visible (bright green colour). This is most likely because the fouling layer is much thinner and therefore closer to the surface, see figure 4.6. The chlorine patches potentially occurred as the fouling layer was disrupted and broken up during backwashing. Figure 4.8.D illustrates a much more even distribution of the elements after the fouling layer is exposed to deionised water for 30 minutes causing it to swell as the water molecules enter the fouling layer and dilute the solutes within it.

4.6.3 Scanning electron cryomicroscopy

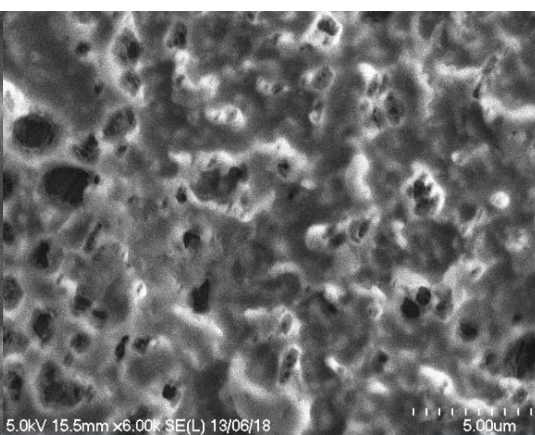
Ion interference, physical disruption and removal of the fouling layer will result in significant changes to the fouling layer structure. Scanning electron cryomicroscopy (Cryo SEM) was used to observe and compare the surface morphology of the fouled and backwashed membranes. The advantage of cryo SEM is that the samples do not need to be dried, instead the fresh samples were frozen in liquid nitrogen and imaged in the SEM. The results are shown below in figure 4.9.



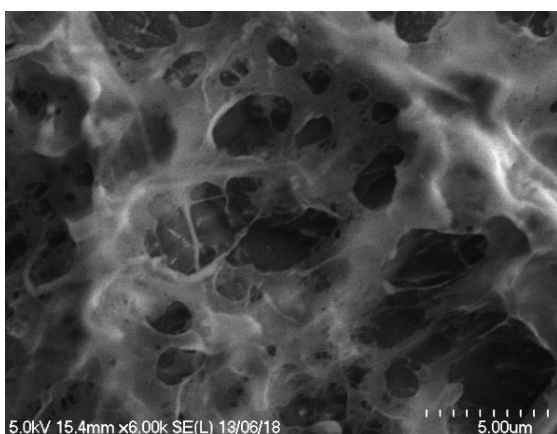
A: Fouled Membrane



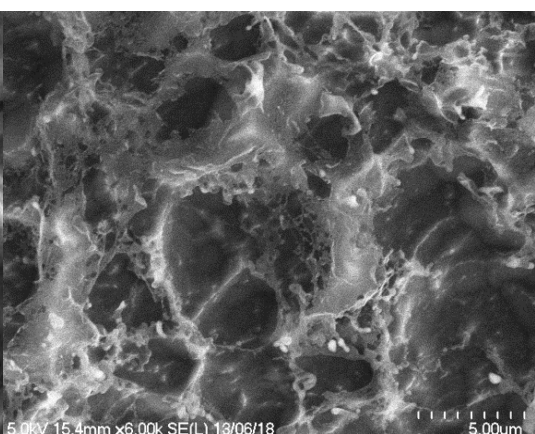
B: Backwashed with 0.7 M NaCl



C: Backwashed with 0.7 M NaCl and PWF
tested



D: Backwashed with 0.5 M CaCl₂



E: Backwashed with 0.5 M CaCl₂ and PWF
tested

Figure 4.9: Cryo SEM images of the surface of the fouled and backwashing membranes.

Each cleaning process has an effect on the morphology of the fouling layer. As the salt solution comes in contact with the fouling layer, ion exchange may occur as well as partial

removal. There is a stark contrast in appearance between the fouled membrane (Figure 4.9.A) and the membrane backwashed with NaCl (Figure 4.9.B). During backwashing the membrane is disrupted and removed (See figure 4.7) resulting in change in the fouling layer structure. Comparing figures 4.9.B and 4.9.C, after the fouling layer is subjected to PWF testing the morphology changes again. The layer is more porous in appearance. This is likely due to the swelling of the layer that occurs during the second pure water flux run after backwashing with NaCl.

There also a contrast in appearance between the fouled membrane (Figure 4.9.A) and the membrane backwashed with CaCl_2 (Figure 4.9.D). During this backwashing step the membrane is disrupted by Ca^{2+} ions interacting with and diffusing into the fouling layer (See figure 4.7) which also results in change in the fouling layer structure. Once this layer is subjected to PWF testing the morphology changes again, (Figure 4.9.E) but not to the same extent as backwashing with NaCl. This confirms that the layer in the CaCl_2 solution does not swell to the same extent as the layer in the NaCl solution. Comparing figures 4.9.C and 4.9.E, the membrane exposed to the CaCl_2 solution does not have a porous structure of that exposed to NaCl this again confirms it does not swell. More images are available in appendix C.

4.6.4 AFM Analysis

Atomic force microscopy was used to determine the elasticity and adhesive force of each fouling layer sample to see how backwashing affects these properties. The results are presented in table 4.6. Elasticity is determined from the Young's modulus: a stiff material has a high Young's modulus while a flexible material has a low Young's modulus.

Table 4.6: AFM force measurements of fouling on RO membranes. The adhesive force is a measure of how sticky the membrane sample is and is determined by the “pull-off” force of the silicon nitride tip of 60 nm radius AFM probe. The elastic force is a measure of how stiff the membrane sample is.

Sample	Adhesive Force (nN)	Elastic Force (kPa)
Virgin membrane	40.11 ± 12.37	45270 ± 16810
Fouled membrane	28.18 ± 11.46	54.41 ± 112.65
Backwashed with NaCl	66.14 ± 19.1	28475 ± 46883
Backwashed with NaCl & PWF tested	45.16 ± 26.35	3046 ± 10653
Backwashed with CaCl ₂	80.04 ± 1.63	112.03 ± 162.69
Backwashed with CaCl ₂ & PWF tested	52.34 ± 9.27	114.03 ± 172.9

The backwashed membranes display the highest adhesion forces, with the membrane backwashed with CaCl₂ displaying adhesion forces twice that of the virgin membrane, 80 ± 1.63 nN vs 40.11 ± 12.37 nN. Lee and Elimelech, [30] determined that for alginate fouling, the adhesion forces between the foulants on the membrane surface and the foulants in the bulk solution were highest in the presence of Ca²⁺ ions due to these ions forming complexes with alginate carboxyl groups. This does not explain how the fouled membrane displays the lowest adhesion forces, this is potentially due to experimental error during AFM. In both cases, PWF testing, which exposed the fouling layer to deionised water, caused the adhesive forces of the samples to decrease suggesting that some of the Ca²⁺ ions are removed during this stage of the experiment. After PWF testing the sample backwashed with NaCl exhibits adhesive forces closest to that of the virgin membrane. This supports the results obtained from SEM EDS analysis where no elemental calcium was observed on this sample, (Table 4.5).

In terms of the elastic forces, the sample backwashed with NaCl displays forces similar to that of a virgin membrane which are much higher than the fouled membrane, showing that they are stiffer. This is because the layer becomes much thinner and closer to the membrane surface, (Figure 4.4). After PWF testing, the Young’s modulus of this sample decreases as the membrane swells with water therefore becoming less rigid. The fouled membrane sample has the lowest Young’s modulus and is therefore the most flexible and “fluffiest”. After backwashing with CaCl₂ the Young’s modulus increases but remains much lower than after backwashing with NaCl. The fouling layer remains flexible after PWF testing as the elasticity does not change as little swelling occurs. This supports the results

shown in figure 4.4 as it is expected that thicker fouling layers are more flexible or “fluffier”. Raw data for these results can be found in appendix E.

The Hertz model was used to determine the elastic forces. The fit of the model was not ideal with R^2 values ranging from 0.93 for the virgin membrane to 0.77 for the membranes backwashed with NaCl and CaCl_2 and then subjected to pure water flux testing. This shows that these AFM tests need to be repeated further in order to obtain more meaning results.

4.7 Flux decline during fouling

In every experiment the membranes were fouled with 200 mg/L alginate acid and subjected to variations in either initial flux or feed solution chemistry. The fouling behaviour is illustrated in figures 4.10 and 4.11 below. Figure 4.10 illustrates flux decline due to CaCl_2 concentration.

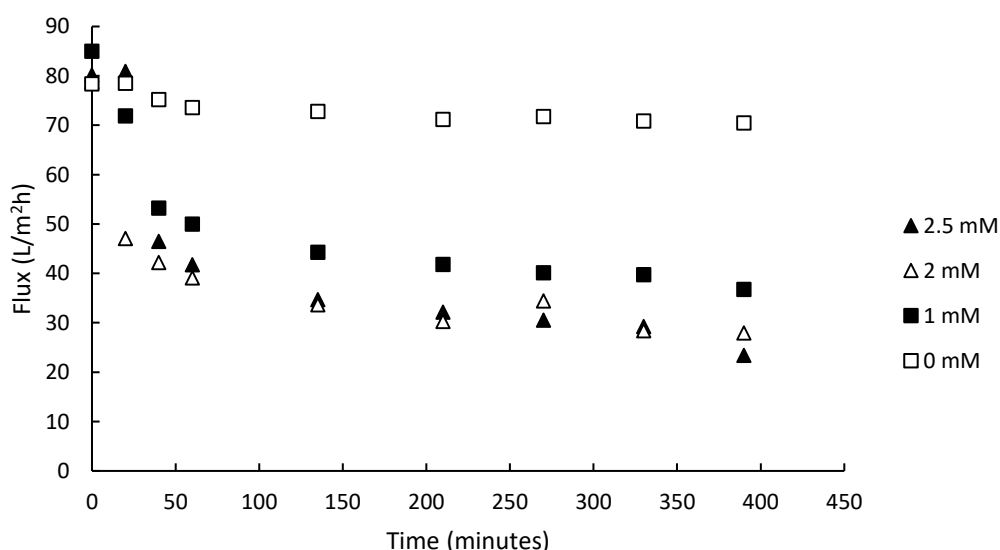


Figure 4.10: Chemical effects on fouling behaviour: Flux results of membrane samples subjected to fouling in cross-flow Fouling conditions: FS = 200 mg/L AA. Initial flux = 80 L/m²h (Applied pressure ranged from 22 to 23 bar). Fouling duration = 6.5 hours. Membrane = BW30. Mode = AL-FS.

Most of the flux reduction occurs in the first hour of the experiment. The presence and concentration of CaCl_2 has a significant influence on flux behaviour. The flux declined by only 10% in the absence of calcium compared to 69% in the presence of 2.5 mM CaCl_2 . As previously stated, this is due to formation of the thick gel layer caused by the complexation of the Ca^{2+} ions and carbocyclic groups in the alginate layer.

Figure 4.11 below illustrates flux decline due to initial flux (due to operating pressure). The initial fluxes range from 25 to 100 L/m²h. Typical RO membranes operate at 14-18 L/m²h, [122], but can operate at fluxes much higher. This study examined high fluxes to illustrate the effect fouling can have on flux in a short period of time.

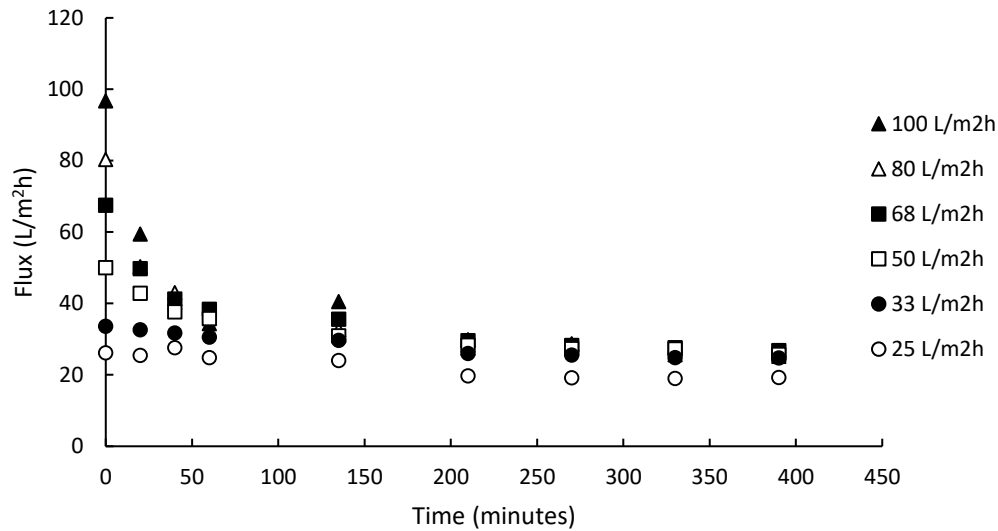


Figure 4.11: Physical effects on fouling behaviour: Flux results of membrane samples subjected to fouling in cross-flow Fouling conditions: FS = 200 mg/L AA. 2.5 mM CaCl₂. Fouling duration = 6.5 hours. Membrane = BW30. Mode = AL-FS. The initial fluxes corresponded to different membrane fluxes which were produced by adjusting the pressure for each membrane coupon. They are as follows: 100 L/m²h = 29-30 Bar, 80 L/m²h = 22-23 Bar, 65 L/m²h = 18-19 Bar, 50 L/m²h = 15-16 Bar, 30 L/m²h = 1-12 Bar, 25 L/m²h = 8-9 Bar.

Again, most of the flux reduction occurs in the first hour of the experiment. The initial flux and therefore operating pressure has a significant influence on flux behaviour. The flux declined by only 19% for an initial flux of 25 L/m²h compared to 75% for an initial flux of 100 L/m²h.

4.8 Conclusion

Osmotic backwashing alone cannot restore organically fouled reverse osmosis membrane operation completely in terms of both flux restoration and fouling layer removal. Also, although flux restorations of 100% were achieved for initial fluxes of 25 and 33 L/m²h, foulant layers of 9 µm and 25 µm remained on the membrane surface respectively. This shows that flux restoration alone cannot indicate how efficient cleaning is as high values have been reported even when significant fouling remains on the membrane surface.

Fouling removal by osmotic backwashing in reverse osmosis depends heavily on the fouling layer characteristics, namely the density due to increased pressure or calcium concentration. However backwashing efficiency does not depend on the fouling layer thickness but rather the compactness of the layer. Increasing the backwashing flux by means of a higher concentration draw solution can increase removal. However, the type of salt used in the backwashing draw solution is extremely important as even 1 minute of backwashing is enough contact time for divalent salts to diffuse into and form complexes with carboxyl groups within the alginate layer. This results in a denser fouling layer that the hydrodynamic drag force of backwashing cannot remove. Therefore flux restoration cannot be achieved.

Possible ways of improving backwashing are to increase the backwashing duration or to combine backwashing with another cleaning method such as surface flushing or air scouring. Backwashing alone may be efficient for membranes subjected to inorganic fouling, colloidal fouling, or low organic fouling conditions (e.g. low calcium concentrations in the feed and low operating pressure), but these would have to be studied in more detail.

Chapter 5: Investigating chemical free cleaning of organic fouling on forward osmosis membranes: Effects of fouling and cleaning conditions

5.1 Introduction

In chapter 4 osmotic backwashing was implemented on organically fouled RO membranes and performed to varying extents. It was found that backwashing efficiency depended on both the feed solution properties and operating pressure during fouling. Backwashing was optimal at removing fouling layers formed under low operating pressures in RO. As FO membrane processes require low or no hydraulic pressure to produce flux, it therefore has lower irreversible fouling tendency than RO, [15]. This lower irreversible fouling propensity indicates greater potential for cleaning in FO without the use of harmful chemicals. As with RO, fouling solution chemistry and membrane flux effect the rate and extent of fouling in FO, [24]. These factors will in turn effect cleaning efficiency and this will be examined in this chapter.

The use of forward osmosis (FO) membrane technology in wastewater reclamation has been reported for many different types of wastewater with encouraging results, [44, 52, 77, 99, 106, 123, 124]. As outlined in the literature review, water can be recovered from wastewater by using it as the feed solution and high salinity water such as seawater as the draw solution in FO. High salinity brines, which have recently been reported as a huge threat to the environment, [4], can be diluted to safe concentrations using FO. As the seawater draw is diluted it can then be desalinated using reverse osmosis at lower pressures. This can potentially lower energy requirements and costs [14, 41]. Gebreyohannes, et al, [44] used FO to successfully dehydrate olive mill wastewater with 98% rejection. Hickenbottom, et al, [77], used FO to reclaim 80% of water from contaminated drilling wastewater with 99% rejection of dissolved organic carbon.

However, the presence of organic contaminants in the wastewater can lead to one of the largest problems associated with membrane processes: membrane fouling. Fouling leads to a reduction in permeate quality and flux, and therefore productivity. Mi and Elimelech, [18], reported a 60% decrease in FO membrane flux in 24 hours due to organic fouling. In a

separate study [24], a 56% decrease in flux due to organic fouling in the presence of calcium was reported. Similarly, Wu et al, [124], reported a rapid decrease of flux during fouling with municipal wastewater. Therefore, research into fast and effective cleaning methods for organic fouling removal is needed. Understanding fouling behaviour during operation and cleaning is important when optimising cleaning methods for membrane processes.

Currently, both chemical and chemical free cleaning methods are carried out in membrane processes. Chemical methods include cleaning with chlorine and detergent solutions, [29, 40, 42]. However, chemical cleaning can harm the environment and damage the membrane [3, 38]. Other downsides associated with membrane cleaning are costs including the costs due to cleaning time losses. Physical cleaning is carried out by increasing the cross flow rate, air scouring or rinsing the membrane with deionised water, [17, 25, 99]. Boo et al, [25], restored 95% of the permeate flux lost due to fouling with silica nanoparticles in FO by increasing the crossflow velocity from 8.5 to 25.6 cm/s. However when the feed solution pH was increased from pH 4 to pH 9 this method was less effective as only 80% of the flux was restored. This shows cleaning efficiency is highly dependent on feed characteristics.

Valladares et al, [99], used air scouring to restore 89.5% of the initial flux of membranes fouled with natural organic matter. Motsa, et al, [17], showed that surface flushing with ultra-pure water could restore 98%, 93% and 91% of the flux for three consecutive fouling and cleaning cycles. Surface flushing is performed by simply increasing the crossflow rate across the membrane or by rinsing the surface of the fouled membrane with deionised water. Surface flushing loses efficiency after three cycles as the fouling layer becomes more difficult to remove. However, no surface imaging was carried out in any of these studies, which is important when evaluating cleaning efficiency.

Osmotic backwashing is carried out on FO membranes where the flux is reversed from the draw side to the feed side either by switching the circulating solutions or by injecting a pulse of high salt concentration into the feed side. As shown in the literature review, reports on backwashing of FO membranes produce widely varying results from unsuccessful, [52, 100], to highly effective, [17, 77, 104].

This shows that osmotic backwashing restores the initial flux to varying extents in FO due to concentration polarisation and fouling layer characteristics. These results invite studying parameters affecting osmotic backwashing efficiency using imaging as well as flux

measurements. Limited information is provided on fouling layer properties after backwashing in the literature. This study will use flux measurements and membrane imaging to obtain a more complete picture of backwashing as a method to overcome organic fouling in FO.

5.2 Chemical effect of feed solution chemistry on FO fouling and cleaning

As explained and demonstrated in chapter 4, Ca^{2+} ions form complexes with carboxyl groups present in alginic acid and therefore varying the quantity of CaCl_2 in the fouling feed solution will produce different levels of fouling with which to assess the efficiency of cleaning methods. To what extent feed solution chemistry affects chemical cleaning in FO will be assessed in this chapter.

Membrane surface flushing and osmotic backwashing with different DS concentrations were applied to FO membranes fouled with alginic acid and compared, as results presented in the literature vary widely. The membranes were fouled with different feed characteristics through the variation of CaCl_2 concentration in the feed, and their efficiency on cleaning was assessed. This is shown in figure 5.1 where differences in fouling layer thicknesses are formed through increased CaCl_2 concentration. Figure 5.2 shows representative images of the fouling layer thickness produced by the confocal microscope.

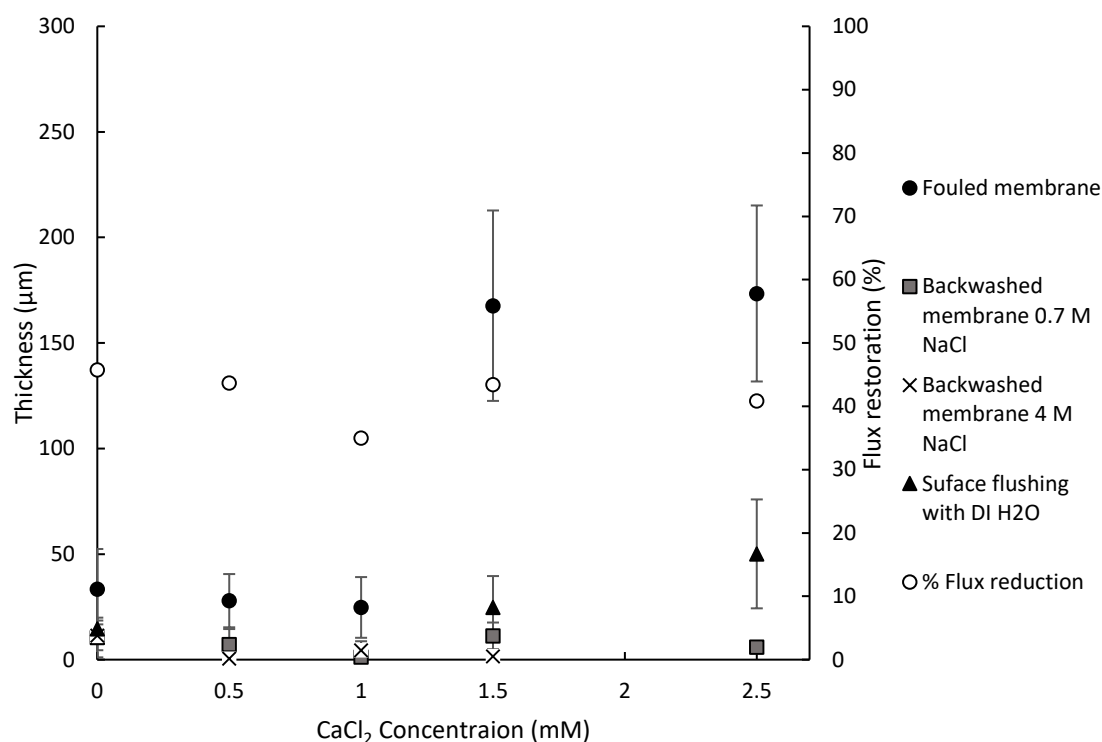


Figure 5.1: Chemical effects of fouling and cleaning in FO: Confocal microscopy results of membrane samples subjected to fouling in cross-flow showing the thickness of the fouling layer before and after cleaning. Fouling conditions: Membrane: Aquaporin Inside™. Draw = 0.7 M NaCl, Feed = 200 mg/L alginate acid, 20 mM NaCl, 1 mM NaHCO₃ and where stated, varying concentrations of CaCl₂. Fouling duration = 18 hours. Backwashing was carried out by changing the feed solution to 0.7 M NaCl and the draw solution to deionised water, thus reversing the flow through the membrane. Backwashing duration = 1 minute. Error bars show standard deviation.

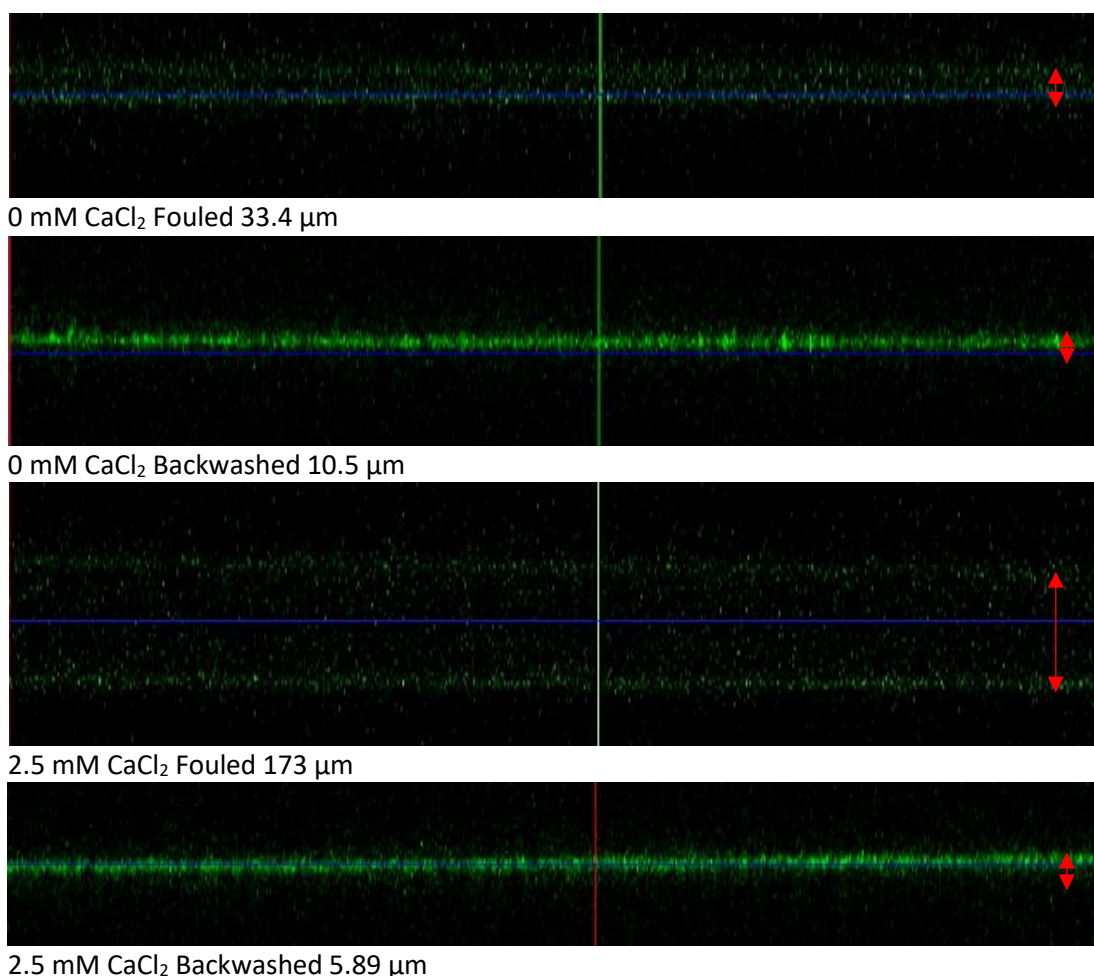


Figure 5.2: Representative confocal images of fouled and cleaned membranes. Membranes were fouled with 200 mg/L alginic acid fouling solutions with CaCl_2 solution concentrations shown.

As shown in figure 5.1, the fouling layer thickness increased from 33 μm , in the presence of 0 mM Ca^{2+} up to 1 mM Ca^{2+} , to 168 μm for Ca^{2+} concentrations higher than 1.5 mM. This occurs as Ca^{2+} forms complexes with the carboxyl groups in alginate fouling, neutralizing the negative charge of alginate molecules, resulting in a thick alginate gel layer which fouls the membrane [23, 34].

Alginate fouling layers on FO membranes have been described as loosely formed and fluffier than those for RO membranes, [18]. For this reason, the CaCl_2 concentration had little effect on the flux reduction which was 43% of the initial flux in the absence of CaCl_2 and 41% in the presence of 2.5 mM CaCl_2 despite the much thicker fouling layer produced, see figure 5.1. The fact that the much thicker fouling layer offered no resistance to flux shows that FO fouling is less detrimental to flux compared to RO fouling, as in chapter 4 it was demonstrated that the fouling layer of 179 μm resulted in a flux reduction of 69% after

just 6 hours of fouling, (See figure 4.1). Motsa et al, [17], studied organic fouling in FO and found that the deposition of alginate onto the membrane resulted in a loose and less compact fouling layer that allowed water permeation. Lee et al, [15], compared organic fouling in RO and FO and showed that the compactness and thickness of the fouling layer are the main factors controlling the flux during fouling. This shows that the FO fouling layer is softer and loosely formed and therefore doesn't contribute to the hydraulic resistance to the extent that the RO fouling layer does. The question now arises as to how this fouling layer affects cleaning efficiency.

Surface flushing for 1 minute with deionised water, which has been reported by Motsa et al, [17], to be effective for organic fouling with alginic acid for 10 hours of fouling in FO, [17], showed a reduced cleaning efficiency when increasing CaCl_2 concentration in the feed solution in this study: in the absence of Ca^{2+} , 14.6 μm of the fouling layer remained on the surface, increasing to 25 μm for Ca^{2+} concentration of 1.5 mM and 50 μm for at 2.5 mM Ca^{2+} concentration. The flux restoration showed a similar trend with an increase in calcium concentration, reducing from 97% at 0 mM Ca^{2+} to 83% at 1.5 mM and 76% at 2.5 mM Ca^{2+} . Lee and Elimelech, [30] found that adhesion forces for alginate fouling of RO membranes were highest in the presence of Ca^{2+} ions. In the absence of Ca^{2+} the flux reduced by 5% after 18 hours of fouling while concentrations of 0.05 mM and 1 mM CaCl_2 caused flux declines of 25% and 65%, respectively. Hence the higher the Ca^{2+} concentration, the higher the adhesion forces between the foulant and the membrane and the lower the surface flushing efficiency is. This explains why surface flushing eventually does not work, figure 5.1.

In terms of the use of surface flushing as a cleaning technique for FO membranes, more promising results are reported in the literature. A surface flushing duration of 15 minutes was used by Motsa et al, [17], and the crossflow rate was doubled during cleaning. In another study by Mi and Elimelech [18], surface flushing was carried out for 15 minutes and the crossflow rate was increased from 8.5 cm/s to 21 cm/s. They both achieved flux recoveries of 98% but did not use visualisation techniques to examine the membrane surface after cleaning which means that the true efficiency of this surface flushing is not known. The drawback of longer surface flushing times is higher cleaning times losses and increasing the cross flow rate will result in higher energy requirements which should be

avoided. Therefore osmotic backwashing is used to try to restore membrane performance in more extreme fouling cases.

As discussed in chapter 4, alginate gel swelling can occur due to changes in the ionic strength of the solution surrounding the gel layer. The reduction in ionic strength of the surrounding solution will result in the swelling of the layer which has been shown by Tow et al, [16], to facilitate removal. Surface flushing involves the introduction of deionised water into the feed side which may result in fouling layer swelling. However any potential swelling of the layer did not aid removal as surface flushing was deemed inadequate in this study.

The effect of high salinity pulse (HSP) concentration, and hence backwashing flux, was tested for 0.7 M and 4 M NaCl backwashing solutions. These concentrations translated to backwashing fluxes of 8.3 ± 2.9 L/m²h and 26.4 ± 3.7 L/m²h., respectively. As can be seen in Figure 5.1, both concentrations are efficient in removing the fouling layer from the membrane surface, as well as restoring the flux to $99.9 \pm 5.9\%$ and $113.1 \pm 12.8\%$, respectively, showing a superior efficiency in cleaning compared to surface flushing for a cleaning time of 1 minute. Backwashing is more efficient than surface flushing for 2 reasons. Firstly, it offers high permeate drag perpendicular to the fouling layer which can remove the layer by shear force. Secondly, exposing the fouling layer to a high salt solution during backwashing results in competition between the salts in the backwashing solution and the salts in the fouling layer resulting in ion exchange between the competing salts and therefore structural changes to the fouling layer. These structural changes weaken the fouling layer therefore making it easier to physically remove, [43]. Another important consideration is the swelling of the remaining fouling layer once it is exposed to pure water as demonstrated in chapter 4. Here, the high removal of fouling due to backwashing indicates that there is potentially a lower swelling tendency as there is very little fouling left on the surface to swell.

As already shown for RO processes, the backwashing flux increases as the fouling layer thickness increases, (shown in chapter 4). As in the case with RO, for FO, the fouling layer thickness also offered no resistance to backwashing flux. The fouling layer thickness increases from 25 μ m to 168 μ m as the CaCl₂ concentration increases from 1 to 1.5 mM. The resulting backwashing fluxes were determined to be 5.24 L/m²h and 6.25 L/m²h, respectively. As explained and demonstrated in chapter 4, the fouling layer thickness does not necessarily

offer resistance to the backwashing flux. During backwashing, the direction of the transmembrane flux is reversed by replacing the draw solution with pure water and replacing the feed solution with a high concentration of salt solution. This concentration difference is the driving force for flux. Therefore, the high concentration fouling layer will increase the concentration difference which is the driving force for backwashing flux.

As 0.7 M solution showed high efficiency for cleaning and flux recovery for all tested Ca^{2+} concentrations in the feed, providing similar results to 4 M (Figure 5.1), even lower backwashing draw solution concentrations were tested to optimize DS cleaning concentration. This is shown in figure 5.3.

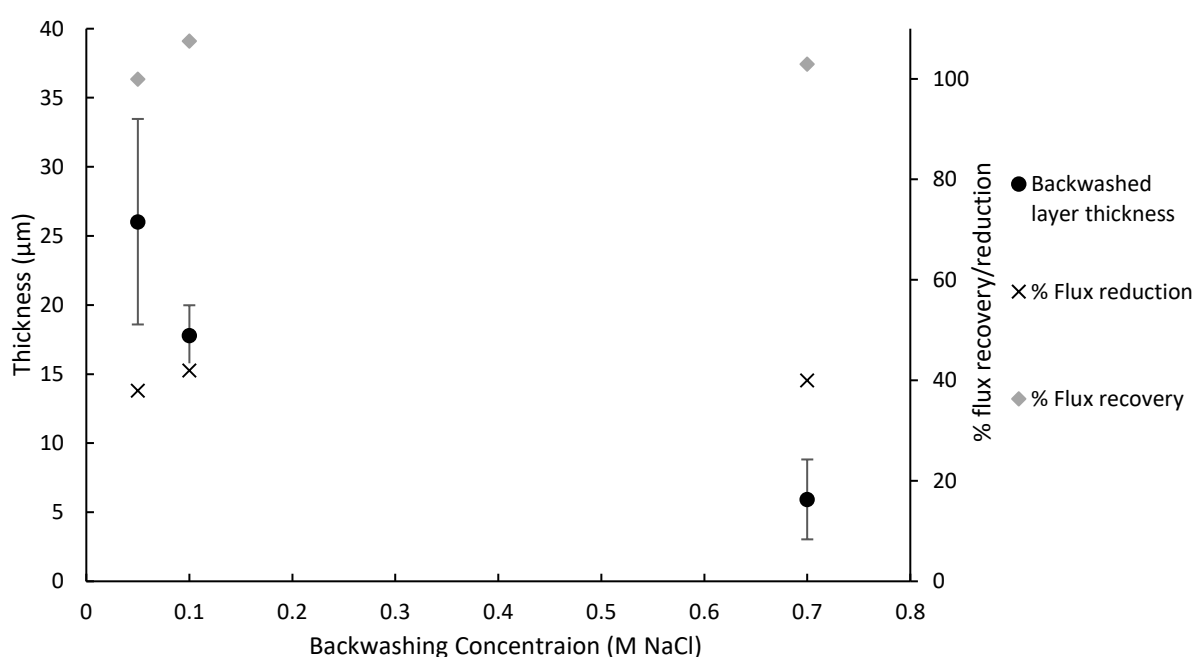


Figure 5.3: Effect of backwashing draw solution in FO: Confocal microscopy results of membrane samples subjected to fouling in cross-flow showing the thickness of the fouling layer after backwashing with 0.05 M, 0.1 M and 0.7 M NaCl. Fouling conditions: Membrane: Aquaporin inside™. Draw = 0.7 M NaCl, Feed = 200 mg/L alginate, 20 mM NaCl, 1 mM NaHCO_3 and 2.5 mM CaCl_2 . Fouling duration = 18 hours. Backwashing duration = 1 minute.

The reduction in backwashing DS concentration resulted in a reduction in the fouling removal efficiency, as thicknesses of the fouling layer after backwashing were 26 μm for 0.05 M NaCl, reducing to 18 μm for 0.1 M NaCl, reducing further to 8 μm for 0.7 M NaCl. This shows that the lower backwashing draw concentration did not offer enough permeate drag to remove the fouling layer to the same extent as 0.7 M NaCl. Flux restoration was however high for all cases with a recovery of $103.5 \pm 3.7\%$, (Note that flux recoveries of

over 100% have previously been reported in the literature, [43]. This is potentially due to any small quantities of remaining alginate fouling making the membrane surface more hydrophilic, [43, 125]) showing that despite a high flux recovery, there is still fouling on the surface, which can accumulate with subsequent fouling cycles.

All backwashing concentrations show a high efficiency but incomplete removal of fouling, with 0.7 M being the optimum. The higher backwashing solution has a higher osmotic pressure which is the driving force for permeation through the membrane. The higher permeation rate results in a higher permeate drag force to overcome the adhesion forces between the organic foulant and the membrane surface and thus detachment of the fouling layer. Also, exposing the fouling layer to a higher ionic concentration during backwashing results in greater ion exchange between the salts in the backwashing solution and the salts in the fouling layer. This causes break-up of the calcium bonds and weakening the fouling layer making it easier to remove, [43].

In chapter 4, backwashing with CaCl_2 solutions was performed and it was determined to be inefficient due to the interaction between Ca^{2+} ions in the feed solution and the alginate fouling layer which resulted in an enhanced fouling layer that could not be removed. Here, backwashing with CaCl_2 was tested to determine if it could influence alginate fouling in FO despite high removal efficiencies with NaCl backwashing. The results are shown in figure 5.4 below.

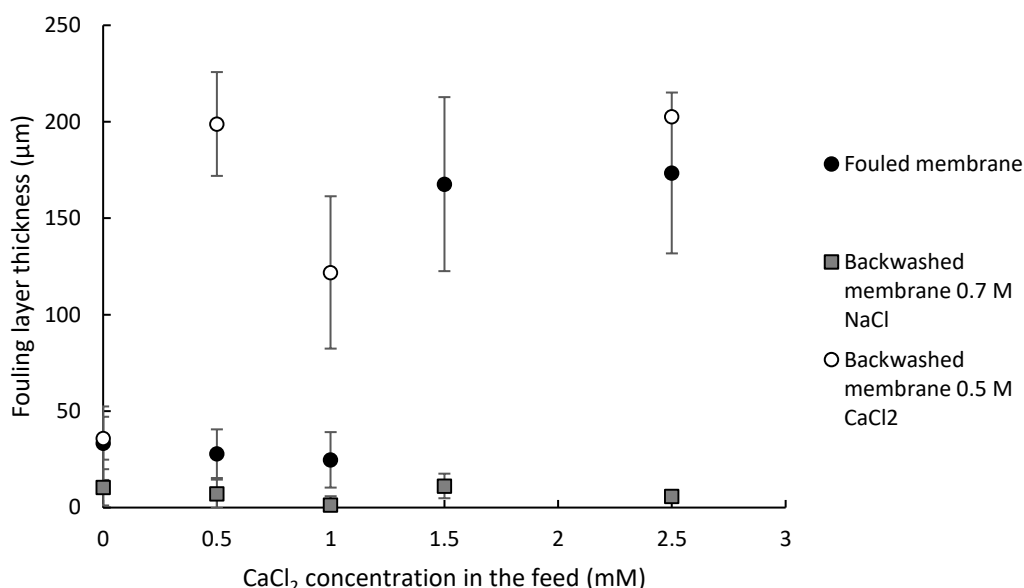


Figure 5.4: Effect of backwashing salt type in FO: Confocal microscopy results of membrane samples subjected to fouling in cross-flow showing the thickness of the fouling layer after backwashing with 0.7 M NaCl and 0.5 M CaCl₂. Fouling conditions: Membrane: Aquaporin inside™. Draw = 0.7 M NaCl, Feed = 200 mg/L alginic acid, 20 mM NaCl, 1 mM NaHCO₃ and 2.5 mM CaCl₂. Fouling duration = 18 hours. Backwashing duration = 1 minute.

Figure 5.4 above compares backwashing of membranes fouled under the same conditions with 0.7 M of NaCl to backwashing with 0.5 M CaCl₂. The 0.5 M CaCl₂ backwashing solution is ineffective at removing the fouling layer and in fact increases the fouling layer thickness. The fouling layer thickness after fouling in the presence of 0.5 mM, 1 mM and 2.5 mM CaCl₂ increased by 171 μm, 97 μm, and 29 μm respectively after backwashing with 0.5 M CaCl₂. The Ca²⁺ ions in the backwashing solution bind with the carboxyl groups in the alginate layer and increase surface adhesion as explained in chapter 4, [24, 30]. This increase in adhesion could not be overcome by the perpendicular force of the backwashing flux.

Backwashing with CaCl₂ was also inefficient at restoring the initial pure water flux of the membrane due to the increase in fouling layer thickness and adhesion energy. Flux restorations of 100%, 83%, 91% and 77% were achieved after fouling with 0 mM, 0.5 mM, 1 mM and 2.5 mM CaCl₂ respectively. This reinforces the results from chapter 4 which show that CaCl₂ is not a suitable backwashing solution as the Ca²⁺ ions in the backwashing solution will interact with the alginate fouling layer and exacerbate the effects of fouling. The high removal efficiencies of NaCl solutions show that monovalent ion solutions are superior for backwashing.

5.3 Physical effects of permeate flux on FO fouling and cleaning

The draw solution concentration during fouling was varied to increase the initial membrane flux and assess its impact on fouling and its removal, figure 5.5. Membrane flux is known to impact on the fouling characteristics by, for example, increasing fouling layer thickness with increasing membrane flux [23, 24, 86]. Therefore an assessment of how this will impact on cleaning efficiency is required.

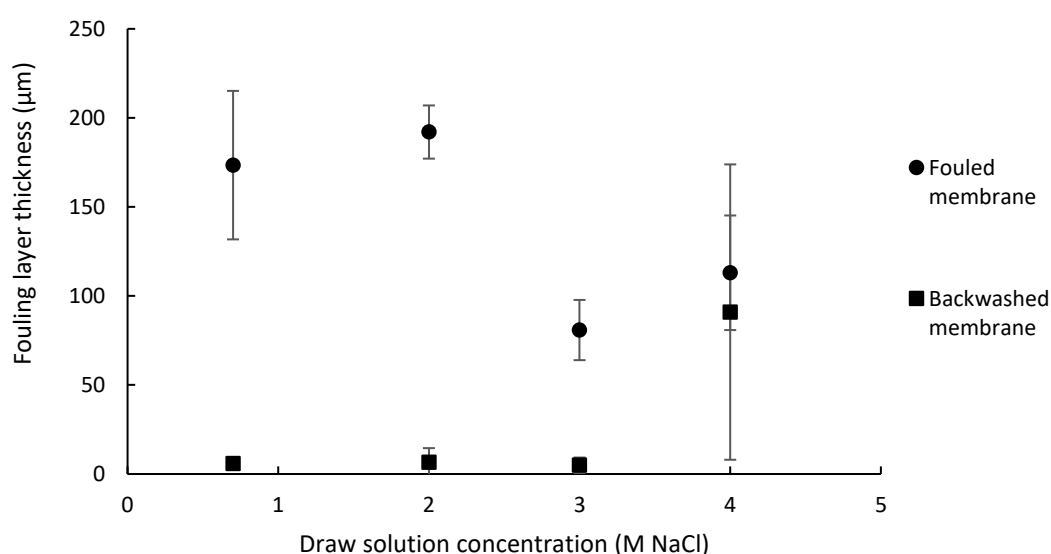


Figure 5.5: Effect of initial flux on backwashing in FO Confocal microscopy results of membrane samples subjected to fouling in cross-flow showing the thickness of the fouling layer. Fouling conditions: Membrane: Aquaporin inside™. Feed = 200 mg/L alginic acid, 20 mM NaCl, 1 mM NaHCO₃ and 2.5 mM CaCl₂. Fouling duration = 18 hours. Backwashing draw = 0.7 M NaCl. Backwashing duration = 1 minute. Error bars show standard deviation.

Figure 5.6 below shows representative images of the fouling layer thickness produced by the confocal microscope.

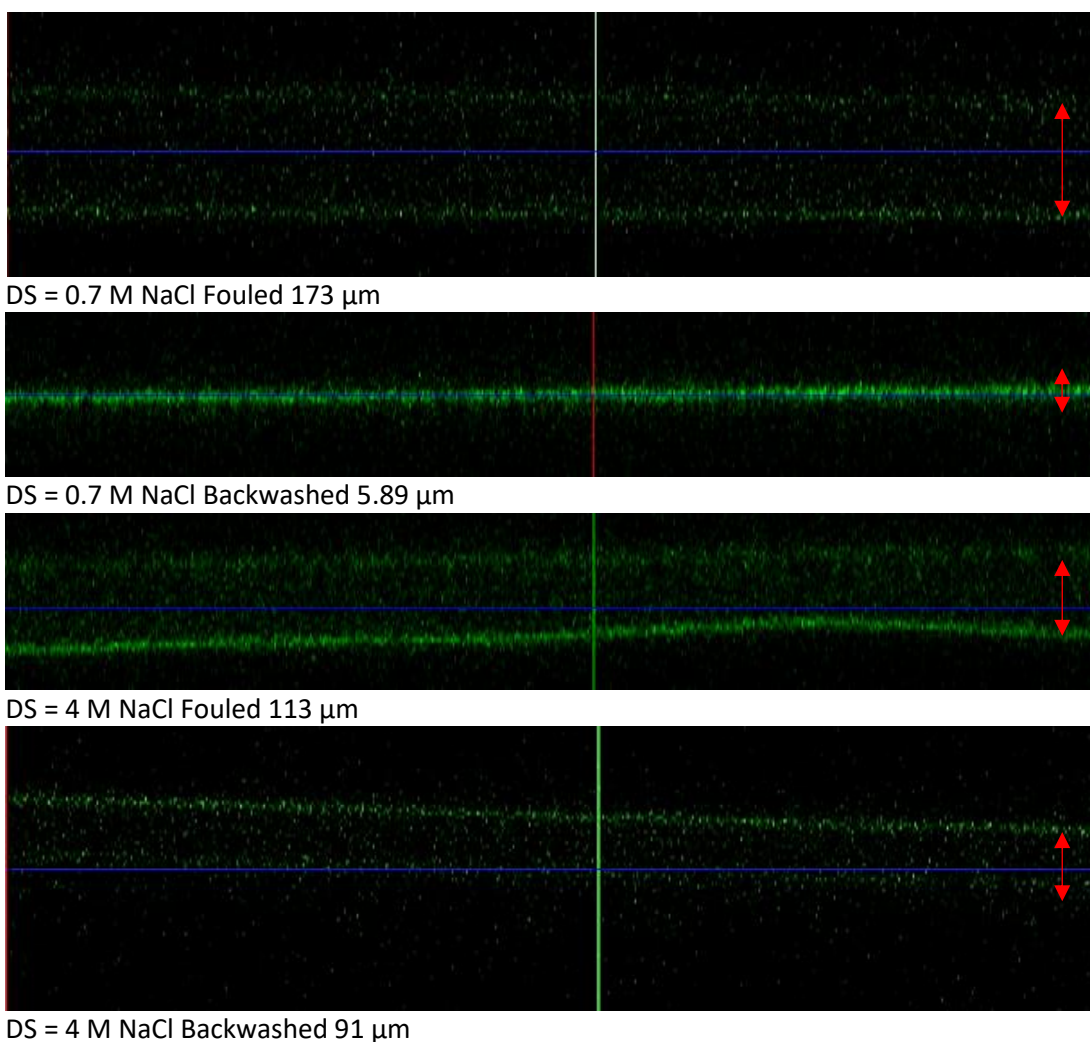


Figure 5.6: Representative confocal images of fouled and cleaned membranes. Membranes were fouled with 200 mg/L alginate acid fouling solutions with 2.5 mM CaCl_2 solution concentrations and fouling draw solutions shown.

Increasing DS concentration from 0.7 M NaCl to 4 M NaCl increases the membrane flux from 6 to 20 $\text{L}/\text{m}^2\text{h}$. This causes a reduction in the fouling layer thickness (Figure 5.5). Xie et al, [118], used confocal microscopy to show that the drag force across the membrane can contribute to compression of the alginate layer which explains the results shown in figure 5.4 where the fouling layer becomes thinner but denser. Total organic carbon analysis of the feed solution was recorded and a mass balance of carbon in the system showed that the amount of carbon deposited on the membrane surface was approximately 36.3 mgC/L and 34.4 mgC/L for draw solutions of 0.7 M NaCl and 4 M NaCl, respectively. This shows that the layer produced with 4 M NaCl in the draw is denser as it is 60 μm thinner, yet contains almost the same amount of carbon as the 0.7 M NaCl layer.

The ionic strength of the feed solution may also explain the decrease in fouling layer thickness. The draw solution concentration had a significant influence on reverse salt flux which increased from 12.1 g/m²h for a draw solution of 0.7 M NaCl, to 26 g/m²h for a draw solution of 4 M NaCl. This is due to the higher driving force for reverse salt flux due to the higher transmembrane concentration difference as per Fick's law, (equation 1.3): $J_s = B\Delta c$. This result is important as observations by de Kerchove and Elimelech, [85] determined that, in the presence of Ca²⁺ ions, increasing the monovalent salt concentration from 0 mM to 100 mM KCl resulted in an increase in alginate layer thickness from 25 nm to > 150 nm. However, when the KCl concentration was increased to 300 mM, the fouling layer thickness decreased from 150 nm to 50 nm. This is observed here also where, the reverse flux of monovalent Na⁺ ions from the draw into the feed increased the feed solution ionic strength resulting in a decrease in fouling layer thickness, figure 5.5. The increase in ionic strength due to reverse salt flux may result in de-swelling of the layer as shown in figure 4.7 where exposing the fouling layer to high and low solution concentrations resulted in fouling layer swelling and de-swelling respectively. This result reinforces the conclusion that alginate fouling layers can be unstable and therefore unpredictable.

As with RO fouling, increasing the initial flux during FO fouling will result in a higher rate of flux decline, see table 5.1.

Table 5.1: Flux decline due to increase in initial flux in FO

Draw Solution (M NaCl)	Initial Flux (L/m ² h)	Flux (t=230 minutes) (L/m ² h)	% flux decline
0.7	6	4.93	18
2	14	10.40	26
3	17	13.19	22
4	21	14.19	32

As the Initial flux was increased from 6 L/m²h to 21 L/m²h, the % flux decline increased from 18% to 32%. This is due to two factors. Firstly, as with RO, the higher initial flux offers higher perpendicular force on the membrane surface resulting in a denser fouling layer, (figure 5.5) that exhibits a higher resistance to flux. Secondly, unlike in RO, an increase in draw solution concentration will result in an increase in reverse salt flux and therefore an

increase in internal concentration polarisation (ICP). ICP occurs in the membrane support where the solute concentration differs on the boundaries of the support layer (see figure 2.3 in the literature review, chapter 2). This reduces the osmotic pressure difference across the active layer and reduces the flux [70, 71]. Therefore the increase in the rate of flux decline is due to both the increase in initial flux and the increase in ICP.

The initial fluxes of 14 L/m²h and 17 L/m²h result in similar flux declines (Table 5.1) and backwashing is effective for both of these initial fluxes in terms of flux restoration and fouling layer removal (Figure 5.5). This suggests that the larger thickness of the 2 M fouling layer and the higher density of the 3 M fouling layer offer similar resistance to flux and submission to backwashing.

100% of the fouling was removed for the draw solution of 0.7 M NaCl. For the cases of 2 M and 3 M draw solutions, only 6.6 µm and 4.9 µm of fouling remained on the membrane surface after backwashing. Cleaning with 0.7 M NaCl is hence effective for all draw solutions tested, as can be seen in figure 5.4, with the exception of the 4 M NaCl draw solution. At a draw solution of 4 M NaCl, 91 µm of the fouling layer remained on the surface showing that the fouling layer cannot be removed with 0.7 M NaCl backwashing. The fouling layer was too dense and compact with adhesion forces potentially too high for the backwashing flux to overcome. A higher backwashing solution concentration or a longer backwashing duration could potentially remove this fouling layer completely.

In all cases, the flux was fully restored, including for 4 M NaCl draw solution, despite 91 µm of fouling remaining on the membrane surface, showing once again that complete flux recovery does not translate into a total removal of the fouling layer. This result again shows the importance of surface imaging to determine the true efficiency of membrane cleaning methods as flux restoration alone could suggest that cleaning was efficient at completely removing the fouling layer.

Although fluxes were largely restored and only a small amount of fouling remained on the membrane, this remaining fouling could affect subsequent fouling adhesion and flux decline rates. As shown by Lee and Elimelech, [30], adhesion forces are proportional to fouling rate. Therefore even a small number of adhesive sites due to organic matter fouling on the membrane surface can increase membrane fouling potential and therefore potentially decrease subsequent cleaning efficiency [18].

In order to determine if the remaining fouling layer affects further membrane fouling and cleaning in forward osmosis, five consecutive fouling and cleaning cycles were performed. This is outlined in the next section.

5.4 Fouling and cleaning cycles

In order to test the true efficiency of osmotic backwashing, it should be tested for numerous consecutive fouling and cleaning cycles as adhesive sites of fouling on the surface increases membrane fouling potential and decrease cleaning efficiency [18]. The fouling and backwashing experiment was repeated for five consecutive cycles, where the fouling was carried out for 22 hours with a draw solution of 0.7 M NaCl for each cycle. The feed solution of the highest fouling propensity was used which is a feed solution of 200 mg/L alginic acid and 2.5 mM CaCl_2 , (See figure 5.1). Fouling was followed by 1 minute of backwashing with 0.7 M NaCl as this was determined to be the optimum backwashing draw, (Figure 5.3). At the end of the 5 cycles the PWF was retested.

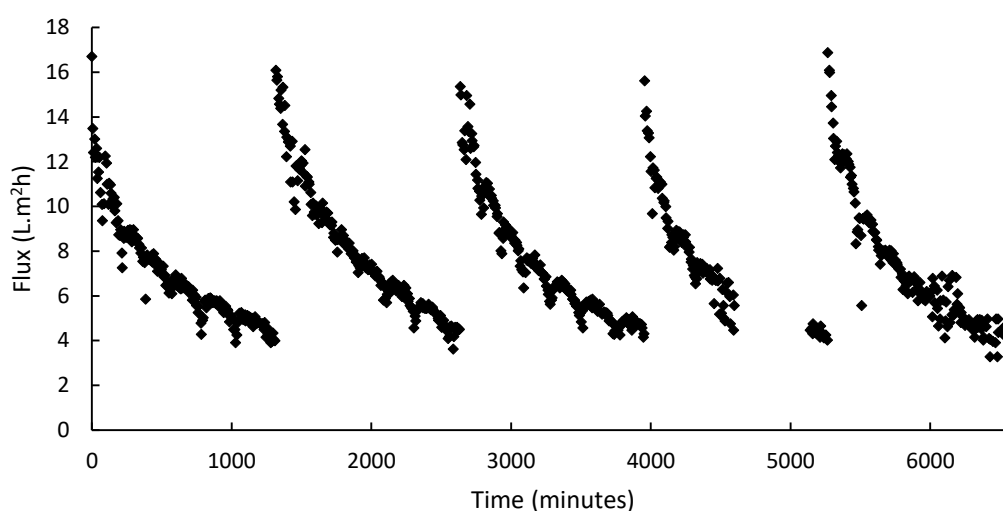


Figure 5.7: Flux decline of membranes subjected to five consecutive cycles of fouling and cleaning in crossflow. Fouling conditions: Membrane: Aquaporin Inside™. Draw = 0.7 M NaCl. Feed = 200 mg/L alginic acid, 20 mM NaCl, 1 mM NaHCO_3 and 2.5 mM CaCl_2 . Fouling duration = 22 hours. Backwashing draw = 0.7 M NaCl. Backwashing duration = 1 minute.

For every 22 hour cycle, the membrane flux decreases from around 16 $\text{L/m}^2\text{h}$ to 4 $\text{L/m}^2\text{h}$. The flux is restored to 16 $\text{L/m}^2\text{h}$ after each 1 minute backwash with 0.7 M NaCl. The reverse salt flux remained relatively consistent for each cycle also, increasing only slightly from 18 $\text{g/m}^2\text{h}$ in cycle 1 to 20 $\text{g/m}^2\text{h}$ in cycle 5. This shows that the fouling behaviour remains consistent throughout each cycle which shows that backwashing is very effective.

The backwashing flux decreased after 3 cycles from 33.8 ± 5.9 L/m²h to 19.4 ± 1.1 L/m²h in the next 2 cycles. The layer may become more resistant to backwashing after numerous cycles. However this backwashing flux is still enough to remove the fouling layer after 5 cycles. This is accompanied by a remaining fouling layer thickness of 3.07 ± 1.97 μm and a reduction of flux restoration from 103 to 97%. The high reversibility due to backwashing is due to the loose fouling gel layer on the membrane surface [18].

This result is similar to those reported by Motsa et al, [17], who used backwashing to restore 100%, 99% and 93% of the flux after cleaning cycles 1, 2, and 3 respectively for organically fouled membranes. Recovery reduces with each cycle, probably due to the fouling layer remaining on the membrane surface.

To further test the efficiency of osmotic backwashing, it was tested for five consecutive fouling and cleaning cycles at a higher permeate flux to test if the higher fouling potential would decrease the backwashing efficiency. The fouling and backwashing experiment with a draw solution of 4 M NaCl (see figure 5.8) was repeated for five consecutive cycle to examine how the 91 μm fouling layer remaining on the membrane surface (figure 5.4) will affect further fouling and cleaning. Once again, the feed solution of the highest fouling propensity was used which is a feed solution of 200 mg/L alginic acid and 2.5 mM CaCl₂, (See figure 5.1). Fouling was followed by 1 minute of backwashing with 0.7 M NaCl to compare the results with those of the lower permeate flux, (Figure 5.5). At the end of the 5 cycles the PWF was retested.

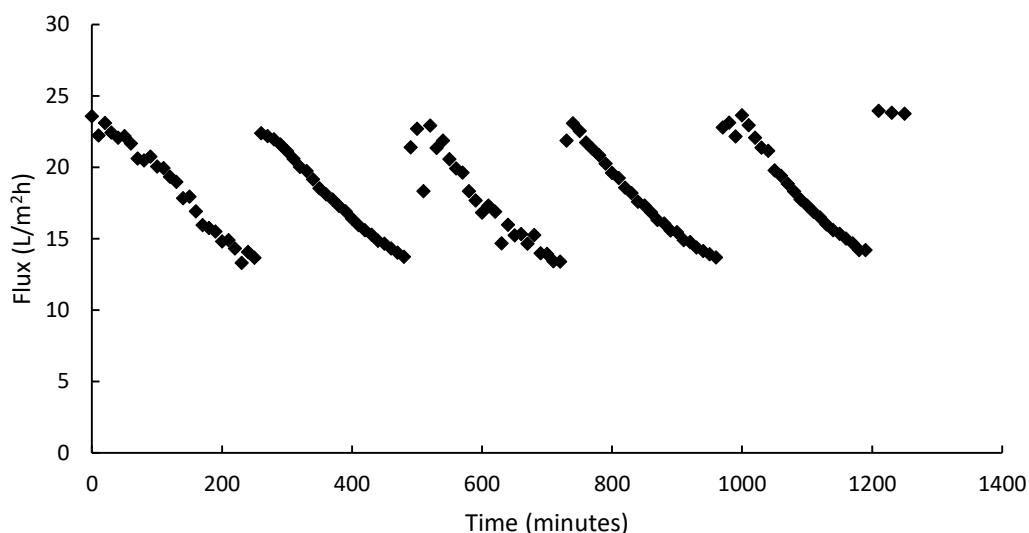


Figure 5.8: Flux decline of membranes subjected to five consecutive cycles of fouling and cleaning under higher permeate flux rates. Fouling conditions: Membrane: Aquaporin Inside™. Draw = 4 M NaCl. Feed = 200 mg/L alginic acid, 20 mM NaCl, 1 mM NaHCO₃ and 2.5 mM CaCl₂. Fouling duration = 4 hours. Backwashing draw = 0.7 M NaCl. Backwashing duration = 1 minute.

The results shown in figure 5.8 are promising and similar to those for the lower fouling flux (figure 5.7). The pure water flux was determined to be 23.6 L/m²h. For every 4 hour cycle, the membrane flux decreases from around 22.5 L/m²h to 14 L/m²h. The flux is restored after each 1 minute backwash with 0.7 M NaCl. The similar rate of fouling shows that the fouling layer remaining on the membrane surface had no effect on the flux even after 4 subsequent fouling experiments.

Total organic carbon analysis of the feed and draw solutions at the start and end of each experiment was used to perform a mass balance of carbon in the system and showed that the amount of carbon accumulated on the membrane was approximately 37.5 mgC/L for cycle 1 and 37.4 mgC/L for cycle 5, again showing that the rate of fouling did not change significantly as repeat fouling took place. Recall that the reverse salt flux of a membrane fouled with a 4 M NaCl draw solution was 26 g/m²h. Subsequent fouling cycles resulted in similar reverse salt fluxes of 22.2 ± 1.4 g/m²h.

The backwashing flux was also relatively unaffected decreasing from 18 L/m²h to 16 L/m²h for cycles 1 and 5 respectively. Being able to maintain a constant backwashing flux is important as each backwashing cycle is optimal and has a high enough permeate drag to remove the fouling layer.

Osmotic backwashing is a good cleaning technique for organically fouled forward osmosis membranes even under extreme fouling conditions and subjected to numerous fouling and cleaning cycles. This is because the fouling layer is loosely formed in the absence of applied pressure and therefore its effects are easier to reverse.

5.5 Flux decline during fouling

In every experiment, the membranes were fouled with 200 mg/L alginic acid and subjected to variations in either initial flux by varying the draw solution concentration or feed solution chemistry by varying the CaCl_2 concentration in the feed. The fouling behaviour is illustrated in figures 5.9 and 5.10 below. Figure 5.9 illustrates flux decline due to CaCl_2 concentration.

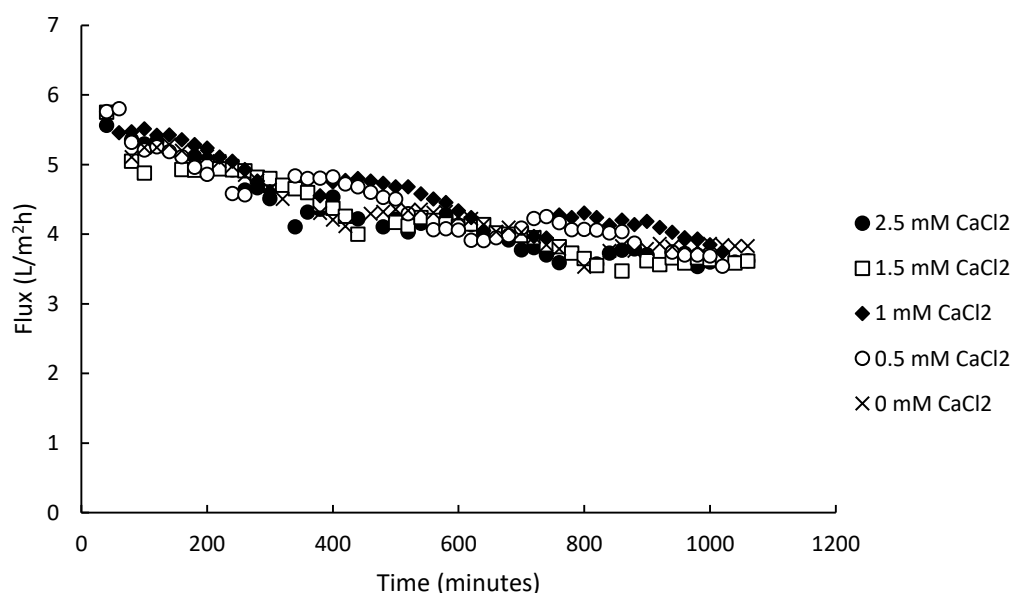


Figure 5.9: Chemical effects on fouling behaviour in FO: Flux results of aquaporin membrane samples subjected to fouling in cross-flow Fouling conditions: FS = 200 mg/L AA. DS = 0.7 M NaCl. Fouling duration = 18 hours. Membrane = Aquaporin Inside™. Mode = AL-FS. Note that as previously stated, the initial flux is much lower here than in figure 5.5 due to a change in the membrane speciation following updates in the manufacturing process.

The flux reduces at a constant rate throughout the experiment. The presence and concentration of CaCl_2 does not have a significant influence on flux behaviour. As previously described, alginate fouling layers on FO have been described as loosely formed and fluffier than those for RO membranes, [18]. For this reason, the CaCl_2 concentration had little effect on the flux reduction which was 43% of the initial flux in the absence of CaCl_2 and

41% in the presence of 2.5 mM CaCl_2 this is due to the low fouling potential of the forward osmosis process.

Figure 5.10 below illustrates flux decline due to initial flux which was changed by varying the draw solution concentration.

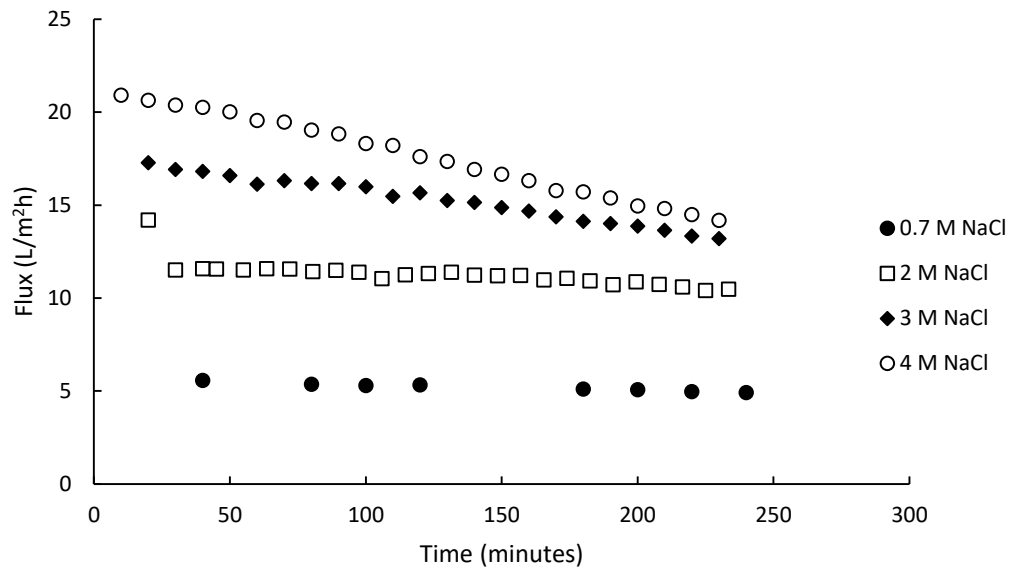


Figure 5.10: Physical effects on fouling behaviour in FO: Flux results of membrane samples subjected to fouling in cross-flow Fouling conditions: FS = 200 mg/L AA. 2.5 mM CaCl_2 . Fouling duration = 4 hours. Membrane = Aquaporin Inside™. Mode = AL-FS.

Again, reduction occurs at a constant rate throughout the experiment. The initial flux and therefore the draw solution has a significant influence on flux behaviour. For a draw solution of 0.7 M NaCl the initial flux decreased from 6 L/m²h to 4.5 L/m²h after 4 hours. For a draw solution of 4 M NaCl the flux reduced from 21 L/m²h to 14.2 L/m²h. As already stated, this is due to both a denser fouling layer that exhibits a higher resistance to flux, and an increase in reverse salt flux and therefore internal concentration polarisation due to the increase in draw solution concentration.

5.6 Conclusion

Osmotic backwashing is an effective cleaning technique which restores organically fouled forward osmosis membrane operation completely in terms of both flux restoration and fouling layer removal. This is due to the soft, loosely formed fouling layer formed in the absence of pressure which is easier to remove by reversing the flow of water through the membrane. While increasing the calcium concentration from 0 to 2.5 mM increased the fouling layer thickness from 33 to 173 μm , backwashing with 0.7 M NaCl for just 1 minute effectively removed the entire fouling layer and restored 100% of the flux in both cases. Backwashing with 0.7 M NaCl was just as effective as backwashing with 4 M NaCl. However surface flushing alone with deionised water only restored 76% of the flux for the membrane fouled with 2.5 mM CaCl_2 . This showed that both the ionic interactions between the backwashing solution and the fouling layer and the perpendicular drag force caused by the backwashing solution are important for effective membrane cleaning.

The limits of backwashing in FO processes were discovered when the draw solution during fouling was increased to 4 M NaCl. The increase in draw solution concentration lead to an increase in flux which resulted in a more compact and dense layer of 113 μm thickness. Backwashing with 0.7 M NaCl only removed 22 μm of this fouling layer. Despite this poor removal rate, 100% of the initial flux was restored. This reinforces one of the conclusions from chapter 4 which is that flux measurements alone cannot guarantee effective cleaning in membrane processes.

In order to test the true efficiency of backwashing in FO processes, 5 consecutive fouling and backwashing cycles were performed with fouling draw solutions of 0.7 M and 4 M of NaCl. In both cases 100% of the flux was restored after 5 cycles. This shows that osmotic backwashing is a very effective technique in FO processes due to the lack of applied pressure during fouling. The resulting loose fouling layer can be removed easily in most cases by just 1 minute of backwashing. This eliminates the need for cleaning chemicals and reduces the time lost to cleaning.

Chapter 6: Factors effecting osmotic backwashing efficiency of forward osmosis membranes subjected to initial bacterial adhesion

6.1 Introduction

As already discussed, membrane fouling is a serious and unavoidable challenge for membrane processes. Membrane fouling with organic material was discussed and it was shown that cleaning by osmotic backwashing is an effective technique for fouling reversal in FO processes. Raw wastewater and seawater also contain a lot of diverse microbial species that can cause an even more severe type of fouling: biofouling.

Biofouling is the accumulation of bacteria and other microorganisms in the membrane surface and it is particularly severe in membrane processes due to the strong adhesion of the microorganisms to each other and to the membrane surface and the excretion of exopolymeric substances (EPS) resulting in the formation of a biofilm [8, 88]. EPS is made up of polysaccharides, proteins, nucleic acids, lipids, and other polymeric compounds, [89]. Biofouling occurs in two stages. Firstly, initial surface adhesion of the bacteria onto the membrane followed by further development of a biofilm. In order for the initial adhesion to occur, the energy barrier between the negatively charged cells and the negatively charged membrane surface needs to be overcome, [79]. Mass transport of the cells towards the membrane surface occurs as water permeates from the feed to the draw side. This brings the cells in close proximity to the membrane surface where forces such as Van der Waals attraction forces, electro- static forces, hydrophobic interactions and steric forces allow adhesion to occur, [126]. Adhesion is advantageous for the cells as it is easier for them to survive and nutrients tend to accumulate on solid surfaces including membranes due to the effects of concentration polarisation, [35, 127]. This primary adhesion stage is described as reversible, [35, 79]. The subsequent development of the biofilm after initial adhesion occurs as the community of adhered cells become enclosed in a self-produced 3 dimensional exopolymer matrix and protects them. This strong biofilm is therefore irreversible, [35], and has a serious impact on membrane processes.

In membrane processes, the biofilm coats the membrane surface resulting in greater resistance to flux and therefore disruption of the performance including reduction of permeate flux and quality, [8]. In 2001, Abdul Azis et al, [128], estimated that biofouling cost the desalination industry 10 billion pounds in the effort to fight its effects. It is therefore necessary to find an effective method of biofouling control in membrane processes.

As discussed in chapter 5, forward osmosis (FO) membrane technology can be used to reclaim wastewater and encouraging results have been reported in the literature with many different types of wastewater explored, [44, 52, 77, 124]. This could potentially lower the pressure requirements associated with RO desalination resulting in lower fouling potential and therefore a more reversible fouling layer as shown in Chapter 4.

Biofouling of RO membranes has been widely reported in the literature. Kwan et al, [80], reported a 30% decrease in RO membrane flux due to biofouling with *Pseudomonas aeruginosa* for 17-18 hours. Herzberg and Elimelech, [129], reported a flux decline of over 80% caused by the same bacteria for 19 hours. This shows the negative effect biofouling has on RO membrane performance and as well as the severe reduction in flux, biofouling in RO is largely irreversible. Creber et al, [109], reported that chemical cleaning of biofouled RO membranes with NaOH and sodium dodecyl sulphate was not efficient at removing the fouling layer. Also chemical cleaning with chlorine has been shown to damage the selective layer of the membrane and therefore reduce the permeate quality, [3, 6]. Cleaning of biofouled RO membranes through osmotic backwashing has been demonstrated by Bar-Zeev and Elimelech, [102]. They used a 50 to 60 second pulse of 1.5 M NaCl to clean RO membranes fouled with artificial wastewater and *Pseudomonas aeruginosa*. This cleaning method restored 80-90% of the flux but could not completely remove the fouling layer. Effective measures to reduce the effects of biofouling are therefore necessary and the method of introducing forward osmosis prior to RO could reduce the high pressures required in RO and therefore its irreversible fouling propensity.

Limited information on biofouling of forward osmosis membranes has been reported in the literature. Kwan, et al, [80], reported a 10% flux decline for FO membranes fouled with 2×10^6 CRU/ml *Pseudomonas aeruginosa* for 18 hours. Yoon et al, [81], reported a 20% reduction in flux after fouling for 55 hours with 10^7 CRU/ml of the same bacteria. This is significantly lower than the 80% reduction in flux reported by Herzberg and Elimelech for

RO fouling [129]. The lower fouling potential in FO processes is due to the lack of applied pressure on the membrane FO compared to the high pressures in RO. This has been explained in terms of organic fouling, [15] and biofouling [80].

The lower fouling potential in FO compared to RO means that FO fouling is largely reversible while RO fouling is more challenging to remove as shown in this thesis and various reports in the literature, see table 2.3 in the literature review section. However, limited information is provided in the literature on chemical free cleaning of biofouled FO membranes. Zhang et al, [82], reported an over 45% flux decline due to biofouling of a forward osmosis membrane bioreactor. They used intervals of 15 minutes of tap water rinsing to mitigate the biofouling but after approximately 70 hours of fouling this method was no longer effective. Water rinsing offers shear force across the surface of the membrane but not perpendicular force or any chemical reaction that could weaken the fouling layer. For this reason it is inefficient at removing severe fouling.

Osmotic backwashing, which offers both perpendicular force and salt interaction between the fouling layer and the backwashing solution has been demonstrated in chapters 4 and 5. In the literature it has been used to mitigate fouling in FO for many different types of foulant to varying extents, [17, 99, 100]. In terms of biofouling control however, little work has been performed with backwashing of FO membranes as of yet. Yoon et al, [81], fouled FO membranes with 10^7 CRU/ml of *Pseudomonas aeruginosa* in the presence of 10 mM NaCl and 1 mM CaCl_2 . They used physical stress with increased crossflow rate from 4 to 33 cm/s and induced osmotic backwashing by replacing the feed solution with 4 M NaCl and the draw with deionised water but neither of these methods restored the flux. This shows that reversal of biofouling is very difficult even in FO processes.

This prompts the need for more research into bacteria adhesion and biofouling in forward osmosis and also into the development of efficient and cost effective cleaning techniques to restore membrane performance and prolong membrane life.

A different approach to osmotic backwashing of biofouled membranes is therefore necessary to improve its performance. Creber et al, [109], showed that the earlier chemical cleaning with sodium dodecyl sulphate and NaOH is carried out in RO, the more effective the cleaning is. This is due to the extent of the development of the biofilm the membrane surface. The more mature the biofilm, the more resilient it is to cleaning. It is therefore potentially more worthwhile to examine backwashing during the initial bacterial adhesion

stage of the biofouling. Implementing backwashing before the biofilm has a chance to develop, may help control the extent of biofouling effectively.

The aim of this study is to examine osmotic backwashing as a method to control initial bacterial adhesion (bioadhesion) in FO. For the purpose of this research, initial adhesion of *Pseudomonas putida* on aquaporin based forward osmosis membranes was performed and osmotic backwashing was carried out on the fouled membranes. This study will use flux measurements and membrane surface imaging to determine backwashing efficiency under different adhesion and backwashing conditions.

6.2 Effect of osmotic backwashing draw solution concentration on bacteria removal

It is anticipated that mass transfer of the water in the opposite direction of adhesion during backwashing will remove adhered cells from the membrane surface thus preventing further biofouling from developing. The effectiveness of backwashing to remove the bacteria cells was tested.

Different NaCl backwashing draw solutions of varied concentrations were applied to membranes subjected to initial bacterial adhesion to determine an optimal draw concentration for efficient cleaning. Membranes were subjected to bioadhesion under the same conditions and the backwashing draw cleaning efficiency was assessed. Higher backwashing draw solution concentrations will result in higher transmembrane flux, see table 6.1, during cleaning and therefore potentially higher bacteria removal rates. This is shown in figure 6.1 where the removal efficiency increased with NaCl concentration in the draw solution.

Table 6.1: Backwashing fluxes for increasing NaCl draw solution concentrations in FO

Concentration (M NaCl)	Backwashing flux (L/m ² h)
0.1	8.65
0.7	20.17
1.5	31.00
2	30.25
3	36.00

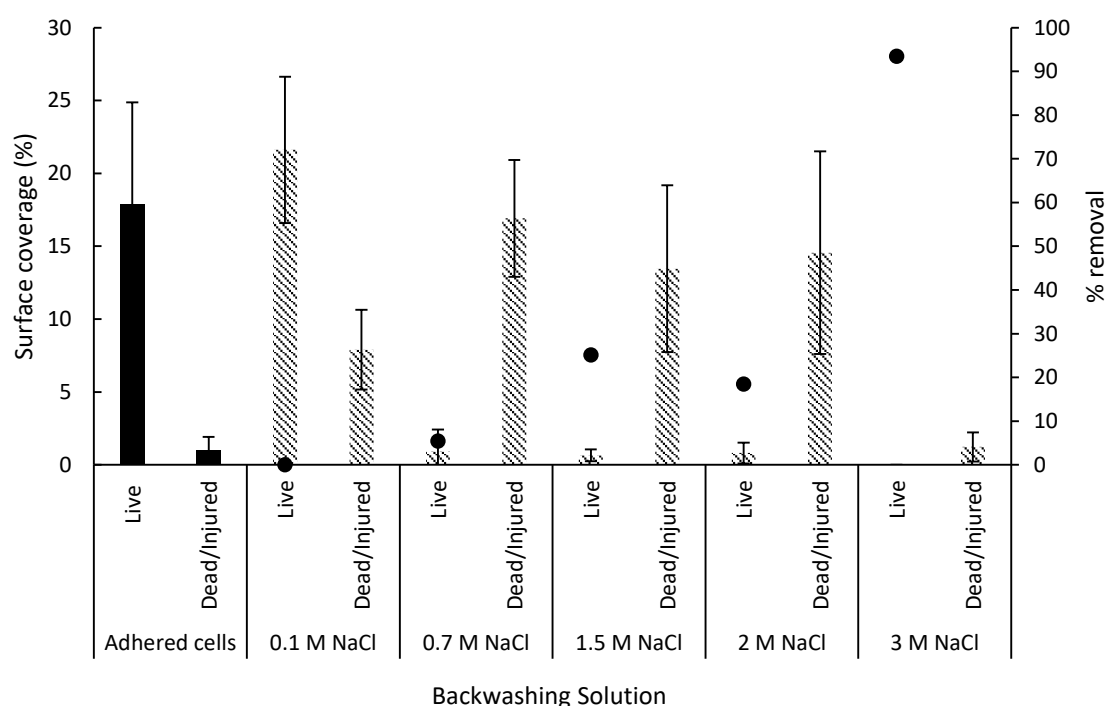


Figure 6.1: Effect of backwashing solution concentration for cell removal in FO: Microscopy results of membrane samples subjected to bacteria adhesion in cross-flow showing % surface coverage of live and dead cells and % removal of all cells on secondary axis. Fouling conditions: Membrane: Aquaporin inside™. Draw = 0.7 M NaCl Feed = 200 ml of media containing *P. Putida* (10^7 cells/ml) in 0.1 M NaCl. Adhesion duration = 30 minutes. Backwashing duration = 1 minute. Error bars show standard deviation of the count determined from 10 areas on the membrane surface.

For each adhesion stage, 30 minutes of adhesion resulted in an average membrane surface coverage of 17.9% live cells and 0.98% dead/injured cells, see figure 6.1. Initial bioadhesion in FO has not yet been reported in the literature. However the adhesion rates in figure 6.1 are expected to be severe in comparison to most FO membranes due to the extremely hydrophobic nature of the Aquaporin Inside™ membrane surface. Li and Logan, [130] show that hydrophobicity of a surface can increase bacterial adhesion. The active layer of the aquaporin membrane is extremely hydrophobic with a contact angle of 96.2 ± 5.5 degrees, compared to that of the popular Hydration Technology Innovations cellulose triacetate FO membrane which has an active layer contact angle of just 62 ± 7.2 degrees, [131]. It is therefore expected that this is a severe case of adhesion after just 30 minutes.

To further show that the Aquaporin Inside™ membrane is particularly susceptible to bacterial adhesion it can be compared to pressure driven membrane processes. Semião et

al, [132], examined the effects of permeate flux on initial bacteria adhesion of *Pseudomonas fluorescens* on a number of nanofiltration and reverse osmosis membranes for 30 minutes. They found that for both ESNA LF and ESNA LF2 membranes, with contact angles of 68.8 ± 0.6 degrees and 62.4 ± 0.6 degrees respectively, [132], the surface coverage was less than 20% for a flux of 15 L/m²h. They showed that for NF90 membranes (contact angle 58.4 ± 0.6 degrees, [132]) the surface coverage was roughly 15% and for BW30 membranes (contact angle 8.2 ± 0.5 degrees, [132]) it was less than 10% for a flux of roughly 15 L/m²h. In this case, the membrane flux was 16 L/m²h and resulted in surface coverage 17.9% live cells despite the lack of applied pressure. The lower adhesion rates reported for the NF and RO membranes are potentially due to the lower contact angles of these membranes compared to the Aquaporin Inside™ membrane.

This initial surface coverage however, did not affect the flux which remained at 16.2 ± 1.8 L/m²h throughout the adhesion stage. The initial adhesion of bacteria for 30 minutes has no significant effect on the flux as the fouling is not severe enough, since the biofilm has not developed during this short time. Yoon et al, [81], fouled FO membranes with *Pseudomonas aeruginosa* and reported only a negligible flux decline after approximately 2 hours of fouling. Similarly, Semião et al, [93], reported that 30 minutes of initial bacterial adhesion had no effect on the flux on NF and RO membranes. This shows that initial adhesion of cells has no effect on flux as the adhered bacteria offer very little resistance to flux.

As shown in Figure 6.1, as the adhered cells were exposed to the backwashing draw solutions they underwent osmotic stress and were either injured or died. Osmotic stress is the response of cells as they adapt to changes to their external environment in order to continue to function, [133]. As the high concentrations of the backwashing salt solutions come into contact with the adhered cells, they undergo osmotic stress and become damaged or die as they try to adapt to their new environment. Even the lowest backwashing concentration of 0.1 M NaCl resulted in a 7.9% surface coverage of dead or injured cells. As the draw solution was increased to 0.7 M and 1.5 M NaCl, the percentage of cells remaining on the membrane surface that became injured or died increased to 16.9% and 19.7%, respectively.

Increasing the backwashing solution concentration from 0.1 M to 1.5 M NaCl increases the dead or injured cells on the membrane surface from 7.9% to 16.91% but does not remove

them. The increase in salt concentration will increase mortality as the cells are subjected to more stress. This was shown by Katebian and Jiang, [134], who used 0.55 M of NaCl to induce hyperosmotic stress on *Shewanella sp.* which is a biofilm producing bacteria, resulting in a greater than 99.5% mortality rate. Dead bacteria cannot produce EPS, [129], and therefore biofouling is potentially avoided. However the remaining dead cells may still have consequences during subsequent fouling cycles. Herzberg and Elimelech, [129], used SEM to show that adhered cells, dead or alive, obstruct the back diffusion of salt during fouling causing a higher osmotic pressure on the membrane surface. This results in a decrease in permeate flux and salt rejection. Therefore an efficient backwashing method should aim to remove all cells from the membrane surface.

As the draw solution concentration was increased from 1.5 M to 2 M and 3 M NaCl, the backwashing flux increased from 31 to, 30.25, to 36 L/m²h, respectively, see table 6.1. This resulted in increased removal rates of 0%, 19% and 93%, respectively. This is due to the higher permeate drag force pulling the bacteria from the membrane surface. This increase in backwashing flux is accompanied by a possible decrease in water contact angle of the cells. Hachicho et al, [135], demonstrated that the water contact angle of *P. putida* cells decreased with increasing NaCl concentration. They showed that cells in the presence of 0.1 M NaCl had a contact angle of 100° and were therefore hydrophobic while cells in the presence of 0.7 M NaCl had a contact angle of 50° and were therefore intermediate hydrophobic/hydrophilic. When the concentration was increased further to 1 M NaCl the contact angle reduced to 45°. Van Loosdrecht et al, [95], demonstrated that decreasing contact angle resulted in a decrease in adhesion. This is evident here as 1.5 M and 3 M NaCl have similar backwashing fluxes, of 31 and 63 L/m²h respectively, but the 1.5 M solution did not remove any bacteria while 3 M removed 93%, figure 6.1. This could be due to further reduction of the cell surface contact angle, and therefore the adhesion forces, by the 3 M NaCl solution although it is most likely due to the backwashing flux of 36 L/m²h being sufficient to remove the adhered cells. Therefore, from figure 6.1, backwashing with 3 M NaCl with a 36 L/m²h backwashing flux was deemed the most efficient with a 93% removal rate under these adhesion conditions and therefore this backwashing solution was used for further experiments.

6.3 Effect of bacteria adhesion time on osmotic backwashing efficiency

Membrane cleaning results in both energy and time losses. Therefore, the frequency at which cleaning is carried out should be minimised as cleaning too often may lead to unnecessary time losses and harmful chemical use and disposal. However, cleaning too sporadically may lead to a reduction in cleaning efficiency as fouling starts to become irreversible as it progresses from initial adhesion to fully established biofouling. Bar-Zeev and Elimelech, [102], backwashed RO membranes subjected to 15 hours of biofouling but only restored 80-90% of the flux. Performing backwashing earlier could improve this. There is an optimal point at which to commence cleaning depending on the process conditions. Different bacteria adhesion times were tested to determine the optimal time to perform backwashing. The backwashing draw solution of 3 M NaCl was deemed the most efficient from figure 6.1, and therefore used throughout the rest of this study.

As the adhesion time is increased, the extent of the adhesion increases. BinAhmed et al, [32], showed that *Pseudomonas fluorescens* cells exhibited stronger adhesion to ultrafiltration membranes when cell-surface contact time was increased. They reported that the adhesion force increased from 0.4 nN to over 0.5 nN as the contact time increased from 2 to 5 seconds. This time-dependent trend is shown here in figure 6.2 where longer adhesion times resulted in higher bacteria surface coverage on the membrane: the bacteria surface area coverage increased from 14% to 55% as the adhesion time increased from 15 min, to 60 minutes, respectively.

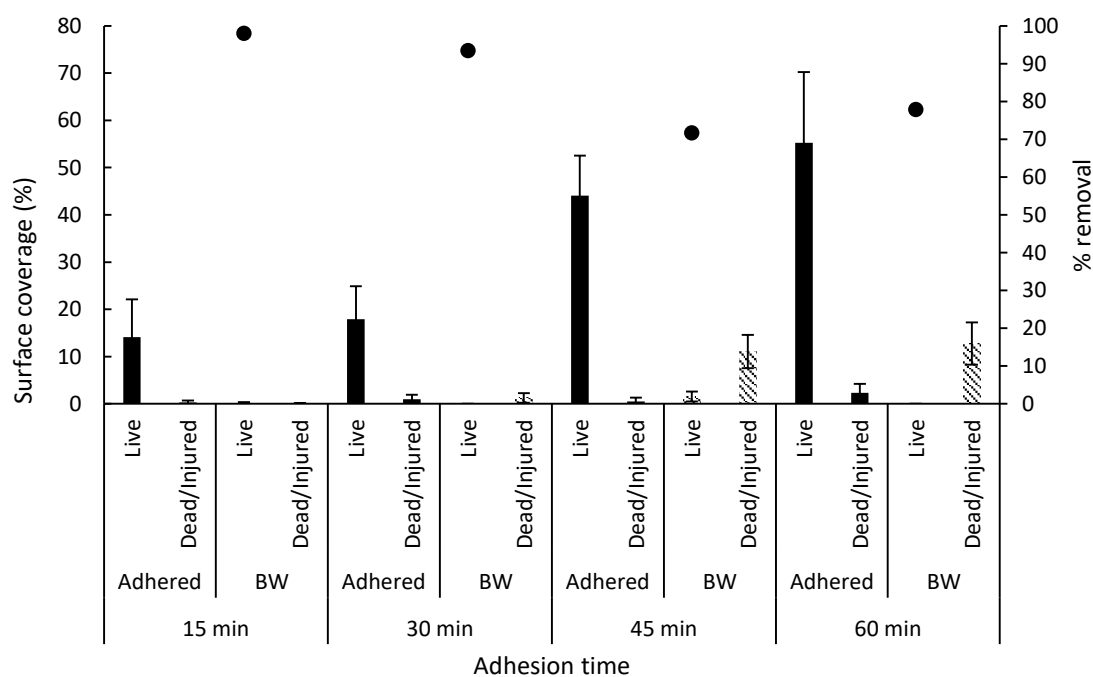


Figure 6.2: Effect of adhesion time on backwashing efficiency: Microscopy results of membrane samples subjected to bacteria adhesion in cross-flow showing % surface coverage of live and dead cells and the % removal of all cells in the secondary axis. Fouling conditions: Membrane: Aquaporin inside™. Draw = 0.7 M NaCl Feed = 200 ml of media containing *P. Putida* (10^7 cells/ml) in 0.1 M NaCl. Backwashing draw = 3 M NaCl. Backwashing duration = 1 minute. Error bars show standard deviation of the count determined from 10 areas on the membrane surface.

A bacteria surface coverage of 14% was obtained after just 15 minutes. This shows the ease of adhesion under these particular conditions. Ridgway et al, [136], studied adhesion of *Mycobacterium sp.* to cellulose diacetate RO membranes under no flux conditions and found that rapid adhesion took place in the first 1 to 2 hours before eventually slowing down. They explained that this is due to the finite number of adhesive sites on the membrane surface becoming occupied.

Just as the membrane flux during initial adhesion was unaffected by the adhesion of cells, the backwashing flux was also unaffected by the increase in adhesion remaining at 37.12 ± 4.7 L/m²h for each adhesion duration. As the adhesion duration increased and more cells adhered to the membrane surface, the cells became more difficult to remove fully. The backwashing efficiency decreased from 98% to 78% in regards to bacteria removal for adhesion times of 15 and 60 minutes, respectively. This is because the adhesion forces between the cells and the surface become stronger as the contact time increases. Evidence for this is provided by studies using AFM in the literature, [32, 91, 137-140]. Vadillo-Rodrigues, [139] who studied the adhesion of *Streptococcus thermophiles* and used AFM to show that the bond between the bacteria cells and a silicon nitride tip of an AFM increased with time. They determined that bond strengthening occurred between the AFM tip and the cell within just 100 seconds of contact. Therefore in this study it is likely that as the adhesion time was increased from 30 minutes to 45 minutes, the bond between the cells and the surface became stronger. For this reason, the cells became more difficult to remove for longer adhesion times with this backwashing method.

In the cases of 45 and 60 minutes of adhesion, 11% and 12.7% of the surface remained covered in dead or injured cells after backwashing. Although the backwashing method is efficient in killing or injuring the bacteria through osmotic shock, it is no longer efficient at removing the remaining cells after longer adhesion times, suggesting that higher BW fluxes would be needed, for example. It is therefore determined that, using this backwashing method, backwashing should be carried out after 30 minutes of adhesion as less frequent backwashing is ineffective. In order to be able to perform cleaning less frequently a

different cleaning method is necessary. This shows that as the longer adhesion time allows more cells to attach to the membrane and the adhesion forces to become stronger, this higher adhesion is therefore too large to be overcome by this backwashing method alone.

It has been shown that *P. Putida* has a division time of 53 minutes, [141], which means that 60 minutes of adhesion is a long enough time to potentially observe significant changes in the adhesion. In this study biofouling was not observed after 60 minutes of adhesion. This could be due to the temperature of 20 °C at which the experiments were carried out.

6.4 Effect of CaCl₂ in the feed solution on adhesion and backwashing efficiency

The feed characteristics have an important effect on the physical, chemical and biological factors affecting adhesion. [97]. Increasing the ionic strength of the feed solution has been shown to increase the cell adhesion, [142]. Divalent ions such as Ca²⁺ ions are known to affect the physiology of bacteria and increase adhesion, [33]. Safari et al, [33], used AFM to show that increasing the calcium concentration will increase the adhesion force between the cells and the membrane surface. Therefore, varying the quantity of CaCl₂ in the feed solution will produce different levels of adhesion with which to evaluate the efficiency of backwashing.

Varying concentrations of CaCl₂ from 0 mM to 5 mM were added to the feed and adhesion was carried out for 30 min. The impact of feed CaCl₂ concentration on the cleaning efficiency was assessed, as shown in Figure 6.3. As the calcium chloride concentration increased from 0 to 5 mM in the feed solution, the percentage surface coverage increased significantly. The addition of 5 mM CaCl₂ in the feed resulted in a 50% increase in surface coverage, compared to adhesion in the absence of Ca²⁺, from 17.87% to 26.8% live cell coverage.

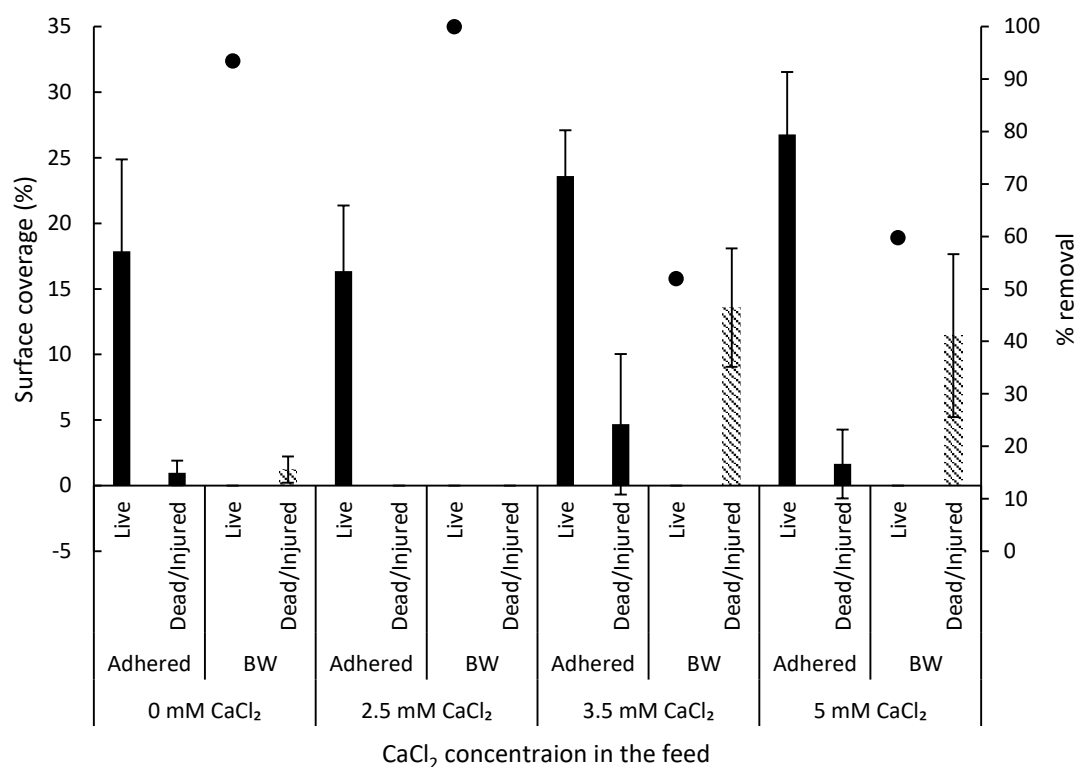


Figure 6.3: Effect of CaCl₂ concentration in the feed on backwashing efficiency: Microscopy results of membrane samples subjected to bacteria adhesion in cross-flow showing % surface coverage of live and dead cells and the % removal of all cells in the secondary axis. Fouling conditions: Membrane: Aquaporin inside™. Draw = 0.7 M NaCl, Feed = 200 ml of media containing *P. Putida* (10⁷ cells/ml) in 0.1 M NaCl and the stated concentration of CaCl₂. Adhesion duration 30 minutes. Backwashing draw = 3 M NaCl. Backwashing duration = 1 minute. Error bars show standard deviation of the count determined from 10 areas on the membrane surface.

Three different factors affect the cell adhesion on the membrane surface in this case. The ionic strength (concentration) of the feed solution, the type of salt (monovalent or divalent) and the specific influence of calcium on bacteria adhesion. Firstly, the ionic strength of the feed solution increased with the addition of CaCl₂. The conductivity increased by 10% (from 10.42 to 11.46 mS/cm) as the CaCl₂ concentration was increased from 0 to 5 mM. This is similar to reports by Sadr Ghayeni et al, [142], who reported a 25% increase in *Pseudomonas* adhesion onto BW30 membranes when the ionic strength of the fouling solution was doubled. This increase in adhesion is predicted by the DLVO theory, [143]. At lower ionic strengths, the electric double layer surrounding each cell is larger and therefore the repulsive forces between the cells and the membrane surface occur at these larger distances. As the ionic strength of the surrounding solution is increased, the electric double layer begins to compact and thus the cells are brought closer to the membrane surface, enabling adhesion of the cells to the membrane surface. This increase in charge

interactions due to the increase in ionic strength also occurs in the presence of divalent ions. Hong and Brown, [143], showed that Ca^{2+} ions cause the zeta potential of *E. coli* and *Bacillus brevis* to become less negative. This will result in greater adhesion onto a surface such as a membrane. Fetcher, [97], reported that the addition of cations decreased the cell-surface separation distance as the cations reduce the repulsive force between the negatively charged cells and the negatively charged membrane surface therefore increasing adhesion.

Divalent ions such as Ca^{2+} and Mg^{2+} may promote adhesion by ion-bridging between anionic groups on the membrane surface and on the cell surface, [144-146]. For the purpose of this study, the influence of Ca^{2+} ions will be examined. Several studies have examined the influence of calcium on bacteria cell adhesion. Ca^{2+} has been shown to increase the surface adhesion of various types of bacteria cells, [33, 96, 97]. Safari et al, [33], reported a 61% increase in bio volume of *P. fluorescens* biofilm formed in the presence of 15 mM of CaCl_2 compared to the absence of CaCl_2 . They showed that increasing the CaCl_2 concentration increased surface coverage during initial adhesion. They also showed that the presence of CaCl_2 leads to an increase in EPS and higher adhesion forces. This increase in bio volume and adhesion is due to the increase in binding sites for crosslinks by bridging of Ca^{2+} ions with alginate which is a major component of the EPS. *Pseudomonas putida* also produces alginate, [147], and therefore this binding can explain the increase in adhesion in the presence of CaCl_2 .

The cells may also present a physiological response to calcium in the backwashing draw solution. Ca^{2+} has been shown to bind with the protein LapF, a key protein for the maturation of biofilm development of *Pseudomonas putida*, and form large aggregates in biofouling, [96]. They reported an 11% increase in attached biomass on an LB agar plate containing *Pseudomonas putida* after 2 hours of contact with 10 mM CaCl_2 . This occurred as Ca^{2+} promotes the interaction between the LapF molecules in adjacent bacteria and therefore the cell to cell interactions. This increase in cell interaction will promote microcolony formation leading to an increase in biomass. This occurrence could also explain the increase in surface coverage upon addition of Ca^{2+} to the feed solution and the decrease in backwashing efficiency.

McEldowney and Fletcher, [145], determined that cell adhesion cannot be credited to any one type of adhesive interactions. Therefore neither the described possible physiological or

physiochemical effects resulting from increasing the CaCl_2 feed concentration is solely responsible for the increase in adhesion. It is likely a combination of the increase in ionic strength, the introduction of the divalent ions and the specific effect of Ca^{2+} ions on *Pseudomonas putida* cells that lead to this increase.

This increase in adhesion caused by the increase in CaCl_2 concentration in the feed from 0 mM to 5 mM, led to a decrease in backwashing efficiency from 93% to just 60%. As the increase in Ca^{2+} ions allows more cells to attach to the membrane, the higher surface coverage is too large to be overcome by this backwashing method. Also, the adhesion force between the cells and the surface becomes stronger with increasing Ca^{2+} concentration. de Kerchove and Elimelech proposed that the greater bacterial adhesion in the presence of divalent cations, such as Ca^{2+} , is governed by strong bonds between the surface of the cell and the divalent cations, [148]. They demonstrated an increase in attachment efficiency of *Pseudomonas aeruginosa* onto clean and conditioned surfaces in the presence of divalent cations. Safari et al, [33], also demonstrated higher adhesion of biofilms formed in the presence of CaCl_2 . They used AFM to show that adhesion forces increased from 1.61 ± 0.56 nN to 2.06 ± 1.03 nN as the CaCl_2 concentration was increased from 0 to 15 mM. As the bond strength increases with increasing CaCl_2 concentration, this backwashing method becomes inefficient as it needs to overcome stronger interaction forces between the cells and the membrane surface.

6.5 Use of CaCl_2 as an osmotic backwashing draw solution for bacteria removal

The results displayed in figures 6.2 and 6.3 show that the backwashing solution of 3 M NaCl is effective under low adhesion conditions, for calcium concentrations up to 2.5 mM and adhesion durations up to 30 minutes. However, as the adhesion conditions become more severe after longer adhesion durations or higher CaCl_2 concentrations, this backwashing method is no longer effective. One way to increase the backwashing efficiency is to increase the driving force for backwashing; the backwashing solution osmotic pressure. CaCl_2 backwashing solutions can be used to do this as they have a much higher osmotic

pressure than NaCl solutions, see table 6.2. However backwashing with CaCl₂ may have drawbacks. As shown in chapters 4 and 5, just one minute of backwashing with CaCl₂ solutions is enough time for Ca²⁺ ions to interact with alginate fouling layers and reduce the backwashing efficiency. As Ca²⁺ ions have been shown to affect the adhesion of *Pseudomonas putida* (See figure 6.3), backwashing with CaCl₂ has the potential to enhance adhesion rather than detach the bacteria with the backwashing flux, as the Ca²⁺ ions come into contact with the adhered bacteria. This will be investigated in this section.

Different CaCl₂ backwashing draw solution concentrations were used to clean membranes subjected to initial bacterial adhesion to compare cleaning efficiency of NaCl and CaCl₂ solutions and to determine if 1 minute of backwashing with Ca²⁺ ions is enough contact time for them to influence adhered cells. Membranes were fouled for 30 minutes in the absence of calcium and the backwashing draw solution cleaning efficiency was assessed.

As shown in table 6.2, an increase in CaCl₂ backwashing draw solution concentrations resulted in increased transmembrane fluxes during cleaning, ranging between 23.7 L/m²h and 55.8 L/m²h, for concentrations of CaCl₂ ranging between 0.1 M and 3 M. Furthermore, BW fluxes for CaCl₂ were higher compared to the same concentrations for NaCl, which is expected since the osmotic pressure of CaCl₂ is higher than NaCl (see table 6.2).

Backwashing fluxes above the maximum NaCl could offer, i.e. 36 L/m²h, were obtained for CaCl₂ concentrations of 2 and 3 M, i.e. 47.5 L/m²h and 55.8 L/m²h.

Table 6.2: Backwashing flux values for increasing draw solution concentrations and their corresponding osmotic pressures.

Concentration (M)	Backwashing flux (L/m ² h)		Osmotic pressure (atm)	
	NaCl	CaCl ₂	NaCl	CaCl ₂
0.1	8.65	23.7	4.8	7.2
0.7	20.17	34	33.4	50.1
1.5	31	-	71.6	-
2	30.25	47.5	95.5	143.2
3	36	55.8	143.2	214.8

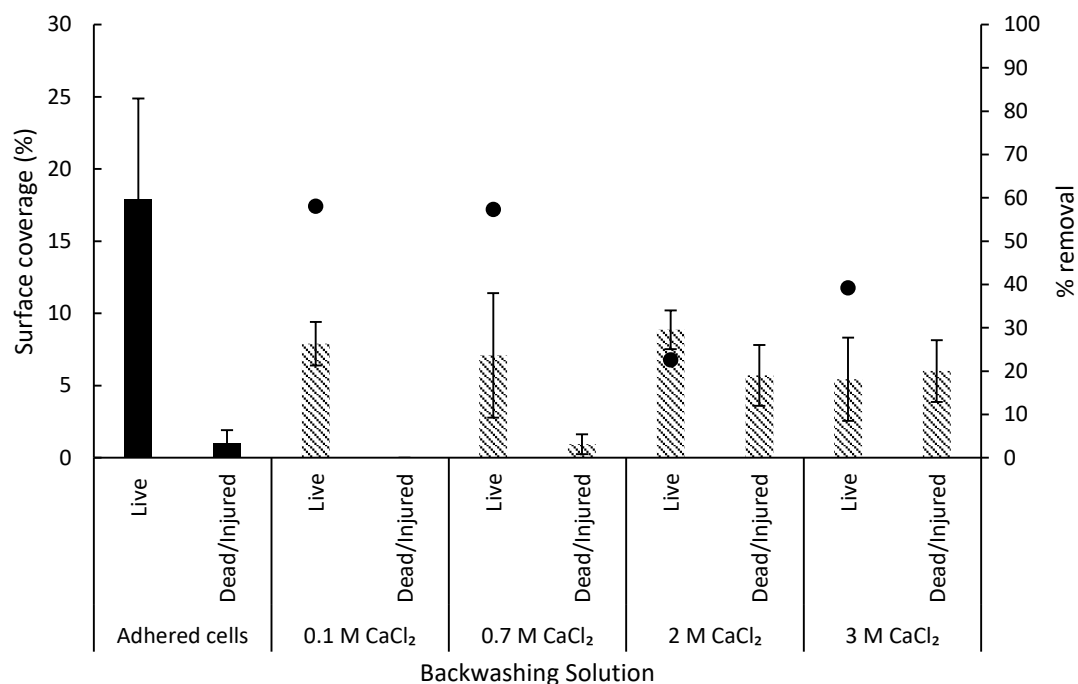


Figure 6.4: Effect of backwashing concentration of CaCl₂: Microscopy results of membrane samples subjected to bacteria adhesion in cross-flow showing % surface coverage of live and dead cells and the % removal of all cells in the secondary axis. Fouling conditions: Membrane: Aquaporin inside™. Draw = 0.7 M NaCl Feed = 200 ml of media containing *P. Putida* (10⁷ cells/ml) in 0.1 M NaCl. Adhesion duration 30 minutes. Backwashing duration = 1 minute. Error bars show standard deviation of the count determined from 10 areas on the membrane surface.

Each membrane was subjected to identical adhesion conditions resulting in an average surface coverage of 17.9% live cells, as can be seen in Figure 6.4. As the CaCl₂ concentration in the backwashing solution was increased, the backwashing flux increased (see table 6.1), and therefore higher backwashing efficiency through the reduction of adhered bacteria would be expected. This was shown to happen with NaCl in figure 6.1, particularly when the NaCl backwashing concentration increased from 2 to 3 M, translating to a BW flux increase from 30 to 36 L/m²h and a bacterial adhesion reduction from 15.4% to 1.2%. However, this did not occur with the CaCl₂ backwashing solution.

As the backwashing draw solution was increased from 0.1 M to 3 M CaCl₂, the % dead cell coverage increased from 0% to 6%, and the live cell coverage decreased from 8% to 5.5%. This is shown in figure 6.4. The increasing percentage of dead cells is due to the increasing osmotic pressure, see table 6.2, which causes osmotic shock and therefore higher numbers of dead/injured cells are obtained for higher CaCl₂ concentrations. When comparing total cells remaining after backwashing, the percentage increases from 7.89% and 8.04% for

CaCl₂ concentrations of 0.1 M and 0.7 M to 14.58% and 11.45% for CaCl₂ concentrations of 2 M and 3 M. This shows that backwashing with CaCl₂ is becoming less efficient as the backwashing solution concentration increases despite the fact that the backwashing flux is increasing. It has been reported that *P. putida* produce alginate in response to stress, [147, 149]. Sarkisova et al, [150], showed that Ca²⁺ ions increased production of EPS including alginate during biofilm formation with *P. aeruginosa*. Chang et al, [147], showed that *P. putida* produces alginate to create a hydrated microenvironment that increases cell stress tolerance under water-limiting conditions. The production of alginate in the presence of CaCl₂ will therefore protect the cells and increase the cell adhesion, [33], therefore making them more difficult to remove and kill/damage. For this reason the increasing concentration of CaCl₂ in the backwashing solution is becoming less efficient, figure 6.4.

This result also shows that the cells are potentially more difficult to both kill/damage via backwashing when CaCl₂ is present compared to backwashing with NaCl. Backwashing with NaCl and CaCl₂ are compared in terms of backwashing flux and osmotic pressure. The osmotic pressure of the backwashing solutions is calculated by the following equation:

$$\pi = iMRT \quad (6.1)$$

Where π is the osmotic pressure, i is the van't Hoff factor of the solute, ($i = 2$ for NaCl, $i = 3$ for CaCl₂), M is the molarity of the solution (mol/L), R is the ideal gas constant (0.082 L.atm/mol.K) and t is the temperature in Kelvin (293.2 K).

Results from table 6.2 show that backwashing flux does not depend solely on osmotic pressure but also on the type of salt used. Comparing solutions of similar backwashing fluxes such as 0.7 M NaCl and 0.1 M CaCl₂ which have backwashing fluxes of 20.17 and 23.7 L/m²h but osmotic pressures of 33 atm and 7.2 atm respectively. This could be due to the way that the specific ions react with the adhered bacteria on the membrane resulting in different backwashing fluxes.

Recall from figure 6.1, at the lowest osmotic pressure of 0.1 M NaCl, no cells were removed during backwashing and 37% of the cells remaining on the membrane were injured or died. After backwashing with 0.1 M CaCl₂, the surface coverage was reduced from 17.9% to

7.89% and no dead cells remained on the membrane surface. This could be due to the higher backwashing flux for CaCl_2 at 0.1 M, i.e. 23.7 L/m²h as opposed to 8.65 L/m²h for 0.1 M NaCl, offering a greater perpendicular drag force across the membrane surface and therefore removing a higher percentage of cells. Also, the production of alginate and subsequent formation of a hydrated microenvironment in the presence of Ca^{2+} therefore protects the cells as previously described resulting in a higher cell survival rate.

It therefore is necessary to compare two backwashing solutions with similar backwashing fluxes. Although the backwashing solutions of 0.7 M NaCl and 0.1 M CaCl_2 offered similar backwashing fluxes of 20.17 L/m²h and 23.7 L/m²h respectively (see table 6.2), very different results are obtained with these solutions. For the 0.7 M NaCl solution, most of the cells died and the total surface coverage was reduced by 5% during backwashing (Figure 6.1). For the 0.1 M CaCl_2 solution, the surface coverage is reduced by roughly 58% and no dead/injured cells were detected. The 0.7 M NaCl solution has the higher osmotic pressure of 33.41 atm compared to 7.16 atm for the 0.1 M CaCl_2 solution. This higher osmotic pressure could explain the high mortality rate for the NaCl solution as the cells underwent osmotic shock when exposed to the draw solution and therefore died, as previously explained. This result also suggests that the CaCl_2 backwashing solution is less efficient at killing/damaging the cells than the NaCl solution because, for similar backwashing fluxes, 16.91% of dead cells remain on the membrane surface after backwashing with 0.7 M NaCl, see figure 6.1, compared to 7.89% of live cells remaining after backwashing with 0.1 M CaCl_2 . This further supports the theory that the production of alginate in the presence of CaCl_2 protects the cells.

The second observation is the cells' response to osmotic stress during backwashing with NaCl and CaCl_2 at the same osmotic pressure. The closest comparisons of osmotic pressure can be made between the backwashing solution of 3 M NaCl and the 2 M CaCl_2 which both have osmotic pressures of 143.2 atm. Backwashing with 3 M NaCl results in almost complete removal with 1.23% surface coverage of dead cells remaining on the membrane surface. Backwashing with 2 M CaCl_2 does not remove the bacteria with 8.9% surface coverage of live cells and 5.7% surface coverage of dead cells remaining despite the higher backwashing flux, see table 6.1. Again, this is due to the stress response of the cells resulting in the production alginate. In response to the osmotic stress the cells produce alginate which is hygroscopic, [117], meaning it can hold several times its weight in water

and potentially loses water slowly. This alginate layer can therefore keep the cells protected long enough for them to make metabolic adjustments to increase survival, [147].

Although a flux of 36 L/m²h produced by 3 M of NaCl was sufficient at removing 92% of the bacteria on the membrane, shown in figure 6.1, this flux was not sufficient when backwashing with CaCl₂ concentrations higher than 0.7 M CaCl₂ which produced backwashing fluxes from 34 to 55.8 L/m²h: a BW flux of 55.8 L/m²h produced by 3 M CaCl₂, for example, resulted only in 75% removal of adhered cells. This suggests that cell adhesion forces have been increased by the Ca²⁺ ions in the backwashing solution. This can be explained by the effect of divalent ions on cell adhesion. As already explained, divalent ions aid adhesion by ion-bridging between anionic groups on the membrane surface and on the cell surface, [144-146]. During backwashing with CaCl₂, the cells come into contact with a high concentration of Ca²⁺ ions for 1 minute. This contact time is sufficient for the Ca²⁺ ions to bind with and alginates produced by the cells as a stress response, [147]. Therefore even the high backwashing flux of 55.8 L/m²h could not overcome the increase in adhesion due to the presence of Ca²⁺ ions.

Some discrepancies in results are noted. NaCl backwashing solutions of 1.5 M and 2 M had backwashing fluxes of 31 L/m²h and 30.25 L/m²h respectively, and total cell removal rates of 0% and 19% respectively. However, the 0.1 M CaCl₂ backwashing solution had lower backwashing flux of 23.7 L/m²h and yet a higher total cell removal rate of 59% despite the high adhesion in the presence of Ca²⁺ ions. There are several mechanisms affecting the adhesion and detachment of bacteria including water contact angles, charge interactions, osmotic stress responses and hydrodynamic forces. Therefore, more work is needed to understand the mechanisms behind adhesion of live and dead cells in the absence and presence of Ca²⁺ ions in order to gain a more complete understanding of backwashing of membranes subjected to initial bacteria adhesion.

6.6 Conclusion

Biofouling on membranes has been deemed irreversible, [35], and therefore cleaning at the adhesion stage is necessary to avoid the detrimental effects of biofouling. In this study, it has been shown that osmotic backwashing is potentially an effective cleaning technique for bioadhesion but only under certain circumstances.

Higher backwashing fluxes resulted in higher removal rates due to the increased perpendicular drag force through the membrane. Although 3 M of NaCl was an efficient backwashing solution after 30 minutes of adhesion, longer adhesion times resulted in increased cell adhesion that could not be overcome using this backwashing method. Performing backwashing for longer may be an effective way of overcoming this increased adhesion.

Similarly, increasing the CaCl_2 concentration in the feed resulted in increased cell adhesion that the method of backwashing with 3 M of NaCl could not remove. This is due to the increase in ionic strength of the feed solution, the presence of divalent cations and the specific influence of calcium on bacteria cells which increased the adhesion of the cells therefore making them more difficult to remove. Performing backwashing for longer or at more frequent intervals may be efficient.

This study has shed light on the potential for CaCl_2 to influence adhesion during backwashing. As shown in chapters 4 and 5, it is evident that a backwashing duration of 1 minute is enough time for the backwashing ions to have a significant impact on adhesion due to the differences in results between backwashing solutions of NaCl and CaCl_2 . This difference is the result of the different physicochemical and possible physiological influences of the divalent Ca^{2+} ions and the monovalent Na^+ ions. Firstly, as already explained, divalent ions have been shown to increase adhesion by ion-bridging and during backwashing with CaCl_2 , high concentrations of divalent ions come into contact with the cells and increase their adhesion onto the membrane surface. This results in an increase in adhesion that even high backwashing fluxes of 47.5 and 55.8 $\text{L/m}^2\text{h}$ cannot overcome. Secondly, the high osmotic pressure of the backwashing solutions induces a stress response of the cells resulting in the production alginate, which in the presence of the Ca^{2+} ions in the backwashing solution, act to protect the cells, [147], and therefore cells backwashed with CaCl_2 experience a lower mortality compared to cells backwashed with NaCl.

Longer backwashing durations, higher backwashing solution concentrations or a combination of cleaning techniques may result in more effective cleaning.

Chapter 7: Conclusions and future work

7.1 Conclusions

Fouling remains one of the foremost drawbacks in membrane processes and is largely unavoidable. Current cleaning methods involve the use of chemicals that can harm the environment, [12, 39], and damage the surface of the membrane, [3]. Therefore, effective and sustainable cleaning methods are necessary to minimise the effects of membrane fouling. The main aim of this thesis is to examine alternative cleaning of RO and FO membrane processes without the use of harmful chemicals under a range of different fouling conditions in order to understand how fouling mechanisms influence cleaning efficiency. It was hypothesised that osmotic backwashing is an efficient and sustainable cleaning method to reverse the effects of fouling on RO and FO membranes. To prove this, several parameters influencing organic fouling and biofouling were studied and how these factors subsequently effect cleaning performance was investigated using surface imaging techniques and flux measurements. The main objectives used to accomplish this are outlined below:

- To examine the impact of fouling solution chemistry and initial membrane flux on osmotic cleaning efficiency of RO and FO membranes using both flux measurements and surface imaging. To do this, membranes were fouled with alginic acid and the solution chemistry was varied by increasing the CaCl_2 concentration in the feed from 0 to 2.5 mM. The initial membrane fluxes were varied from 25 to 100 $\text{L/m}^2\text{h}$ for RO by increasing the pressure and for FO the draw solution was increased from 0.7 to 4 M NaCl to increase the initial flux from 6 to 20 $\text{L/m}^2\text{h}$. Combining the use of both flux measurements and surface imaging to verify the efficiency of osmotic backwashing is neglected in the current research on cleaning. However both are necessary as shown in this thesis.
- To understand how factors affecting initial bacterial adhesion in FO influence osmotic backwashing. The literature review identified a gap in the research in this area but this research is important as biofouling is very difficult to overcome without the use of harmful chemicals. Intervening early during initial adhesion could help control biofouling. The factors effecting initial adhesion tested were adhesion duration and CaCl_2 concentration. FO membranes were subjected to

initial adhesion for 30 minutes resulting in a cell surface coverage of 18%. Adhesion was increased by increasing the adhesion duration from 15 to 60 minutes. Also increasing the CaCl_2 concentration in the feed from 0 to 5 mM resulted in a 50% increase in adhesion. How these conditions effected backwashing efficiency was then tested.

- To study the use of CaCl_2 as a backwashing solution: Can the increase in driving force improve reversibility? Or will the presence of Ca^{2+} exacerbate adhesion effects? Backwashing with CaCl_2 was performed for both RO and FO and for both organic fouling and initial cell adhesion. This objective shed light on the influence of Ca^{2+} ions on the fouling layer and adhered bacteria even with just 1 minute of contact time.

In this thesis it was determined that backwashing efficiency depends greatly on feed solution chemistry and initial membrane flux in RO processes. Due to the high pressures involved, organic fouling remained largely irreversible both in terms of flux restoration and fouling layer removal. Although flux restorations of 100% were achieved for initial RO membrane fluxes of 25 and 33 $\text{L/m}^2\text{h}$, foulant layers of 9 μm and 25 μm remained on the membrane surface, respectively. This shows that flux restoration as a sole parameter used to assess cleaning efficiency is not a reliable indicator and should be accompanied by a surface imaging method in order to obtain the full picture of cleaning efficiency. As the initial flux was further increased to 80 and 100 $\text{L/m}^2\text{h}$, backwashing became increasingly inefficient with 141 μm and 115 μm of fouling remaining on the membrane surface respectively. Fouling removal by osmotic backwashing in reverse osmosis depends heavily on the fouling layer characteristics, due to increased pressure or calcium concentration.

Increasing the backwashing flux, by means of a higher concentration draw solution, can potentially increase removal due to the higher permeate drag force acting on the fouling layer. However, the chemistry of the backwashing draw solution has also been found to be extremely important in this thesis. It was shown that 1 minute of backwashing with a 0.5 M CaCl_2 solution is enough contact time for divalent Ca^{2+} ions to interact with the alginate layer formed on the membrane surface during fouling, and form complexes with the carboxyl groups within it resulting in an increase in adhesion forces between the fouling layer and the membrane, [30]. The higher hydrodynamic drag force created by the increase in osmotic pressure cannot overcome this increase in adhesion and the fouling layer cannot

be removed. Therefore flux restoration cannot be achieved using this method of backwashing for alginate fouling. The calcium ions form complexes with carboxyl groups within the alginate layer and therefore backwashing with CaCl_2 may be effective for reversal of fouling that does not contain polysaccharides.

The phenomenon of alginate fouling gel layer swelling should be considered when examining osmotic backwashing. It was shown that, after backwashing with NaCl, exposing the remaining alginate layer to a solution of lower ionic concentration (during testing of the pure water flux) resulted in swelling of the alginate fouling layer and therefore an increase in thickness from 49 μm to 174 μm was observed. Swelling of the fouling layer will result in lowering of the fouling layer density. Therefore this phenomenon can potentially be utilised to improve cleaning in membrane processes as it was shown that less dense fouling layers are easier to remove. The rate and extent of the removal of the swollen fouling layer is dependent on the thickness and adhesion energy of the gel layer, [121], both of which depend on the feed chemistry and initial flux as shown in this thesis. In reality, seawater composition varies from source to source and is made up of several different types of contaminants and therefore the fouling layer swelling will potentially behave differently depending on the source. Also, freshwater and wastewater have low salt concentrations and therefore after backwashing with NaCl the remaining fouling layer may swell during further membrane filtration of these sources. The gel layer swelling occurs when the layer is exposed to a solution of lower ionic strength and the extent of the swelling will depend on this solution ionic strength, [16], which will vary from source to source. Therefore knowledge of the chemistry of the source water is important when considering a chemical free cleaning strategy.

Cleaning was more efficient at lower pressures in RO so therefore as FO does not require any pressure, surface flushing of organic fouling of FO membranes with deionised water was tested. This method was successful after fouling in the absence of CaCl_2 however surface flushing only removed 71% of the layer after severe fouling in the presence of 2.5 mM CaCl_2 . At these fouling conditions, the parallel shear with pure water was not as effective as the combination of perpendicular flow and physio-chemical interactions between ions in the backwashing solution and the fouling layer offered with backwashing.

Osmotic backwashing proved most effective after low pressure fouling conditions (low initial fluxes) in RO, and therefore it's potential as a cleaning method for FO was examined

next. For FO processes, 1 minute of backwashing is effective at reversing fouling and restoring membrane operation in terms of both flux restoration and fouling layer removal.

Unlike in RO, changes to the feed solution chemistry did not reduce the backwashing efficiency in FO where even the effects of the highest calcium concentration of 2.5 mM could be reversed using a 0.7 M NaCl backwashing solution which removed almost the entire fouling layer and restored 100% of the flux. This is due to the soft and loose fouling layer formed in the absence of pressure which is easier to remove by reversing the flow of water through the membrane.

As with RO, increasing the initial membrane flux can reduce the backwashing efficiency in FO. Increasing the FO draw solution concentration from 0.7 M to 4 M NaCl lead to a threefold increase in flux which resulted in a more compact and dense fouling layer of which only 20% could be removed by backwashing. Despite this, 100% of the initial flux was restored reinforcing the conclusion that flux measurements alone cannot confirm that membrane cleaning methods are effective.

An effective cleaning technique should be able to maintain membrane performance for multiple fouling and cleaning cycles in order to increase membrane lifetime and reduce membrane replacement costs and cleaning time losses. Consecutive fouling and backwashing cycles in FO were performed and 100% of the flux was restored after 5 cycles of fouling for 22 hours and backwashing for 1 minute with 0.7 M NaCl. Due to the lack of applied pressure during fouling, backwashing was shown to be a very effective technique in FO processes.

As backwashing was proven to be effective for organic fouling reversal in FO processes, focus was next turned to utilising it for biofouling control in FO. As biofouling on membranes has been deemed irreversible, [35], backwashing at the initial cell adhesion stage was explored to evade the effects of biofouling. It was determined that 3 M of NaCl was an efficient backwashing solution after 30 minutes of adhesion. However lower backwashing solution concentrations were ineffective. Longer adhesion times resulted in increased adhesion. Doubling of the adhesion duration from 30 to 60 minutes resulted in a 200% increase in total adhered cells that even 3 M of NaCl could not remove fully as 12% of the membrane remained covered in dead cells after backwashing. Similarly, increasing the CaCl_2 concentration in the feed from 0 mM to 2.5 mM resulted in a 50% increase in total cell adhesion. Backwashing with 3 M NaCl could not reverse this enhanced cell adhesion.

This is due to the increase in ionic strength of the feed solution, the presence of divalent cations and the specific influence of calcium on bacteria cells all of which increase adhesion. The increase in ionic strength and the presence of Ca^{2+} decreases the cell and membrane surface separation distance due to increased charge interactions resulting in increased adhesion. Also, divalent ions like Ca^{2+} aid adhesion by ion-bridging between anionic groups on the membrane surface and on the cell surface.

In both chapters 4 and 5, it was shown that 1 minute of backwashing with CaCl_2 was enough time for the Ca^{2+} ions to influence the fouling layer and thus reduce backwashing efficiency. To see if Ca^{2+} ions could have the same effect on adhered cells, backwashing solutions of CaCl_2 were tested. Results obtained for backwashing solutions of CaCl_2 were notably different from NaCl backwashing solutions at the same osmotic pressures and backwashing fluxes. This shows that 1 minute of backwashing with CaCl_2 solutions is enough time for Ca^{2+} ions to influence adhered cells. Backwashing solutions of 2 M and 3 M CaCl_2 were less efficient than the 3 M NaCl solution showing that, similar to organic fouling, Ca^{2+} ions in the backwashing solution hinder backwashing by forming complexes with alginates produced by the cells as a stress response which results in poor cell removal. Numerous mechanisms effect adhesion and detachment of bacteria including contact angles, charge interactions, stress responses and the hydrodynamic forces of crossflow and backwashing. Therefore, more work is needed here to obtain a clearer understanding of backwashing of adhered bacteria.

Indeed, seawater and wastewater vary widely in composition from source to source and are made up of several different contaminants and therefore organic fouling is accompanied by many other types of fouling such as biofouling and colloidal fouling. Therefore the chemistry of the feed water needs to be examined before implementing a cleaning strategy. In this study, only one RO and one FO membrane were examined. The type of membrane also influences fouling, [93, 151, 152], and therefore will affect cleaning efficacy. It is therefore also important to examine how the membrane affects fouling and cleaning in order to establish a robust cleaning strategy. The main conclusions from this thesis show that in order to develop an effective membrane cleaning approach, knowledge of the source water and the several factors that influence fouling and how they consequently affect cleaning efficiency need to be understood.

7.2 Future Work

This thesis shows that osmotic backwashing has potential as a means of fouling and biofouling control in membrane processes. However, more research is needed to optimise backwashing as a cleaning method. The necessary further work for each chapter is outlined in this section. It has been shown that flux measurements alone cannot guarantee organic fouling layer removal in RO and FO membrane processes. For this reason, all future work on membrane cleaning should always utilise at least one method of surface imaging as well as flux measurements when examining cleaning efficiency. Where a cleaning method has been determined to be effective, future work should always perform numerous consecutive fouling and cleaning cycles to verify the true efficiency of the cleaning method.

Chapter 4: Osmotic backwashing of organic fouling on reverse osmosis membranes: Influence of fouling and backwashing conditions on cleaning efficiency

In chapter 4, backwashing of organically fouled RO membranes for 1 minute was deemed inadequate at restoring membrane performance at high pressures and therefore more work is needed to optimise backwashing in RO. Although the fouling layer was not removed completely, the membrane was fouled under severe conditions (in the presence of 2.5 mM CaCl_2) and even then it did show promise as a cleaning solution. Possible ways of improving backwashing are to implement it more frequently, thus reducing the time required for fouling to develop or to increase the backwashing duration thus potentially increasing removal. However, increasing the backwashing frequency and/or duration will result in greater time losses due to cleaning. Another way of improving cleaning is to combine backwashing with another cleaning method such as surface flushing or air scouring. In this chapter it was shown that fouling layer swelling occurs when the fouling layer is exposed to a solution of lower ionic concentration after backwashing with NaCl. This swelling will result in a reduction in fouling layer density which may be easier to remove without the use of chemicals. Further work is needed here to determine how fouling layer swelling can be exploited to aid fouling removal and flux restoration.

Organic fouling with alginic acid was tested. Other types of organic fouling such as humic acid and bovine serum albumin (BSA) as well as a combination of these foulants should be tested next. As shown, alginate is hygroscopic, meaning it can hold several times its weight in water. Humic acid and BSA are also hygroscopic, [153, 154], so the rate and extent of

fouling layer swelling and subsequent detachment will potentially be affected. In order to produce a robust cleaning strategy, further research into fouling layer detachment under a range of conditions is needed with the aid of surface imaging and AFM. AFM could be used to gain a better understanding of the fouling layer swelling phenomenon by determining how the swelling affects the adhesion energy of the fouling layer. It is useful to know the adhesion energy of the original fouling layer and the swollen fouling layer to see how these forces effect backwashing efficiency.

Comparative studies on backwashing of inorganic and colloidal fouling and biofouling are also needed as well as a combination of different fouling types. This is important in order to develop a better understanding of how fouling affects cleaning efficiency which can then lead to the establishment of more robust cleaning methods.

Chapter 5: Investigating chemical free cleaning of organic fouling on forward osmosis membranes: Effects of fouling and cleaning conditions

FO coupled with low pressure reverse osmosis is emerging as potential technology to reduce the energy consumption of conventional RO membrane desalination, [41]. This thesis showed that lower pressures in RO resulted in organic fouling layers that were easier to remove with the use of backwashing alone. Therefore FO-RO hybrid technology may not only have lower energy requirements but also higher fouling reversibility. For this reason, sustainable and effective cleaning techniques should be developed to treat FO fouling.

In chapter 5, it was shown that organic fouling in FO is reversible with backwashing due to the lack of required pressure during fouling. Chemical free cleaning of more complex fouling which a combination of organic, inorganic, colloidal and biofouling needs to be examined to reflect real life environments. Longer fouling durations must also be tested as well as more consecutive fouling and cleaning cycles to push the limits of osmotic backwashing and determine its true potential as a cleaning method in FO. Consecutive fouling and cleaning cycles may eventually result in severe fouling that backwashing cannot overcome. Motsa et al, [17], reported that cleaning efficiency decreased from 100% to 93% after 3 cycles of organic fouling of FO membranes. Similarly, Martinetti et al, [105], reported a decrease in backwashing efficiency from 94% to 84% after 2 cycles for FO fouling with concentrated RO brines. In this thesis, 5 consecutive fouling and cleaning cycles were performed but efficiency was not lost. Determination of the point at which backwashing is

no longer an adequate cleaning method is necessary. After the point at which this occurs, chemical cleaning or membrane replacement will be needed.

Chapter 6: Factors effecting osmotic backwashing efficiency of forward osmosis membranes subjected to initial bacterial adhesion

In FO-RO hybrid technology, a source of impaired wastewater can act as the feed solution for the FO step. This increases the potential for a wide variety of fouling and biofouling in FO, increasing the need for further research into the factors effecting cleaning efficiency.

In chapter 6, factors effecting osmotic backwashing of adhered bacteria on FO membranes was examined and backwashing was deemed adequate but only under certain conditions. Further work is needed in this area due to the several physical, chemical and biological factors that influence bacteria during both adhesion and backwashing. Physical factors include crossflow velocity and perpendicular drag due to backwashing. Chemical influences include the ionic strength and pH of the feed solution and draw solution. Potential biological effects include manipulation of the stress responses of the bacteria such that they are easier to remove. The use of AFM to measure adhesion forces of the membrane after backwashing with various solutions would give insight into how different backwashing solutions aid or hinder cell removal.

The production of alginate as a stress response of *P. putida* resulted in higher cell survival rates and higher backwashing efficiencies with CaCl_2 solutions compared to NaCl solutions for lower backwashing fluxes, see table 6.2. However, no CaCl_2 backwashing solution could compete with the 3 M NaCl solution, which removed 93% of the adhered cells, due to the increase in adhesion caused by the interaction between the alginate produced by the bacteria and the Ca^{2+} ions. This invites studying initial adhesion of *P. putida* in the presence of alginate on FO membranes to determine if the alginate presence will hinder or aid backwashing efficiency.

As shown in this thesis, osmotic backwashing is a membrane cleaning method that shows promise, but drawbacks such as ionic salts interacting with the fouling layer need to be overcome. Alternatives to ionic salts to induce osmotic backwashing should be explored further. A good draw solution should be inexpensive, energy efficient, nontoxic and offer high fluxes and low reverse salt fluxes. Recent studies have explored alternatives such as

water soluble ammonium bicarbonate, [62], and magnetic nanoparticles, [155, 156]. McCutcheon et al, [62], studied water soluble ammonium bicarbonate and achieved high fluxes of over 20 L/m²h. Ling et al, [156], showed that magnetic nanoparticles capped with polyacrylic acid could achieve fluxes of 10 L/m²h. Similarly, Ge et al, [155], used hydrophilic superparamagnetic nanoparticles to achieve fluxes of over 10 L/m²h. Draw solutions such as these may help to increase backwashing efficacy but further work is needed here.

Real wastewater contains a multitude of different contaminants including bacteria and organic substances so knowledge of how they interact is important when developing effective cleaning methods. Further work involving cleaning of more complex fouling matrices that mimic real seawater and wastewater is needed.

In this thesis it was shown that cleaning efficiency depends on the fouling characteristics. Therefore tailoring the backwashing method to the rate of fouling may be a way of maintaining efficiency, see figure 7.1.

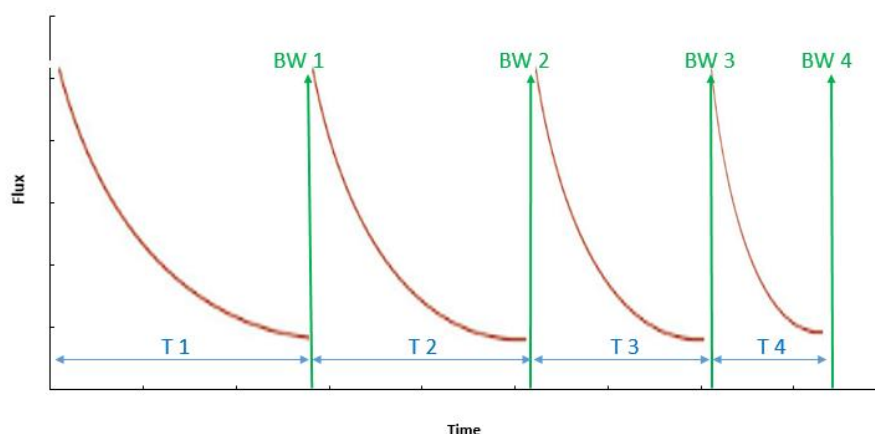


Figure 7.1: Illustration of how backwashing could be employed to restore flux

Backwashing solutions of differing osmotic pressures could be applied to fouled membranes depending on the rate at which the flux reduces to a certain end point. The end flux should be chosen such that fouling effects can be reversed at this point. If the extent of the fouling is indicated by how quickly the flux is lost, an appropriate backwashing solution can be chosen based on this time. This could potentially decrease the cleaning frequency and therefore limit time losses, as well as limiting the use of salts.

Once robust cleaning methods are developed, pilot plant testing of these methods is needed in order for it to be implemented on a larger scale. A simple illustration of how this may be designed is shown below in figure 7.2.

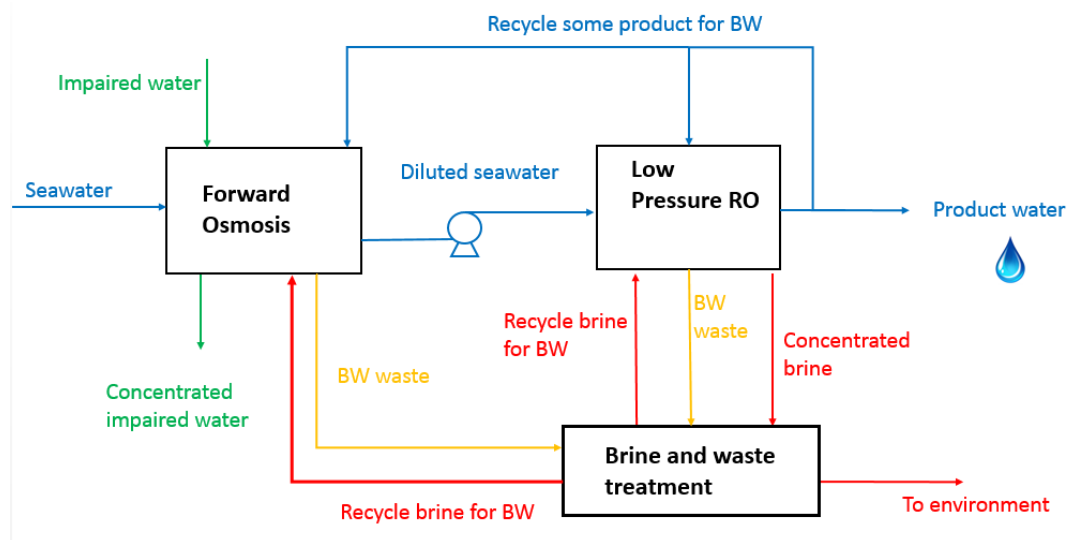


Figure 7.2: Flow diagram of how osmotic backwashing could be employed in a forward osmosis and low pressure osmosis hybrid system

Diluting seawater via FO could be carried out using impaired water as the feed solution. As shown in this thesis, backwashing is a promising cleaning method for forward osmosis so harmful cleaning chemicals may be reduced. Reducing the concentration of seawater using FO will therefore mean that RO desalination can be carried out at lower pressures which will result in fouling layers that are easier to remove via backwashing, as shown in this thesis. Waste brine from RO desalination could be treated and recycled for use during backwashing of both membrane processes as shown in this basic diagram, figure 7.2.

Desalination is a good solution to earth's water crisis however, our ever changing climate, increasing population and industries are effecting our water sources. For this reason, constant and continuous monitoring of feed water is necessary to implement optimal chemical free cleaning strategies in desalination and other membrane processes. FO-RO hybrid technology can potentially reduce cleaning chemical requirements in RO and FO. The use of FO technology to dilute seawater requires a lower concentration impaired water

such as municipal wastewater to act as the feed solution. Therefore, knowledge of the chemistry of this feed water is also important. The chemistry of the seawater is also important as this will affect the initial membrane flux which will affect cleaning efficiency. In reality, a combination of many types of fouling such as organic, colloidal and biofouling effect membrane processes and therefore knowledge of the type of fouling is important when determining the best approach to cleaning. There is likely no “one size fits all” approach to the cleaning of membrane processes without the use of harmful chemicals but cleaning can potentially be tailored to specific fouling conditions and therefore research into its optimisation is worthwhile.

Appendices

Appendix A: Materials and methods

Design, construction and testing of the forward osmosis crossflow system

In order to ensure accurate results were obtained, it was necessary to measure the weight of both the feed and draw solutions. Preliminary experiments were carried out to do this using a feed solution of deionised water and a draw solution of 0.7 M NaCl. This ensured no weight was lost due to fouling build-up on the membrane surface. The membrane used was NF90 and was placed in AL-DS mode and a reading was taken roughly every 10 minutes.

Table A.1: Agreeability of the feed and draw solution weight changes (ΔW). Experiments carried out: 25-06-15

Experiment 1		Experiment 2	
ABS DS ΔW - FS ΔW	% Total DS ΔW	ABS DS ΔW - FS ΔW	% Total DS ΔW
0.03	1.05	0.02	1.03
0.06	1.09	0.04	1.05
0.10	0.87	0.04	1.04
0.26	0.85	0.04	1.04
0.32	0.85	0.01	0.99
0.09	0.97	0.03	0.98
0.40	0.87	0.06	0.98
0.04	1.10	0.11	0.96
		0.14	0.96
		0.27	0.94
		0.39	0.92
		0.33	0.94
Average	0.95	Average	0.99

The weights of both solutions were within 5% of each other on average. This shows that using this method of weighing the draw solution to measure membrane flux is accurate.

To carry out chapter 5, Osmotic Backwashing of Forward Osmosis Membranes after Initial Bioadhesion, the FO crossflow system was modified to allow for 2 membrane cells to operate in parallel. In order to ensure the results from both cells were the same, the pressure and flowrate of both cells on the feed and draw side were tested. These are shown below in table 2.

Table A.2: Pressure and flowrate of cell 1 and cell 2 on the draw side and the feed side. Experiments carried out: 04-05-18

Feed side				Draw Side			
Pressure Cell 1 - 2 (Bar)	% Total Pressure	Flow Cell 1 - 2 (L/min)	% Total Flow	Pressure Cell 1 - 2 (Bar)	% Total Pressure	Flow Cell 1 - 2 (L/min)	% Total Flow
0.004	0.95	0.04	0.87	0.00	1.00	0.03	0.88
0.002	0.98	0.00	1.00	0.001	0.98	0.03	0.92
0.00	1.00	0.02	0.95	0.002	0.98	0.02	0.94
0.00	1.00	0.01	0.98	0.00	1.00	0.02	0.96
0.00	1.00	0.01	0.98	0.00	1.00	0.00	1.00
average	0.99	average	0.96	average	0.99	average	0.94

As well as testing the feed and draw side pressures and flowrates, initial bioadhesion experiments were performed on both cells at the same time to ensure the surface coverage was even and therefore flow was split evenly. Adhesion is measured by surface coverage. The results are shown below in table A.3.

Table A.3: Membrane surface coverage. Experiment carried out 06/06/18 to 07/06/18.

	Cell 1 Live		Cell 2 Live	
Media volume	Area (%)	Stdev	Area (%)	Stdev
100 ml	15.29	5.57	14.84	2.48
200ml	18.58	4.71	20.69	4.95

From tables A.2 and A.3 it is accepted that the flow was divided evenly. For both the draw and feed sides the pressures of both cells agreed within 1% of each other. The flowrates

were within 6% of each other for each recording. The surface coverage was relatively even for both cells for a media volume of 100 ml and 200 ml. These results show that the flow was split evenly between the two cells.

Design, construction and testing of the reverse osmosis crossflow system

In the reverse osmosis bench scale set-up, two cells were fouled in parallel. In order to ensure the results from both cells were the same, the pressure of both cells was tested under an operating pressure of 20 bar. Pressure transducers were attached to both cells and the results are shown below in table A.4.

Table A.4: Difference in pressure between cell 1 and cell2 at 20 bar. Experiment carried out: 29-03-17

Pressure abs(Cell 1 - Cell2) (Bar)	% Total Pressure
0.53	0.97
0.51	0.97
0.80	0.96
0.80	0.96
0.30	0.99
Average	0.97

From table A.4, it has been proven that the flow was split evenly between both cells as the pressures in both cells were within 3% of each other. This shows that results obtained from this crossflow system are accurate.

Appendix B: Calibrations

Calibration of measurement instruments

Thermocouples

The thermocouples were used to measure the temperature of the feed and draw solutions during FO experiments. And the temperature of the feed during RO experiments.

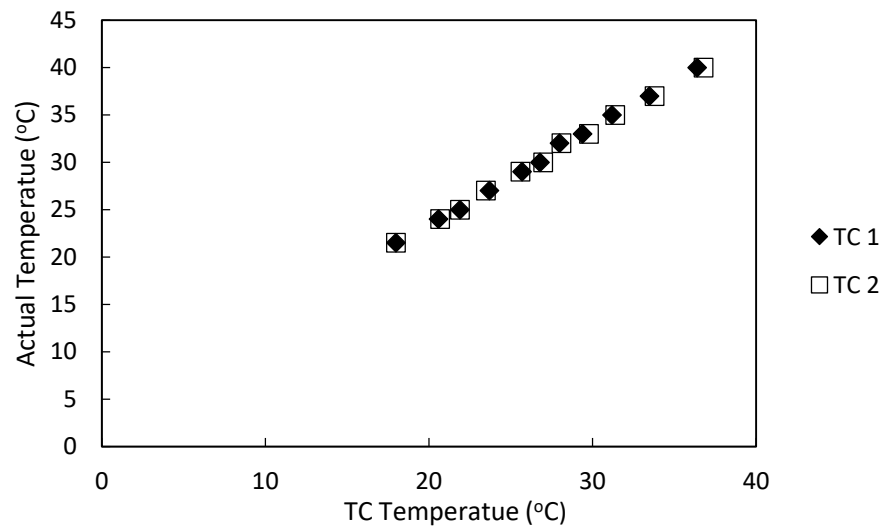


Figure B.1: Calibration of thermocouples

The thermocouples were placed in a water bath of known temperature (measured by a thermometer) and the values given by the thermocouples are plotted in figure 1.

Flowmeters

The flowmeters were used to measure the crossflow rate of the feed and draw solutions.

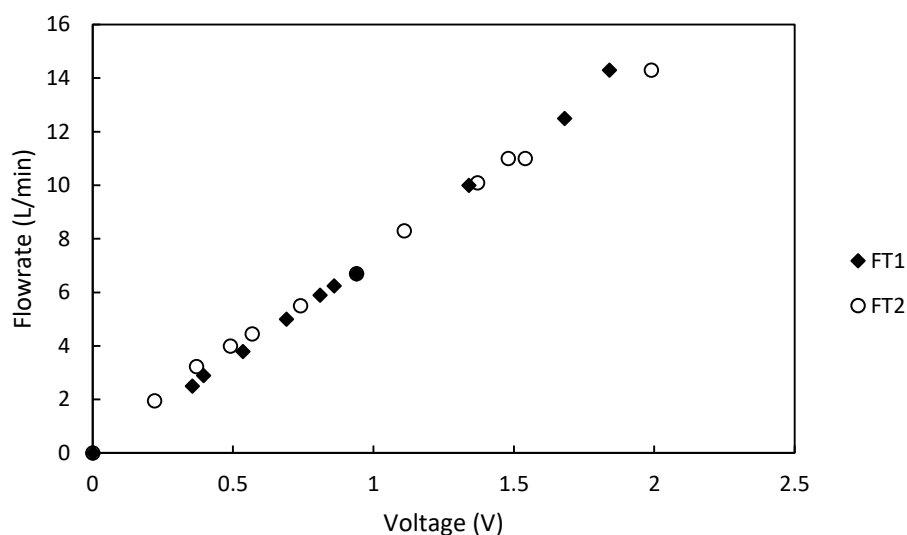


Figure B.2: Calibration of flowmeters for FO crossflow

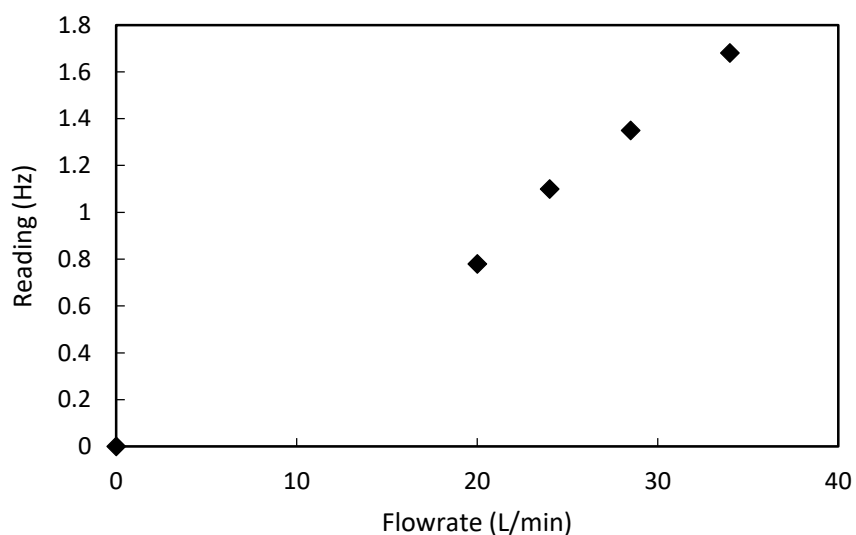


Figure B.3: Calibration of flowmeter for RO crossflow

For both crossflow systems, the flowrate was measured using a graduated cylinder and a stopwatch. This known flowrate was plotted against the recorded frequency and the calibration is shown in figures B.2 and B.3.

Pressure Transducers

In total, 4 pressure transducers were calibrated, 2 for each crossflow system. They were used to measure the pressure in each membrane cell.

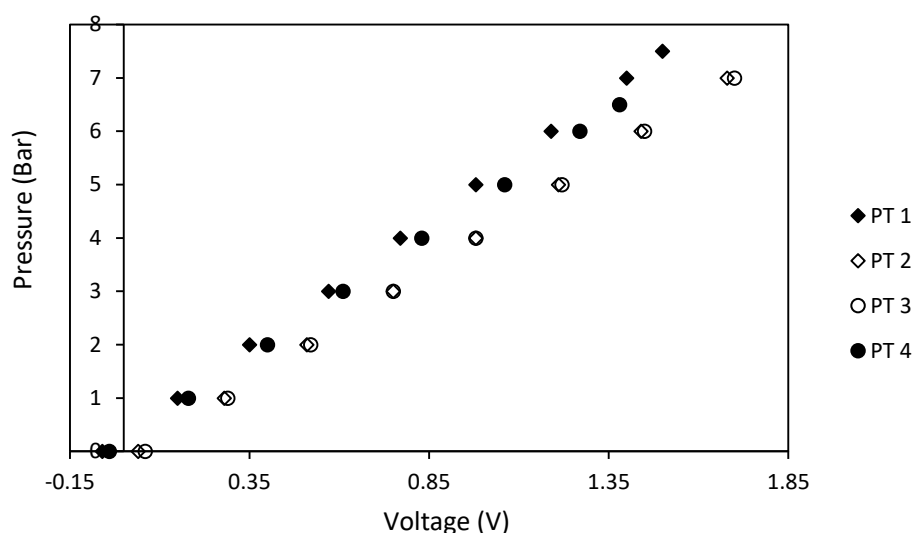


Figure B.4: Calibration of pressure transducers for both FO and RO crossflow

The pressure transducers were calibrated using a Druck calibrator (Scotia Instrumentation). The calibration is shown in figure B.4.

Total Organic Carbon Analyser

For the organic fouling and cleaning experiments, levels of TOC in permeate and feed samples were measured using a total organic carbon analyser (TOC-V CPH) in non-purgeable organic carbon (NPOC) mode (Shimadzu, Milton Keynes, UK). Prior to analysis, the samples were acidified using 2 M HCl to pH 2-3 and sparged for 1.5 minutes with N_2 to remove inorganic carbon (from CO_2 in the sample).

Next, some of the sample is sent to a platinum catalyst, where the organic carbon is burned to form CO_2 at $680^\circ C$. This is sent to a nondispersive infrared detector to obtain a peak. The area of this peak is converted into a concentration by using the relationship in figure B.5.

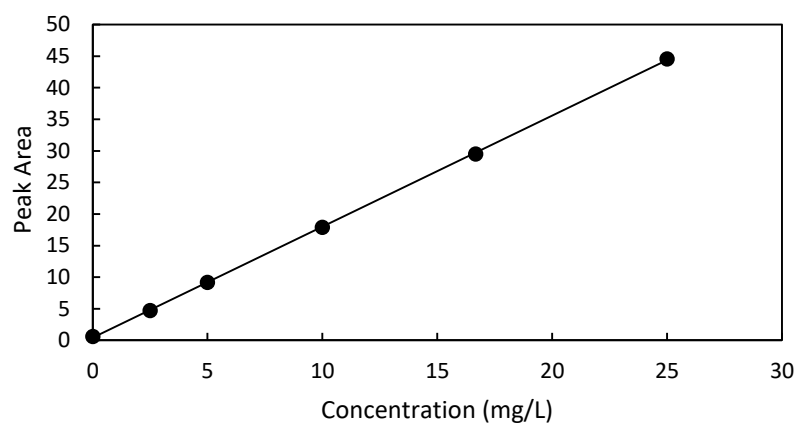
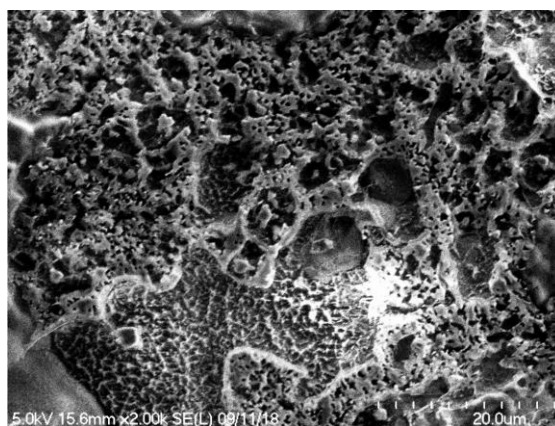


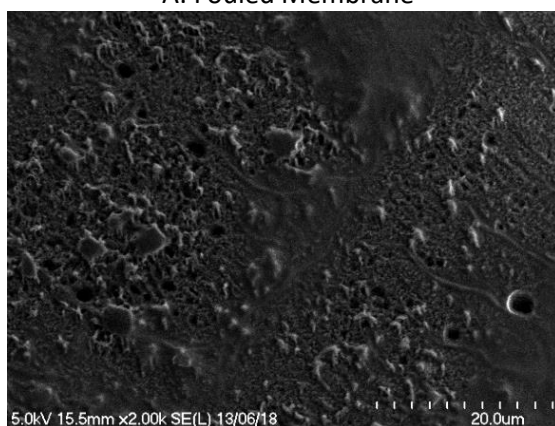
Figure B.5: Calibration of the TOC analyser

In order to produce this calibration curve, known concentrations of potassium hydrogen phthalate (PHP) were made up and ran in the instrument under a built in calibration method in the software. PHP was used as a standard in each run of the instrument

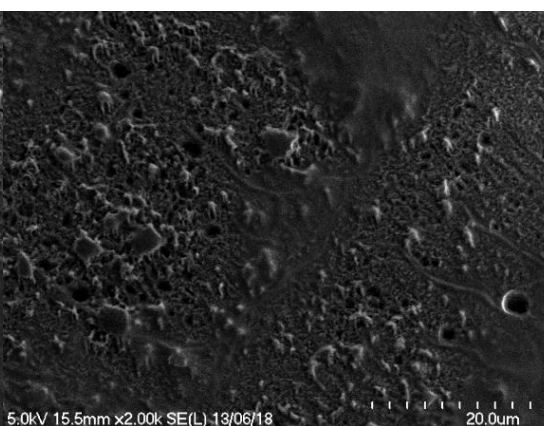
Appendix C: Scanning electron microscopy images



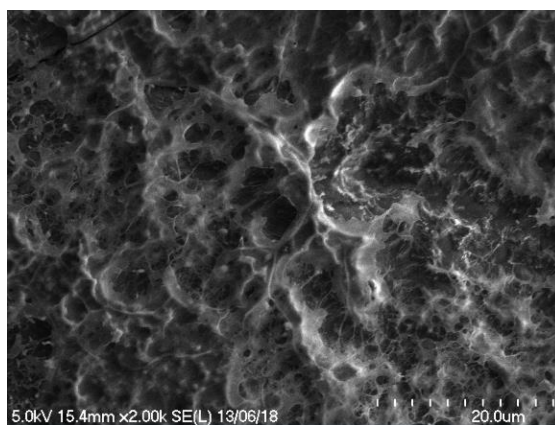
A: Fouled Membrane



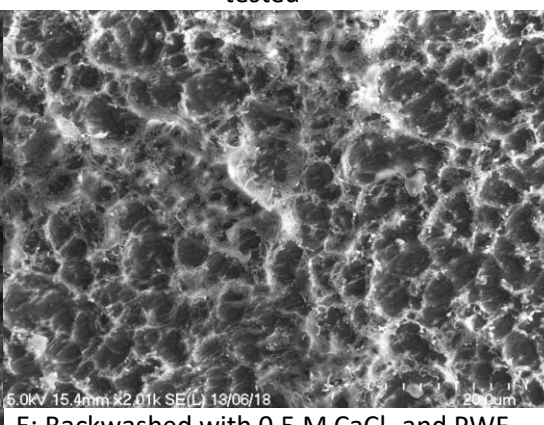
B: Backwashed with 0.7 M NaCl



C: Backwashed with 0.7 M NaCl and PWF tested



D: Backwashed with 0.5 M CaCl₂



E: Backwashed with 0.5 M CaCl₂ and PWF tested

Figure C.1: Cryo SEM images of the surface of the fouled and backwashing membranes. Imaged at 2K magnification

Scanning electron cryomicroscopy (Cryo SEM) was used to observe and compare the surface morphology of the fouled and backwashed membranes in RO.

Appendix D: Scanning electron microscopy energy-dispersive X-ray spectroscopy: Spectrums

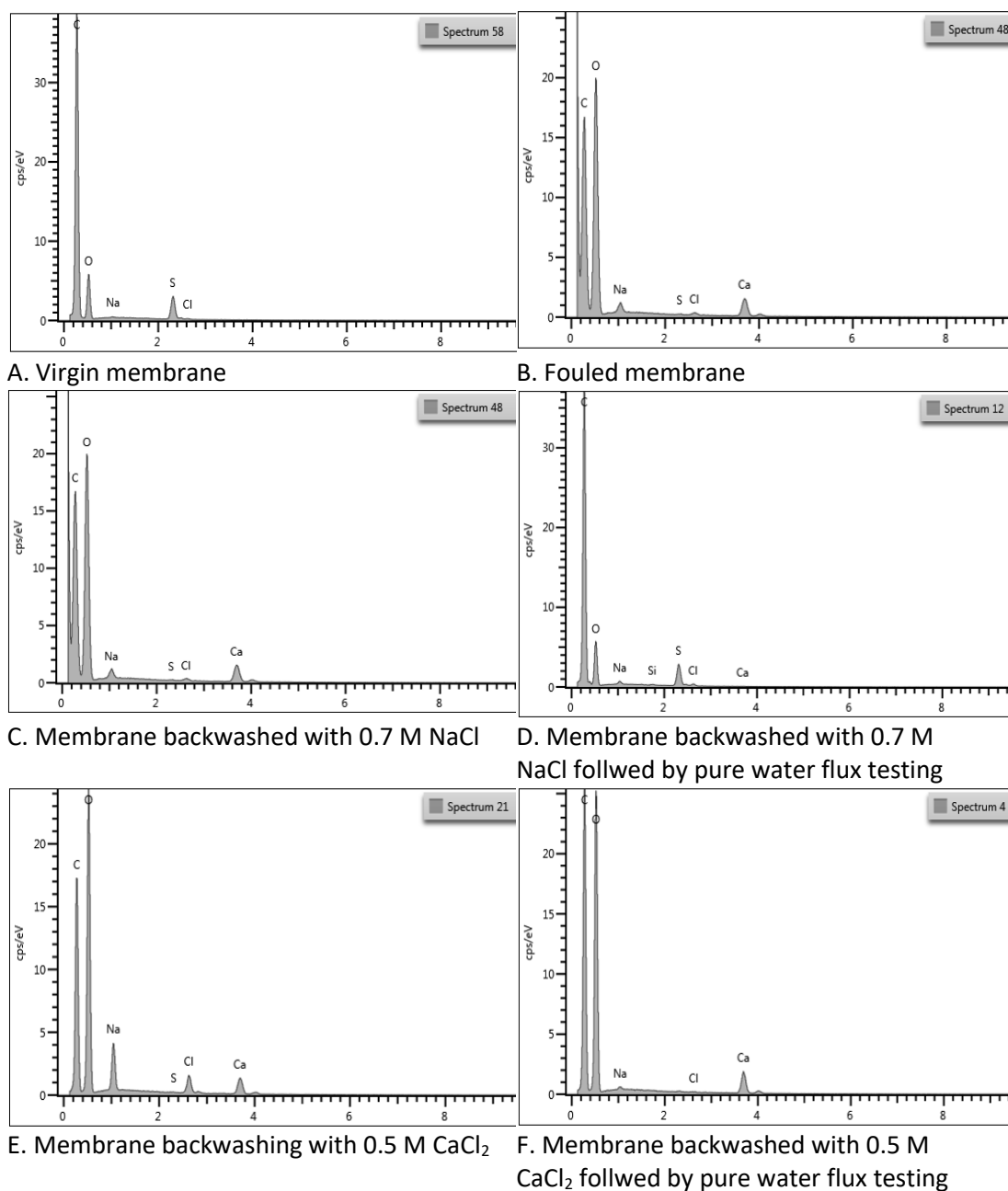


Figure D.1: SEM EDS spectra for virgin, fouled and cleaned membranes.

SEM-EDS was used to determine the elements present on the clean and fouled membrane surfaces. Three spectra each were obtained from three different sites on the membrane surface (9 in total per membrane). Shown in figure D.1 are examples for 1 of these spectra for each membrane studied.

Appendix E: Atomic force microscopy

Atomic Force Microscopy Raw Data

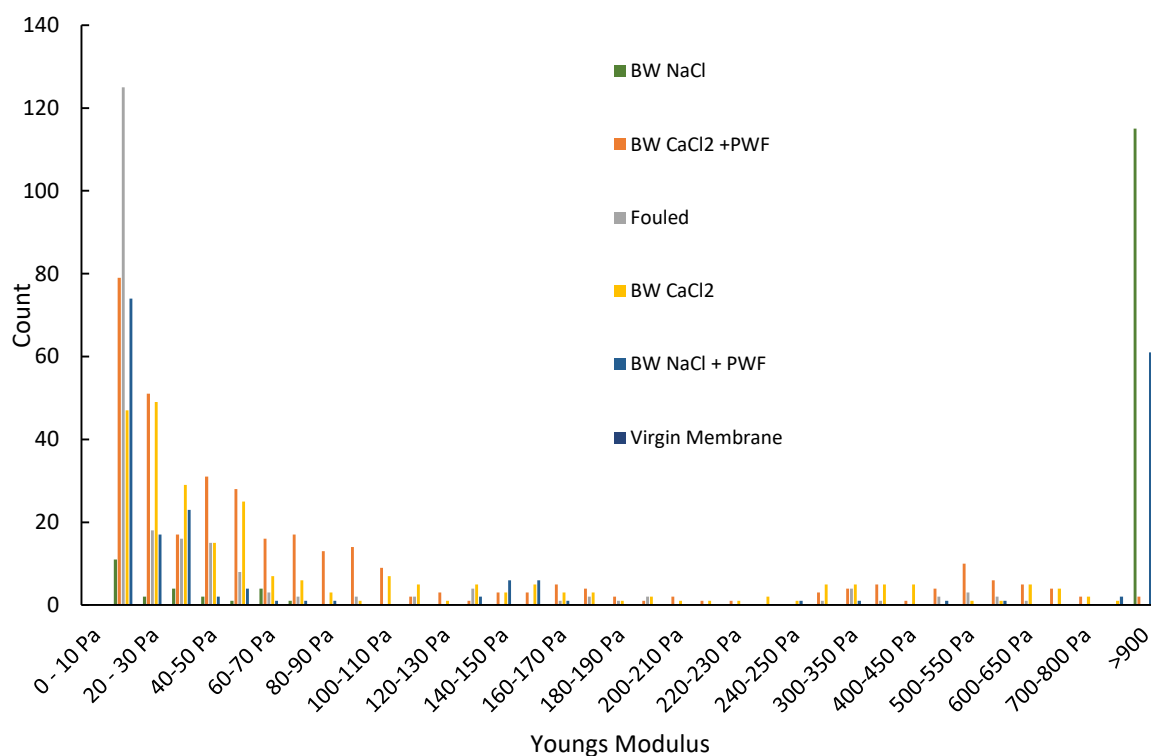


Figure E.1: Atomic force microscopy results showing the Young's modulus for each membrane sample

The Young's modulus (elasticity) and adhesive force of the fouled and backwashed membranes were determined by examining indentation and retraction curves obtained using AFM. The raw data was analysed using the Hertz model fitting with PUNIAS software with a constant Poisson ratio of 0.5. At least 50 measurements of each sample were taken to get average measurements.

References

1. Farooque, A.M., et al., *Parametric analyses of energy consumption and losses in SWCC SWRO plants utilizing energy recovery devices*. Desalination, 2008. **219**(1–3): p. 137-159.
2. Semiat, R., *Energy Issues in Desalination Processes*. Environmental Science & Technology, 2008. **42**(22): p. 8193-8201.
3. Service, R.F., *Desalination Freshens Up*. Science, 2006. **313**(5790): p. 1088-1090.
4. Jones, E., et al., *The state of desalination and brine production: A global outlook*. Science of The Total Environment, 2019. **657**: p. 1343-1356.
5. Hoepner, T. and S. Lattemann, *Chemical impacts from seawater desalination plants — a case study of the northern Red Sea*. Desalination, 2003. **152**(1): p. 133-140.
6. Abd El Aleem, F.A., K.A. Al-Sugair, and M.I. Alahmad, *Biofouling problems in membrane processes for water desalination and reuse in Saudi Arabia*. International Biodeterioration & Biodegradation, 1998. **41**(1): p. 19-23.
7. Alzahrani, S., et al., *Identification of foulants, fouling mechanisms and cleaning efficiency for NF and RO treatment of produced water*. Separation and Purification Technology, 2013. **118**(0): p. 324-341.
8. Flemming, H.-C., *Reverse osmosis membrane biofouling*. Experimental Thermal and Fluid Science, 1997. **14**(4): p. 382-391.
9. Zhu, X. and M. Elimelech, *Colloidal Fouling of Reverse Osmosis Membranes: Measurements and Fouling Mechanisms*. Environmental Science & Technology, 1997. **31**(12): p. 3654-3662.
10. Association, W.R., *Water Desalination Costs*. 2011.
11. Lattemann, S. and T. Höpner, *Impacts of seawater desalination plants on the marine environment of the Gulf*, in *Protecting the Gulf's Marine Ecosystems from Pollution*, A.H. Abuzinada, et al., Editors. 2008, Birkhäuser Basel: Basel. p. 191-205.
12. Lattemann, S. and T. Höpner, *Environmental impact and impact assessment of seawater desalination*. Desalination, 2008. **220**(1–3): p. 1-15.
13. Caldera, U. and C. Breyer, *Learning Curve for Seawater Reverse Osmosis Desalination Plants: Capital Cost Trend of the Past, Present, and Future*. Water Resources Research, 2017. **53**(12): p. 10523-10538.
14. Bamaga, O.A., et al., *Hybrid FO/RO desalination system: Preliminary assessment of osmotic energy recovery and designs of new FO membrane module configurations*. Desalination, 2011. **268**(1): p. 163-169.
15. Lee, S., et al., *Comparison of fouling behavior in forward osmosis (FO) and reverse osmosis (RO)*. Journal of Membrane Science, 2010. **365**(1–2): p. 34-39.
16. Tow, E.W., M.M. Rencken, and J.H. Lienhard, *In situ visualization of organic fouling and cleaning mechanisms in reverse osmosis and forward osmosis*. Desalination, 2016. **399**: p. 138-147.
17. Motsa, M.M., et al., *Organic fouling in forward osmosis membranes: The role of feed solution chemistry and membrane structural properties*. Journal of Membrane Science, 2014. **460**(0): p. 99-109.
18. Mi, B. and M. Elimelech, *Organic fouling of forward osmosis membranes: Fouling reversibility and cleaning without chemical reagents*. Journal of Membrane Science, 2010. **348**(1–2): p. 337-345.

19. Ramon, G.Z., T.-V. Nguyen, and E.M.V. Hoek, *Osmosis-assisted cleaning of organic-fouled seawater RO membranes*. Chemical Engineering Journal, 2013. **218**(0): p. 173-182.
20. Sagiv, A., et al., *Osmotic backwash mechanism of reverse osmosis membranes*. Journal of Membrane Science, 2008. **322**(1): p. 225-233.
21. Ramon, G., Y. Agnon, and C. Dosoretz, *Dynamics of an osmotic backwash cycle*. Journal of Membrane Science, 2010. **364**(1–2): p. 157-166.
22. Li, Z.-Y., et al., *Flux patterns and membrane fouling propensity during desalination of seawater by forward osmosis*. Water Research, 2012. **46**(1): p. 195-204.
23. Hong, S. and M. Elimelech, *Chemical and physical aspects of natural organic matter (NOM) fouling of nanofiltration membranes*. Journal of Membrane Science, 1997. **132**(2): p. 159-181.
24. Mi, B. and M. Elimelech, *Chemical and physical aspects of organic fouling of forward osmosis membranes*. Journal of Membrane Science, 2008. **320**(1–2): p. 292-302.
25. Boo, C., et al., *Colloidal fouling in forward osmosis: Role of reverse salt diffusion*. Journal of Membrane Science, 2012. **390–391**(0): p. 277-284.
26. Liu, Y. and B. Mi, *Combined fouling of forward osmosis membranes: Synergistic foulant interaction and direct observation of fouling layer formation*. Journal of Membrane Science, 2012. **407–408**: p. 136-144.
27. Arkhangelsky, E., et al., *Combined organic–inorganic fouling of forward osmosis hollow fiber membranes*. Water Research, 2012. **46**(19): p. 6329-6338.
28. Tang, C.Y., Y.-N. Kwon, and J.O. Leckie, *Fouling of reverse osmosis and nanofiltration membranes by humic acid—Effects of solution composition and hydrodynamic conditions*. Journal of Membrane Science, 2007. **290**(1): p. 86-94.
29. Valladares Linares, R., et al., *NOM and TEP fouling of a forward osmosis (FO) membrane: Foulant identification and cleaning*. Journal of Membrane Science, 2012. **421–422**(0): p. 217-224.
30. Lee, S. and M. Elimelech, *Relating Organic Fouling of Reverse Osmosis Membranes to Intermolecular Adhesion Forces*. Environmental Science & Technology, 2006. **40**(3): p. 980-987.
31. She, Q., et al., *Relating reverse and forward solute diffusion to membrane fouling in osmotically driven membrane processes*. Water Research, 2012. **46**(7): p. 2478-2486.
32. BinAhmed, S., et al., *Bacterial Adhesion to Ultrafiltration Membranes: Role of Hydrophilicity, Natural Organic Matter, and Cell-Surface Macromolecules*. Environmental Science & Technology, 2018. **52**(1): p. 162-172.
33. Safari, A., et al., *The significance of calcium ions on Pseudomonas fluorescens biofilms – a structural and mechanical study*. Biofouling, 2014. **30**(7): p. 859-869.
34. Li, Q. and M. Elimelech, *Organic Fouling and Chemical Cleaning of Nanofiltration Membranes: Measurements and Mechanisms*. Environmental Science & Technology, 2004. **38**(17): p. 4683-4693.
35. Dunne, W.M., *Bacterial Adhesion: Seen Any Good Biofilms Lately?* Clinical Microbiology Reviews, 2002. **15**(2): p. 155-166.
36. Tang, C.Y., Y.-N. Kwon, and J.O. Leckie, *Fouling of reverse osmosis and nanofiltration membranes by humic acid—Effects of solution composition and hydrodynamic conditions*. Journal of Membrane Science, 2007. **290**(1–2): p. 86-94.
37. Marshall, A.D., P.A. Munro, and G. Trägårdh, *The effect of protein fouling in microfiltration and ultrafiltration on permeate flux, protein retention and selectivity: A literature review*. Desalination, 1993. **91**(1): p. 65-108.

38. Ang, W.S., et al., *Chemical cleaning of RO membranes fouled by wastewater effluent: Achieving higher efficiency with dual-step cleaning*. Journal of Membrane Science, 2011. **382**(1–2): p. 100-106.
39. Pihko, P.M., T.K. Rissa, and R. Aksela, *Enantiospecific synthesis of isomers of AES, a new environmentally friendly chelating agent*. Tetrahedron, 2004. **60**(48): p. 10949-10954.
40. Yoon, H., et al., *Biofouling occurrence process and its control in the forward osmosis*. Desalination, 2013. **325**(0): p. 30-36.
41. Yangali-Quintanilla, V., et al., *Indirect desalination of Red Sea water with forward osmosis and low pressure reverse osmosis for water reuse*. Desalination, 2011. **280**(1): p. 160-166.
42. Ang, W.S., et al., *Fouling and cleaning of RO membranes fouled by mixtures of organic foulants simulating wastewater effluent*. Journal of Membrane Science, 2011. **376**(1–2): p. 196-206.
43. Lee, S. and M. Elimelech, *Salt cleaning of organic-fouled reverse osmosis membranes*. Water Research, 2007. **41**(5): p. 1134-1142.
44. Gebreyohannes, A.Y., et al., *Treatment of Olive Mill Wastewater by Forward Osmosis*. Separation and Purification Technology, 2015. **147**(0): p. 292-302.
45. Qin, J.-J., et al., *Development of novel backwash cleaning technique for reverse osmosis in reclamation of secondary effluent*. Journal of Membrane Science, 2010. **346**(1): p. 8-14.
46. Montgomery, M.A. and M. Elimelech, *Water And Sanitation in Developing Countries: Including Health in the Equation*. Environmental Science & Technology, 2007. **41**(1): p. 17-24.
47. Shannon, M.A., et al., *Science and technology for water purification in the coming decades*. Nature, 2008. **452**(7185): p. 301-310.
48. Drioli, E., A.I. Stankiewicz, and F. Macedonio, *Membrane engineering in process intensification—An overview*. Journal of Membrane Science, 2011. **380**(1–2): p. 1-8.
49. Zhou, Y. and R.S.J. Tol, *Evaluating the costs of desalination and water transport*. Water Resources Research, 2005. **41**(3).
50. Racoviceanu, A.I., et al., *Life-Cycle Energy Use and Greenhouse Gas Emissions Inventory for Water Treatment Systems*. Journal of Infrastructure Systems, 2007. **13**(4): p. 261-270.
51. Cheng, C.-L., *Study of the inter-relationship between water use and energy conservation for a building*. Energy and Buildings, 2002. **34**(3): p. 261-266.
52. Valladares Linares, R., et al., *Water harvesting from municipal wastewater via osmotic gradient: An evaluation of process performance*. Journal of Membrane Science, 2013. **447**(0): p. 50-56.
53. Qin, J.-J., et al., *New option of MBR-RO process for production of NEWater from domestic sewage*. Journal of Membrane Science, 2006. **272**(1–2): p. 70-77.
54. Liu, C., K. Rainwater, and L. Song, *Energy analysis and efficiency assessment of reverse osmosis desalination process*. Desalination, 2011. **276**(1–3): p. 352-358.
55. Liyanaarachchi, S., et al., *Mass balance for a novel RO/FO hybrid system in seawater desalination*. Journal of Membrane Science, 2016. **501**: p. 199-208.
56. Eriksson, P., *Nanofiltration extends the range of membrane filtration*. Environmental Progress, 1988. **7**(1): p. 58-62.
57. Pendergast, M.M. and E.M.V. Hoek, *A review of water treatment membrane nanotechnologies*. Energy & Environmental Science, 2011. **4**(6): p. 1946-1971.

58. Košutić, K., D. Dolar, and B. Kunst, *On experimental parameters characterizing the reverse osmosis and nanofiltration membranes' active layer*. Journal of Membrane Science, 2006. **282**(1): p. 109-114.
59. Ahmad, A.L., L.S. Tan, and S.R. Abd. Shukor, *The role of pH in nanofiltration of atrazine and dimethoate from aqueous solution*. Journal of Hazardous Materials, 2008. **154**(1): p. 633-638.
60. Ying, W., et al., *New insights on early stages of RO membranes fouling during tertiary wastewater desalination*. Journal of Membrane Science, 2014. **466**(0): p. 26-35.
61. Cath, T.Y., A.E. Childress, and M. Elimelech, *Forward osmosis: Principles, applications, and recent developments*. Journal of Membrane Science, 2006. **281**(1–2): p. 70-87.
62. McCutcheon, J.R., R.L. McGinnis, and M. Elimelech, *Desalination by ammonia–carbon dioxide forward osmosis: Influence of draw and feed solution concentrations on process performance*. Journal of Membrane Science, 2006. **278**(1): p. 114-123.
63. Alsvik, I. and M.-B. Hägg, *Pressure Retarded Osmosis and Forward Osmosis Membranes: Materials and Methods*. Polymers, 2013. **5**(1): p. 303.
64. Madsen, H.T., et al., *Use of biomimetic forward osmosis membrane for trace organics removal*. Journal of Membrane Science, 2015. **476**: p. 469-474.
65. Hancock, N.T. and T.Y. Cath, *Solute Coupled Diffusion in Osmotically Driven Membrane Processes*. Environmental Science & Technology, 2009. **43**(17): p. 6769-6775.
66. Jin, X., et al., *Effects of feed water temperature on separation performance and organic fouling of brackish water RO membranes*. Desalination, 2009. **239**(1): p. 346-359.
67. Ge, Q., M. Ling, and T.-S. Chung, *Draw solutions for forward osmosis processes: Developments, challenges, and prospects for the future*. Journal of Membrane Science, 2013. **442**(0): p. 225-237.
68. Mahlangu, T.O., et al., *Influence of organic, colloidal and combined fouling on NF rejection of NaCl and carbamazepine: Role of solute–foulant–membrane interactions and cake-enhanced concentration polarisation*. Journal of Membrane Science, 2014. **471**: p. 35-46.
69. Lee, S., J. Cho, and M. Elimelech, *Influence of colloidal fouling and feed water recovery on salt rejection of RO and NF membranes*. Desalination, 2004. **160**(1): p. 1-12.
70. Gao, Y., et al., *Characterization of internal and external concentration polarizations during forward osmosis processes*. Desalination, 2014. **338**(0): p. 65-73.
71. McCutcheon, J.R. and M. Elimelech, *Influence of concentrative and dilutive internal concentration polarization on flux behavior in forward osmosis*. Journal of Membrane Science, 2006. **284**(1–2): p. 237-247.
72. Tang, C.Y., et al., *Coupled effects of internal concentration polarization and fouling on flux behavior of forward osmosis membranes during humic acid filtration*. Journal of Membrane Science, 2010. **354**(1–2): p. 123-133.
73. Gray, G.T., J.R. McCutcheon, and M. Elimelech, *Internal concentration polarization in forward osmosis: role of membrane orientation*. Desalination, 2006. **197**(1–3): p. 1-8.
74. Zhao, S. and L. Zou, *Relating solution physicochemical properties to internal concentration polarization in forward osmosis*. Journal of Membrane Science, 2011. **379**(1–2): p. 459-467.

75. Mallevialle, J.O., P. E.; Wiesner, M. R., *Water Treatment Membrane Processes*. 1996, New York: McGraw-Hill.
76. Zou, S., et al., *The role of physical and chemical parameters on forward osmosis membrane fouling during algae separation*. Journal of Membrane Science, 2011. **366**(1): p. 356-362.
77. Hickenbottom, K.L., et al., *Forward osmosis treatment of drilling mud and fracturing wastewater from oil and gas operations*. Desalination, 2013. **312**(0): p. 60-66.
78. Flemming, H.-C. and J. Wingender, *The biofilm matrix*. Nature Reviews Microbiology, 2010. **8**: p. 623.
79. Habimana, O., A.J.C. Semião, and E. Casey, *The role of cell-surface interactions in bacterial initial adhesion and consequent biofilm formation on nanofiltration/reverse osmosis membranes*. Journal of Membrane Science, 2014. **454**: p. 82-96.
80. Kwan, S.E., E. Bar-Zeev, and M. Elimelech, *Biofouling in forward osmosis and reverse osmosis: Measurements and mechanisms*. Journal of Membrane Science, 2015. **493**: p. 703-708.
81. Yoon, H., et al., *Biofouling occurrence process and its control in the forward osmosis*. Desalination, 2013. **325**: p. 30-36.
82. Zhang, J., et al., *Membrane biofouling and scaling in forward osmosis membrane bioreactor*. Journal of Membrane Science, 2012. **403-404**: p. 8-14.
83. Pang, C.M., et al., *Biofilm Formation Characteristics of Bacterial Isolates Retrieved from a Reverse Osmosis Membrane*. Environmental Science & Technology, 2005. **39**(19): p. 7541-7550.
84. Subramani, A. and E.M.V. Hoek, *Direct observation of initial microbial deposition onto reverse osmosis and nanofiltration membranes*. Journal of Membrane Science, 2008. **319**(1): p. 111-125.
85. de Kerchove, A.J. and M. Elimelech, *Formation of Polysaccharide Gel Layers in the Presence of Ca²⁺ and K⁺ Ions: Measurements and Mechanisms*. Biomacromolecules, 2007. **8**(1): p. 113-121.
86. Tang, C.Y., Y.-N. Kwon, and J.O. Leckie, *Characterization of Humic Acid Fouled Reverse Osmosis and Nanofiltration Membranes by Transmission Electron Microscopy and Streaming Potential Measurements*. Environmental Science & Technology, 2007. **41**(3): p. 942-949.
87. Seidel, A. and M. Elimelech, *Coupling between chemical and physical interactions in natural organic matter (NOM) fouling of nanofiltration membranes: implications for fouling control*. Journal of Membrane Science, 2002. **203**(1): p. 245-255.
88. O'Toole, G., H.B. Kaplan, and R. Kolter, *Biofilm Formation as Microbial Development*. Annual Review of Microbiology, 2000. **54**(1): p. 49-79.
89. Wingender, J., T.R. Neu, and H.-C. Flemming, *What are Bacterial Extracellular Polymeric Substances?*, in *Microbial Extracellular Polymeric Substances: Characterization, Structure and Function*, J. Wingender, T.R. Neu, and H.-C. Flemming, Editors. 1999, Springer Berlin Heidelberg: Berlin, Heidelberg. p. 1-19.
90. Monroe, D., *Looking for Chinks in the Armor of Bacterial Biofilms*. PLOS Biology, 2007. **5**(11): p. e307.
91. Boks, N.P., et al., *Forces involved in bacterial adhesion to hydrophilic and hydrophobic surfaces*. Microbiology, 2008. **154**(10): p. 3122-3133.
92. Allen, A., et al., *Nanofiltration and reverse osmosis surface topographical heterogeneities: Do they matter for initial bacterial adhesion?* Journal of Membrane Science, 2015. **486**: p. 10-20.

93. Semião, A.J.C., O. Habimana, and E. Casey, *Bacterial adhesion onto nanofiltration and reverse osmosis membranes: Effect of permeate flux*. Water Research, 2014. **63**: p. 296-305.
94. Semião, A.J.C., et al., *The importance of laboratory water quality for studying initial bacterial adhesion during NF filtration processes*. Water Research, 2013. **47**(8): p. 2909-2920.
95. van Loosdrecht, M.C., et al., *The role of bacterial cell wall hydrophobicity in adhesion*. Applied and environmental microbiology, 1987. **53**(8): p. 1893-1897.
96. Martínez-Gil, M., et al., *Calcium Causes Multimerization of the Large Adhesin LapF and Modulates Biofilm Formation by *Pseudomonas putida**. Journal of Bacteriology, 2012. **194**(24): p. 6782-6789.
97. Fletcher, M., *Attachment of *Pseudomonas fluorescens* to glass and influence of electrolytes on bacterium-substratum separation distance*. Journal of Bacteriology, 1988. **170**(5): p. 2027-2030.
98. Jin, X., X. Huang, and E.M.V. Hoek, *Role of Specific Ion Interactions in Seawater RO Membrane Fouling by Alginic Acid*. Environmental Science & Technology, 2009. **43**(10): p. 3580-3587.
99. Valladares Linares, R., et al., *Cleaning protocol for a FO membrane fouled in wastewater reuse*. Desalination and Water Treatment, 2013. **51**(25-27): p. 4821-4824.
100. Arkhangelsky, E., et al., *Effects of scaling and cleaning on the performance of forward osmosis hollow fiber membranes*. Journal of Membrane Science, 2012. **415–416**(0): p. 101-108.
101. Sagiv, A., et al., *Analysis of forward osmosis desalination via two-dimensional FEM model*. Journal of Membrane Science, 2014. **464**(0): p. 161-172.
102. Bar-Zeev, E. and M. Elimelech, *Reverse Osmosis Biofilm Dispersal by Osmotic Back-Flushing: Cleaning via Substratum Perforation*. Environmental Science & Technology Letters, 2014. **1**(2): p. 162-166.
103. Achilli, A., et al., *The forward osmosis membrane bioreactor: A low fouling alternative to MBR processes*. Desalination, 2009. **239**(1–3): p. 10-21.
104. Holloway, R.W., et al., *Forward osmosis for concentration of anaerobic digester centrate*. Water Research, 2007. **41**(17): p. 4005-4014.
105. Martinetti, C.R., A.E. Childress, and T.Y. Cath, *High recovery of concentrated RO brines using forward osmosis and membrane distillation*. Journal of Membrane Science, 2009. **331**(1–2): p. 31-39.
106. Coday, B.D., N. Almaraz, and T.Y. Cath, *Forward osmosis desalination of oil and gas wastewater: Impacts of membrane selection and operating conditions on process performance*. Journal of Membrane Science, 2015. **488**: p. 40-55.
107. Valladares Linares, R., et al., *Impact of spacer thickness on biofouling in forward osmosis*. Water Research, 2014. **57**: p. 223-233.
108. Tang, C.Y., et al., *Effect of Flux (Transmembrane Pressure) and Membrane Properties on Fouling and Rejection of Reverse Osmosis and Nanofiltration Membranes Treating Perfluorooctane Sulfonate Containing Wastewater*. Environmental Science & Technology, 2007. **41**(6): p. 2008-2014.
109. Creber, S.A., et al., *Chemical cleaning of biofouling in reverse osmosis membranes evaluated using magnetic resonance imaging*. Journal of Membrane Science, 2010. **362**(1): p. 202-210.

110. Cath, T.Y., et al., *A multi-barrier osmotic dilution process for simultaneous desalination and purification of impaired water*. Journal of Membrane Science, 2010. **362**(1–2): p. 417-426.
111. Loeb, S. and M.R. Bloch, *Countercurrent flow osmotic processes for the production of solutions having a high osmotic pressure*. Desalination, 1973. **13**(2): p. 207-215.
112. de Groot, B.L. and H. Grubmüller, *Water Permeation Across Biological Membranes: Mechanism and Dynamics of Aquaporin-1 and GlpF*. Science, 2001. **294**(5550): p. 2353-2357.
113. Hester, K.L., J. Luo, and J.R. Sokatch, [14] - *Purification of Pseudomonas putida Branched-Chain Keto Acid Dehydrogenase E1 Component*, in *Methods in Enzymology*, R.A. Harris and J.R. Sokatch, Editors. 2000, Academic Press. p. 129-138.
114. Richardson, S.D., et al., *Occurrence, genotoxicity, and carcinogenicity of regulated and emerging disinfection by-products in drinking water: A review and roadmap for research*. Mutation Research/Reviews in Mutation Research, 2007. **636**(1): p. 178-242.
115. Greenlee, L.F., et al., *Reverse osmosis desalination: Water sources, technology, and today's challenges*. Water Research, 2009. **43**(9): p. 2317-2348.
116. Xie, M., et al., *Comparison of the removal of hydrophobic trace organic contaminants by forward osmosis and reverse osmosis*. Water Research, 2012. **46**(8): p. 2683-2692.
117. Kallenberger, P.A. and M. Fröba, *Water harvesting from air with a hygroscopic salt in a hydrogel-derived matrix*. Communications Chemistry, 2018. **1**(1): p. 28.
118. Xie, M., et al., *Role of pressure in organic fouling in forward osmosis and reverse osmosis*. Journal of Membrane Science, 2015. **493**: p. 748-754.
119. de Kerchove, A.J. and M. Elimelech, *Structural Growth and Viscoelastic Properties of Adsorbed Alginate Layers in Monovalent and Divalent Salts*. Macromolecules, 2006. **39**(19): p. 6558-6564.
120. Moe, S.T., et al., *Swelling of covalently crosslinked alginate gels: influence of ionic solutes and nonpolar solvents*. Macromolecules, 1993. **26**(14): p. 3589-3597.
121. Wang, Q. and X. Zhao, *A three-dimensional phase diagram of growth-induced surface instabilities*. Scientific Reports, 2015. **5**: p. 8887.
122. P.H. Wolf, S.S., *The new generation for reliable RO pre-treatment*, in *International Conference on Desalination Costing*. 2004: Limassol.
123. Hancock, N.T., N.D. Black, and T.Y. Cath, *A comparative life cycle assessment of hybrid osmotic dilution desalination and established seawater desalination and wastewater reclamation processes*. Water Research, 2012. **46**(4): p. 1145-1154.
124. Wu, C.-Y., et al., *Removal of trace-amount mercury from wastewater by forward osmosis*. Journal of Water Process Engineering, 2016. **14**: p. 108-116.
125. Ang, W.S., S. Lee, and M. Elimelech, *Chemical and physical aspects of cleaning of organic-fouled reverse osmosis membranes*. Journal of Membrane Science, 2006. **272**(1): p. 198-210.
126. Carpentier, B. and O. Cerf, *Biofilms and their consequences, with particular reference to hygiene in the food industry*. Journal of Applied Bacteriology, 1993. **75**(6): p. 499-511.
127. Bereschenko, L.A., et al., *Biofilm Formation on Reverse Osmosis Membranes Is Initiated and Dominated by *Sphingomonas* spp.* Applied and Environmental Microbiology, 2010. **76**(8): p. 2623-2632.
128. Abdul Azis, P.K., I. Al-Tisan, and N. Sasikumar, *Biofouling potential and environmental factors of seawater at a desalination plant intake*. Desalination, 2001. **135**(1): p. 69-82.

129. Herzberg, M. and M. Elimelech, *Biofouling of reverse osmosis membranes: Role of biofilm-enhanced osmotic pressure*. Journal of Membrane Science, 2007. **295**(1): p. 11-20.
130. Li, B. and B.E. Logan, *Bacterial adhesion to glass and metal-oxide surfaces*. Colloids and Surfaces B: Biointerfaces, 2004. **36**(2): p. 81-90.
131. Xia, L., et al., *Novel Commercial Aquaporin Flat-Sheet Membrane for Forward Osmosis*. Vol. 56. 2017.
132. Semião, A.J.C., O. Habimana, and E. Casey, *Bacterial adhesion onto nanofiltration and reverse osmosis membranes: Effect of permeate flux*. Water Research, 2014. **63**(Supplement C): p. 296-305.
133. Kültz, D., *Chapter 12 - Osmotic regulation of DNA activity and the cell cycle*, in *Cell and Molecular Response to Stress*, K.B. Storey and J.M. Storey, Editors. 2000, Elsevier. p. 157-179.
134. Katebian, L. and S.C. Jiang, *Marine bacterial biofilm formation and its responses to periodic hyperosmotic stress on a flat sheet membrane for seawater desalination pretreatment*. Journal of Membrane Science, 2013. **425-426**: p. 182-189.
135. Hachicho, N., A. Birnbaum, and H.J. Heipieper, *Osmotic stress in colony and planktonic cells of Pseudomonas putida mt-2 revealed significant differences in adaptive response mechanisms*. AMB Express, 2017. **7**(1): p. 62.
136. Ridgway, H.F., M.G. Rigby, and D.G. Argo, *Adhesion of a Mycobacterium sp. to cellulose diacetate membranes used in reverse osmosis*. Applied and environmental microbiology, 1984. **47**(1): p. 61-67.
137. Harimawan, A., A. Rajasekar, and Y.-P. Ting, *Bacteria attachment to surfaces – AFM force spectroscopy and physicochemical analyses*. Journal of Colloid and Interface Science, 2011. **364**(1): p. 213-218.
138. Thwala, J.M., et al., *Bacteria–Polymeric Membrane Interactions: Atomic Force Microscopy and XDLVO Predictions*. Langmuir, 2013. **29**(45): p. 13773-13782.
139. Vadillo-Rodríguez, V., et al., *Atomic force microscopic corroboration of bond aging for adhesion of Streptococcus thermophilus to solid substrata*. Journal of Colloid and Interface Science, 2004. **278**(1): p. 251-254.
140. Xu, L.-C., V. Vadillo-Rodríguez, and B.E. Logan, *Residence Time, Loading Force, pH, and Ionic Strength Affect Adhesion Forces between Colloids and Biopolymer-Coated Surfaces*. Langmuir, 2005. **21**(16): p. 7491-7500.
141. Mbaye, S., et al., *Influence of hydrodynamics on the growth kinetics of glass-adhering Pseudomonas putida cells through a parallel plate flow chamber*. Biomicrofluidics, 2013. **7**(5): p. 54105-54105.
142. Sadr Ghayeni, S.B., et al., *Adhesion of waste water bacteria to reverse osmosis membranes*. Journal of Membrane Science, 1998. **138**(1): p. 29-42.
143. Hong, Y. and D.G. Brown, *Electrostatic Behavior of the Charge-Regulated Bacterial Cell Surface*. Langmuir, 2008. **24**(9): p. 5003-5009.
144. Gingell, D., D.R. Garrod, and J.F. Palmer, *Divalent Cations and Cell Adhesion*, in *A Symposium on Calcium and Cellular Function*, A.W. Cuthbert, Editor. 1970, Palgrave Macmillan UK: London. p. 59-64.
145. McEldowney, S. and M. Fletcher, *Variability of the influence of physicochemical factors affecting bacterial adhesion to polystyrene substrata*. Applied and environmental microbiology, 1986. **52**(3): p. 460-465.
146. Sobek, D.C. and M.J. Higgins, *Examination of three theories for mechanisms of cation-induced bioflocculation*. Water Research, 2002. **36**(3): p. 527-538.
147. Chang, W.-S., et al., *Alginate Production by *Pseudomonas putida* Creates a Hydrated Microenvironment and Contributes to Biofilm Architecture and*

- Stress Tolerance under Water-Limiting Conditions*. Journal of Bacteriology, 2007. **189**(22): p. 8290-8299.
148. de Kerchove, A.J. and M. Elimelech, *Calcium and Magnesium Cations Enhance the Adhesion of Motile and Nonmotile Pseudomonas aeruginosa on Alginate Films*. Langmuir, 2008. **24**(7): p. 3392-3399.
 149. Sandhya, V. and S.Z. Ali, *The production of exopolysaccharide by Pseudomonas putida GAP-P45 under various abiotic stress conditions and its role in soil aggregation*. Microbiology, 2015. **84**(4): p. 512-519.
 150. Sarkisova, S., et al., *Calcium-induced virulence factors associated with the extracellular matrix of mucoid Pseudomonas aeruginosa biofilms*. Journal of bacteriology, 2005. **187**(13): p. 4327-4337.
 151. Lee, N., et al., *Identification and understanding of fouling in low-pressure membrane (MF/UF) filtration by natural organic matter (NOM)*. Water Research, 2004. **38**(20): p. 4511-4523.
 152. Vrijenhoek, E.M., S. Hong, and M. Elimelech, *Influence of membrane surface properties on initial rate of colloidal fouling of reverse osmosis and nanofiltration membranes*. Journal of Membrane Science, 2001. **188**(1): p. 115-128.
 153. Gysel, M., et al., *Hygroscopic properties of water-soluble matter and humic-like organics in atmospheric fine aerosol*. Atmos. Chem. Phys., 2004. **4**(1): p. 35-50.
 154. Mikhailov, E., et al., *Interaction of aerosol particles composed of protein and salts with water vapor: Hygroscopic growth and microstructural rearrangement*. Vol. 4. 2004. 323-350.
 155. Ge, Q., et al., *Hydrophilic Superparamagnetic Nanoparticles: Synthesis, Characterization, and Performance in Forward Osmosis Processes*. Industrial & Engineering Chemistry Research, 2011. **50**(1): p. 382-388.
 156. Ling, M.M., K.Y. Wang, and T.-S. Chung, *Highly Water-Soluble Magnetic Nanoparticles as Novel Draw Solute in Forward Osmosis for Water Reuse*. Industrial & Engineering Chemistry Research, 2010. **49**(12): p. 5869-5876.